R O S E T T A

FLIGHT REPORTS of RPC–MAG

RO–IGEP–TR–0014

Issue: 4 Revision:

Febuary 4, 2019

Report of the

First Earth Swing by (EAR1)

Time period: March 01 - 07, 2005

Andrea Diedrich
Karl-Heinz Glassmeier
Ingo Richter

Institut für Geophysik und extraterrestrische Physik
Technische Universität Braunschweig
Mendelssohnstraße 3, 38106 Braunschweig
Germany

Contents

1 Introduction

ROSETTA's first Earth Swing by (EAR1) happened in the time period March 01 – 07, 2005. RPC-MAG was switched on in the time between 2005-03-01T00:00:00 and 2005-03-08T00:00:00. The instrument performance was excellent. There were no problems.

This document gives a brief description of the executed activities and show the obtained data. Housekeeping data (Temperature of the OB & IB sensor, Filter Stages A & B, Filter configuration register, Reference voltage, negative and positive 5V supply voltage, and the coarse HK sampled magnetic field data of the OB sensor) are presented as well as magnetic field science data of the OB and IB sensor in the activated modes. Magnetic field data are plotted in s/c coordinates and ECLIPJ2000 coordinates if not otherwise stated. They are calibrated according to the results of the ground calibration and the results of the inflight temperature model 009 using all flight data until 2016. Sensitivity, Misalignment, and Temperature effects are taken into account. The s/c residual field is not subtracted.

The spectra of the magnetic field data measured by the OB sensor are plotted as well in section 7. This time there is no influence of ROSETTAs reaction wheels (refer to section 8) as the instrument was only operated in normal mode SID2.

The data quality and a comparison between OB and IB sensor will be presented in chapter 4.

Additionally to the RPC–MAG instrument the LANDER Magnetometer ROMAP was switched on from 2005-03-01T01:00:00 until 2005-03-07T23:30:00. A comparison with RPCMAG will be shown in section 11.

The activation of the LANDER was associated with the test of some heaters onboard the LANDER. Unfortunately this caused magnetic disturbances presented in section 9.

The close Earth Swing by was a unique chance to check and improve the calibration of the instrument and to compare the measured field with a theoretical model of the earth. These investigations will be presented in chapter 5.

Also the comparison of our magnetic field data with data measured by different spacecrafts (e.g WIND) can give information about the data quality. A comparison to the WIND data can be found in section 6.

A temperature profile for the whole Earth Swing by is shown in section 10.

2 The Swing by Geometry

This section gives an overview about the trajectory during the Swing by. ROSETTA approached through the tail within 4 days (March 1 until March 4), had its closest approach on March 4 at 22:09, and left through magnetopause and bow shock. It performed the closest Swing-By manoeuver ever flown by an interplanetary spacecraft. The minimum distance to earth was 1961 km.

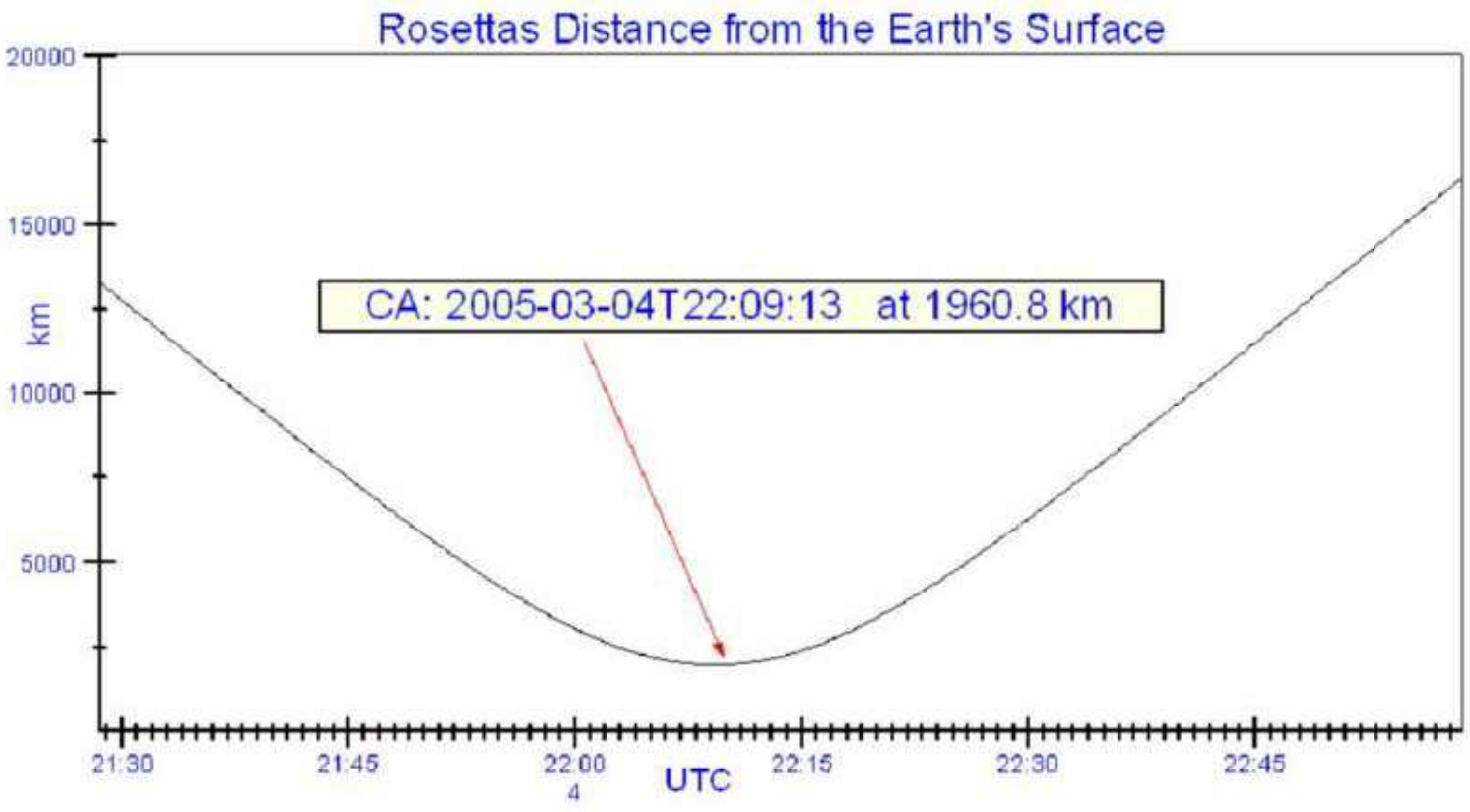

Figure 1: ROSETTA'S Distance to the EARTH'S Surface

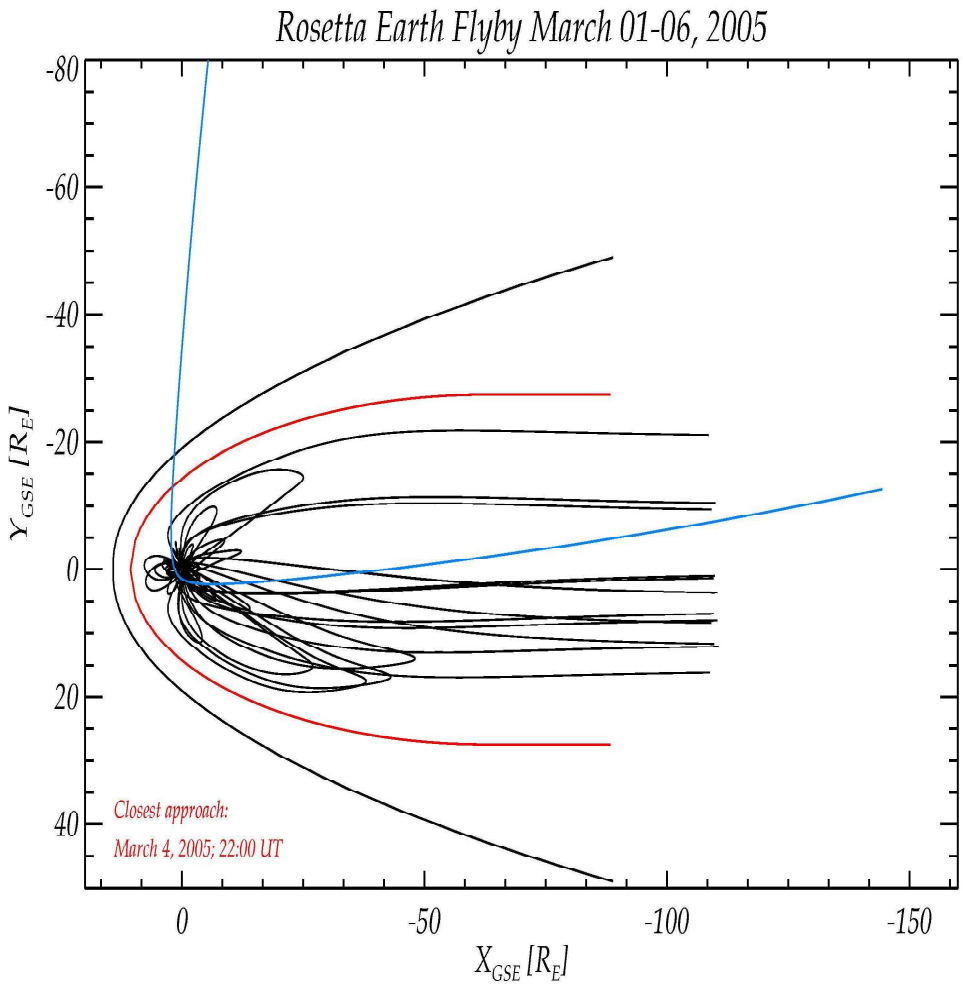

Figure 2: ROSETTA'S Swing by Trajectory in GSE coordinates: XY–Plane

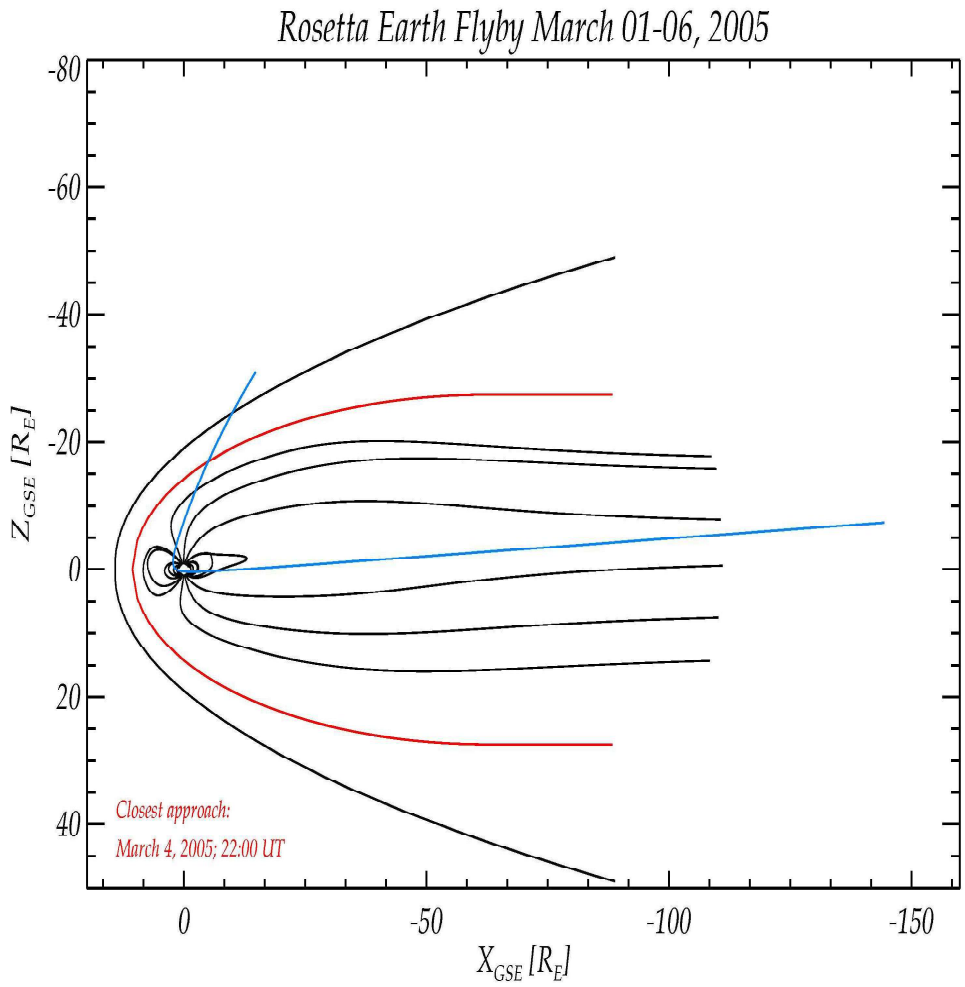

Figure 3: ROSETTA'S Swing by Trajectory in GSE coordinates: XZ–Plane

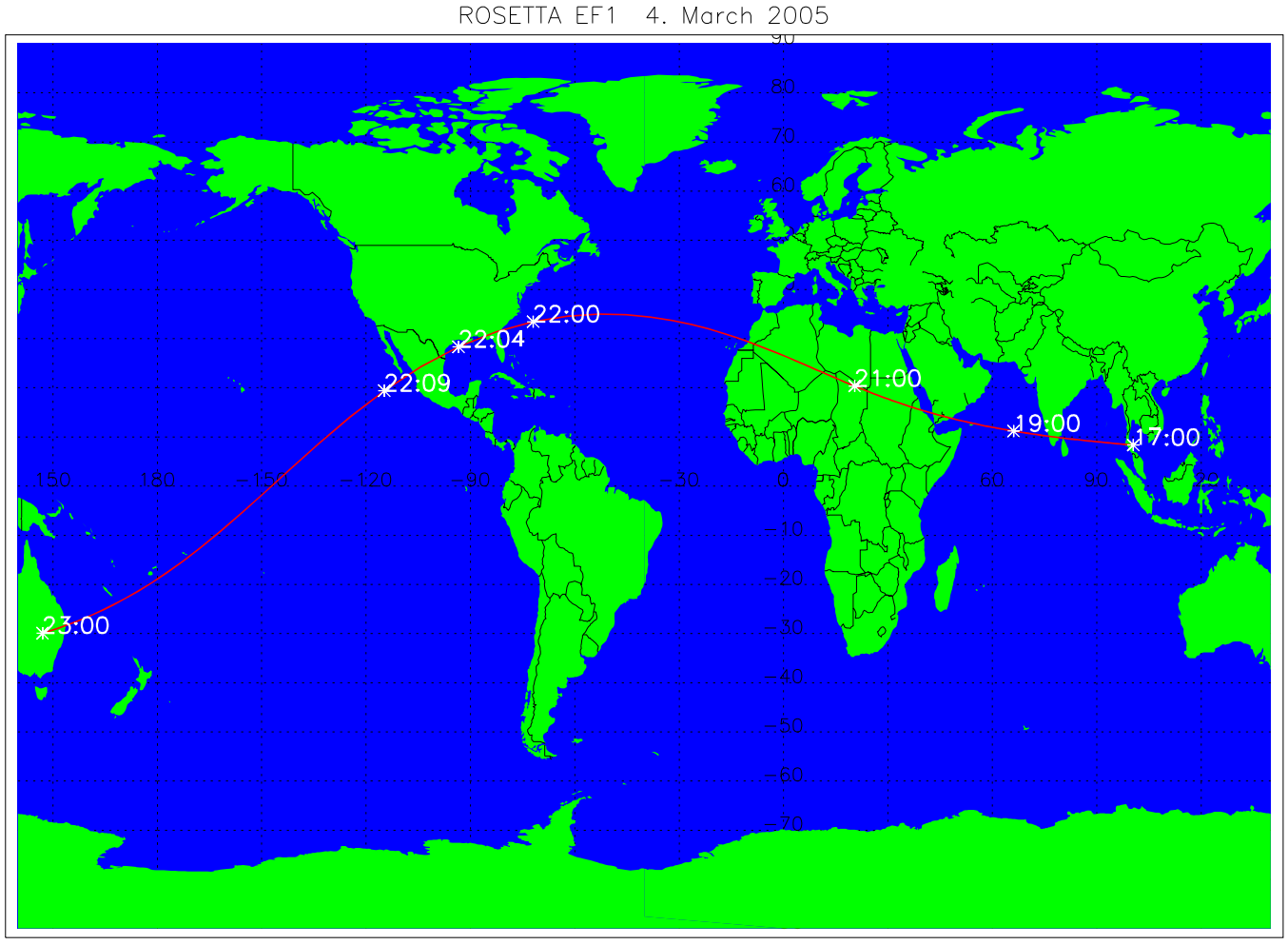

Figure 4: ROSETTA'S Ground Track during the Swing by

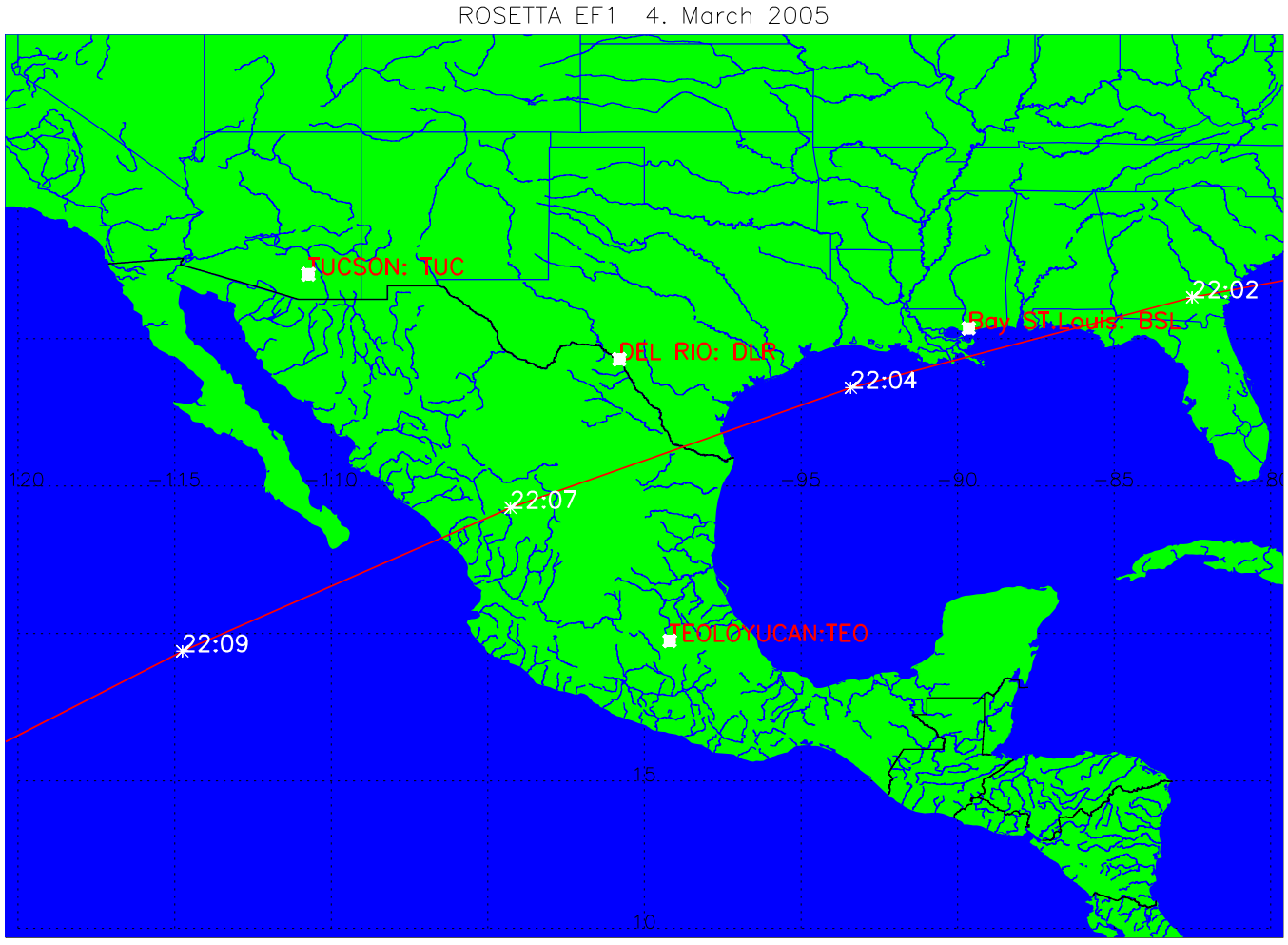

Figure 5: ROSETTA'S Ground Track during the Swing by (Zoomed)

3 Activities and data plots of EAR1

This chapter presents all relevant data /data types measured by RPCMAG day by day:

- Housekeeping data (HK).
- Magnetic field of the OB sensor, sampled with 16 bit in the HK stream.
- Calibrated LEVEL_B data (s/c coordinates) of the IB and OB sensor with the original sampling frequency.
- Calibrated LEVEL_C data (ECLIPJ2000 coordinates) of the IB and OB sensor with the original sampling frequency.

3.1 March 01, 2005:

3.1.1 Actions

MAG was switched on immediately after PIU and set to HK mode at 00:02. The normal mode SID 2 was set at 00:14. All commands passed smoothly and the instrument followed in the expected way.

3.2 Plots of Calibrated Data

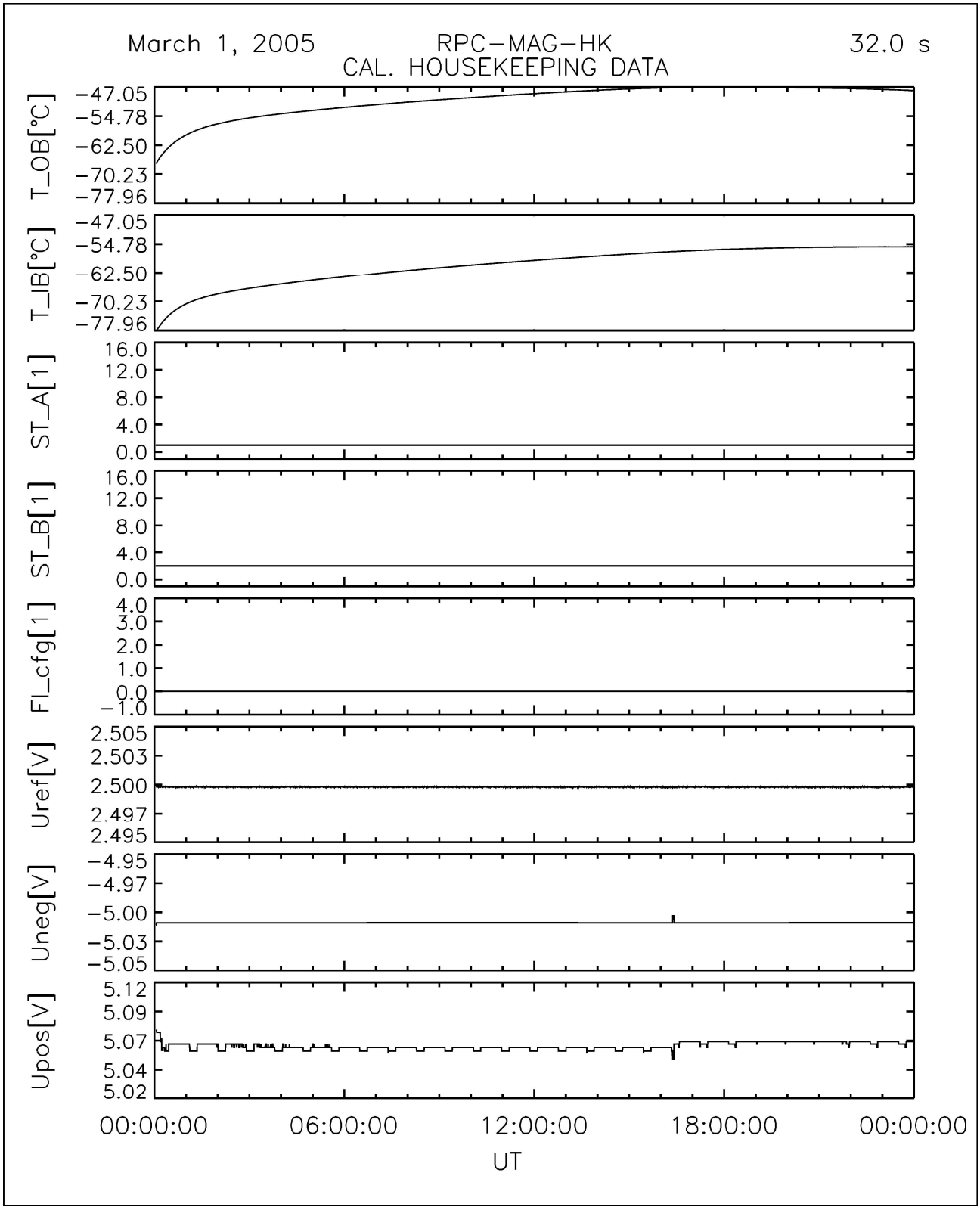

Figure 6: File: RPCMAG050301T0002_CLA_HK_P0000_2400

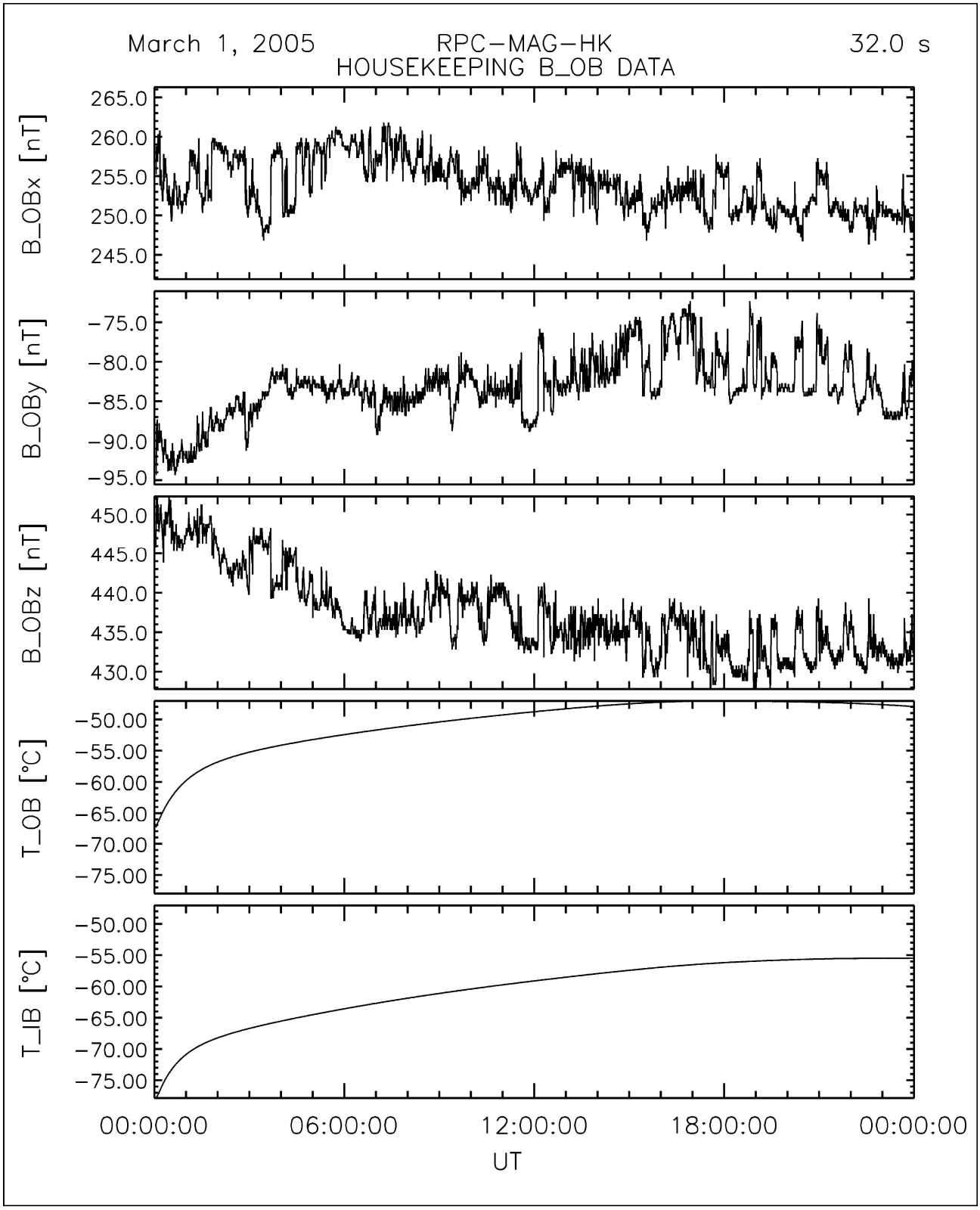

Figure 7: File: RPCMAG050301T0002_CLA_HK_B_P0000_2400

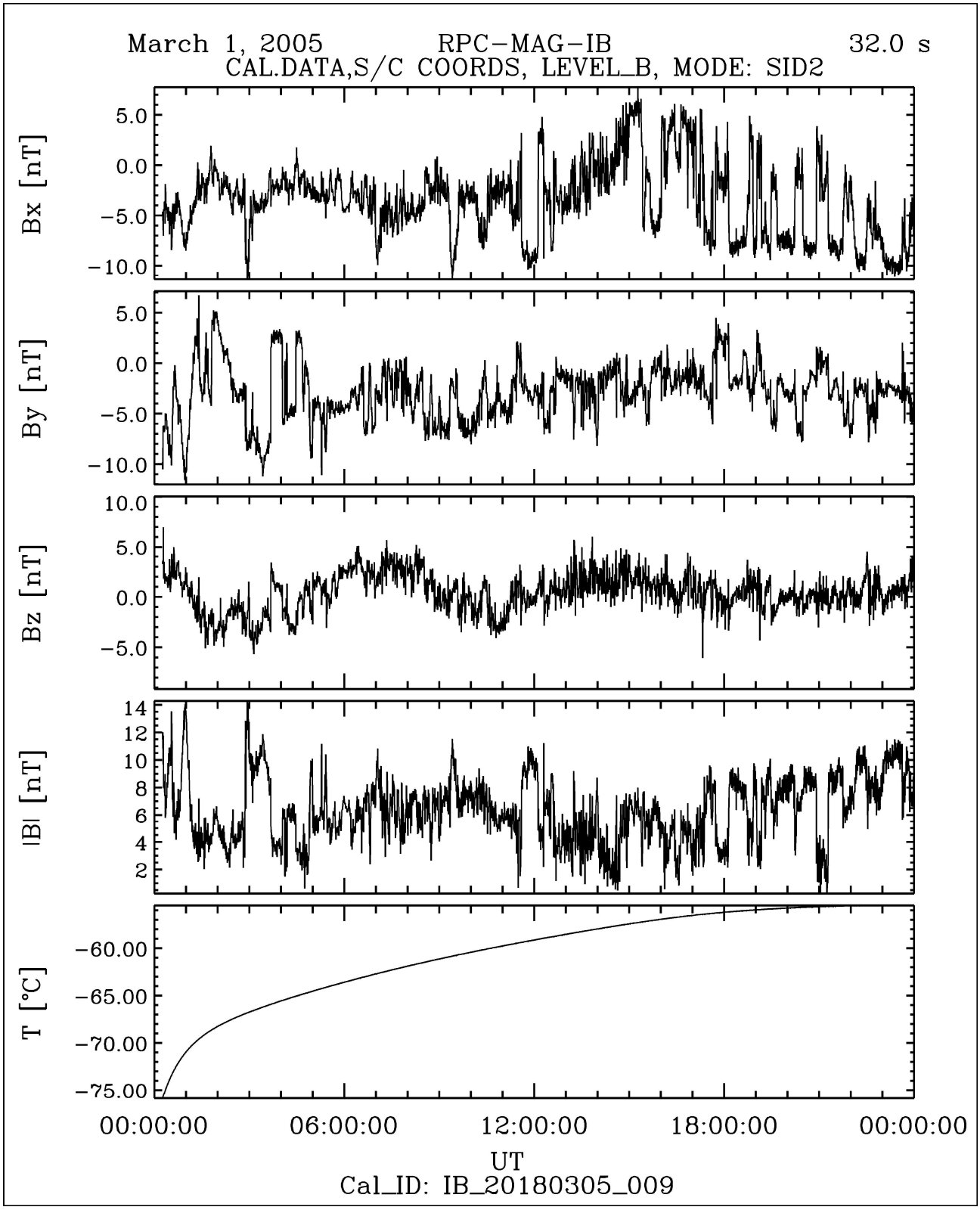

Figure 8: File: RPCMAG050301T0014_CLB_IB_M2_T0000_2400_009

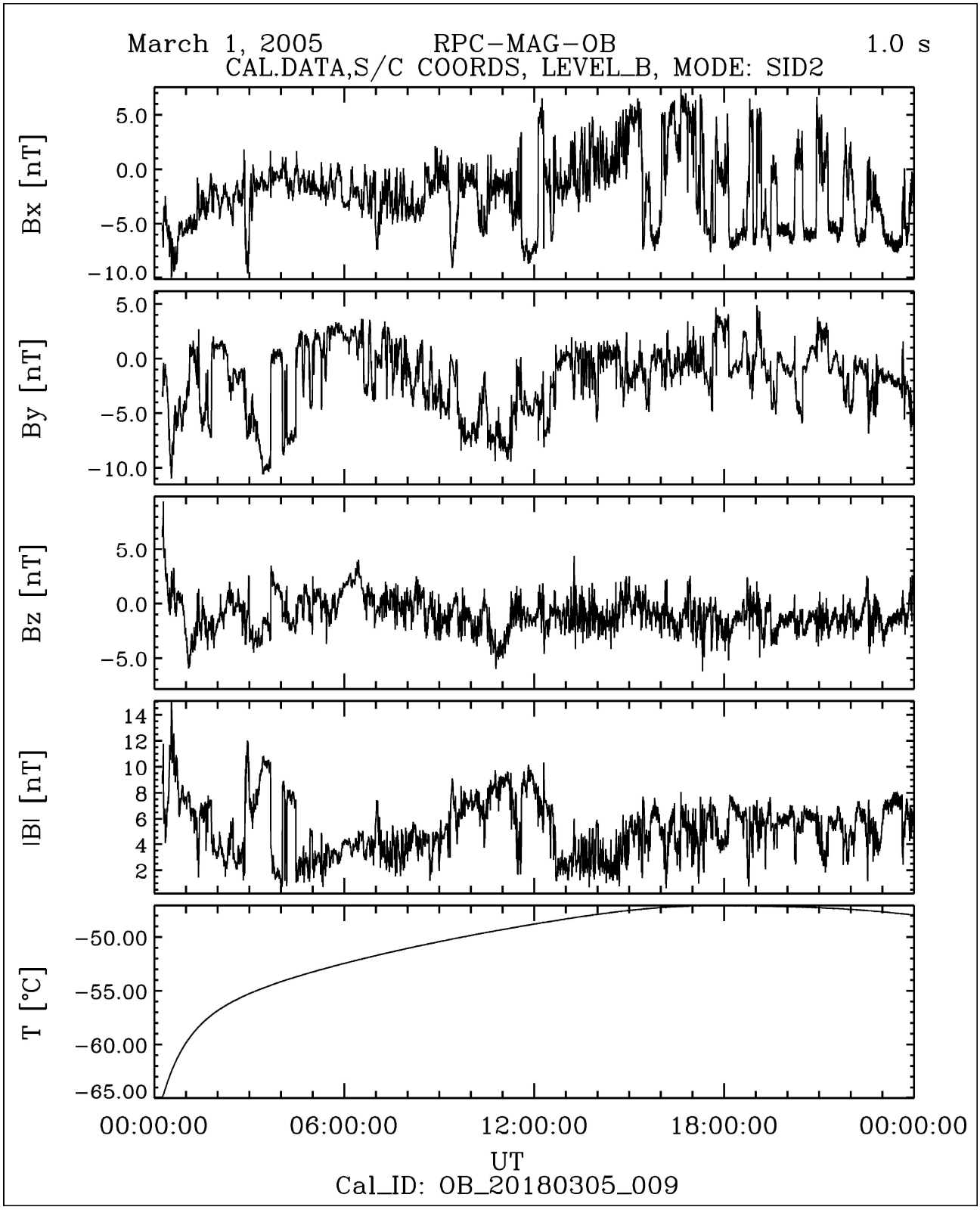

Figure 9: File: RPCMAG050301T0014_CLB_OB_M2_T0000_2400_009

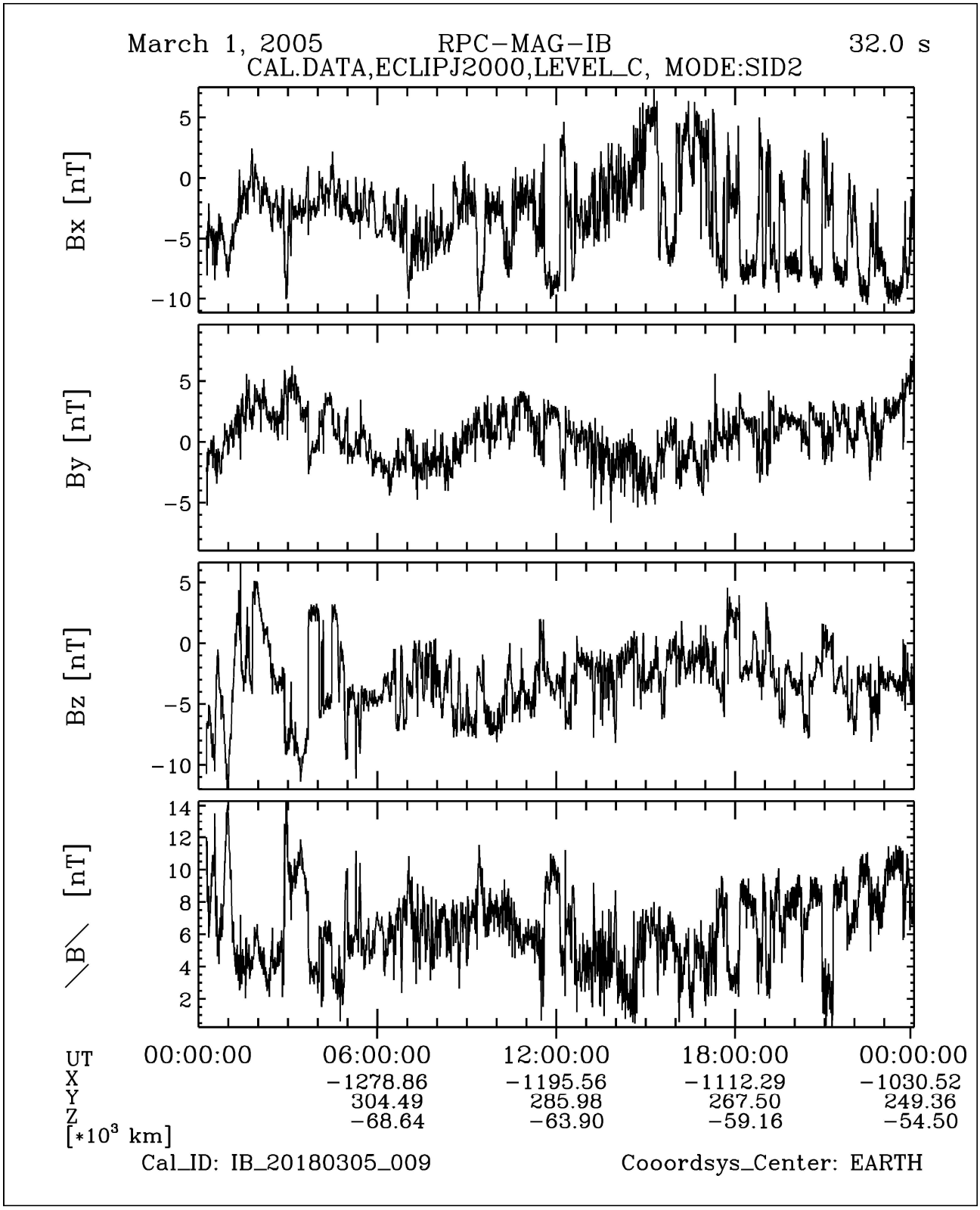

Figure 10: File: RPCMAG050301T0014_CLC_IB_M2_T0000_2400_009

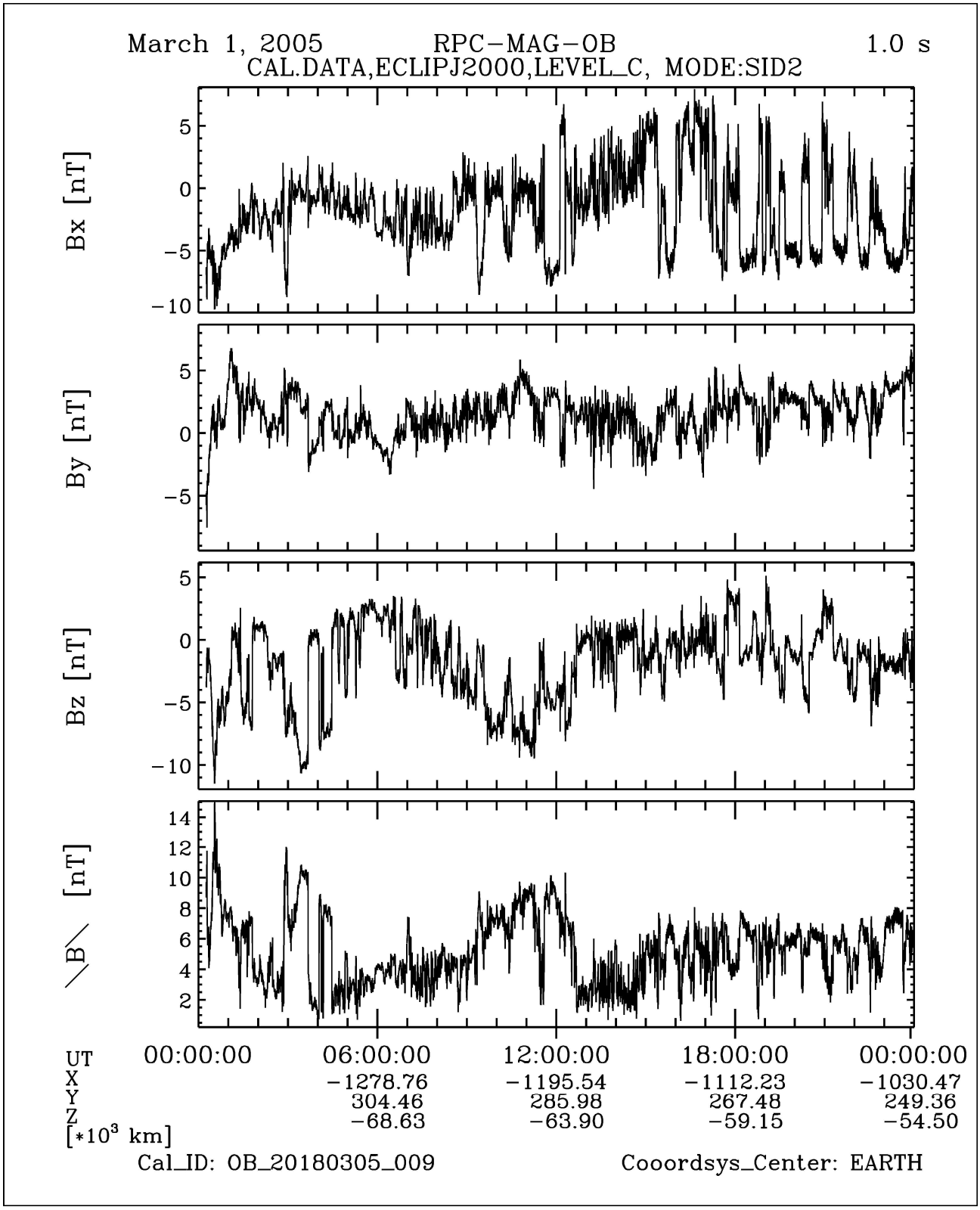

Figure 11: File: RPCMAG050301T0014_CLC_OB_M2_T0000_2400_009

3.3 March 02, 2005:

3.3.1 Actions

MAG stayed in SID 2. No problems occurred.

3.3.2 Plots of Calibrated Data

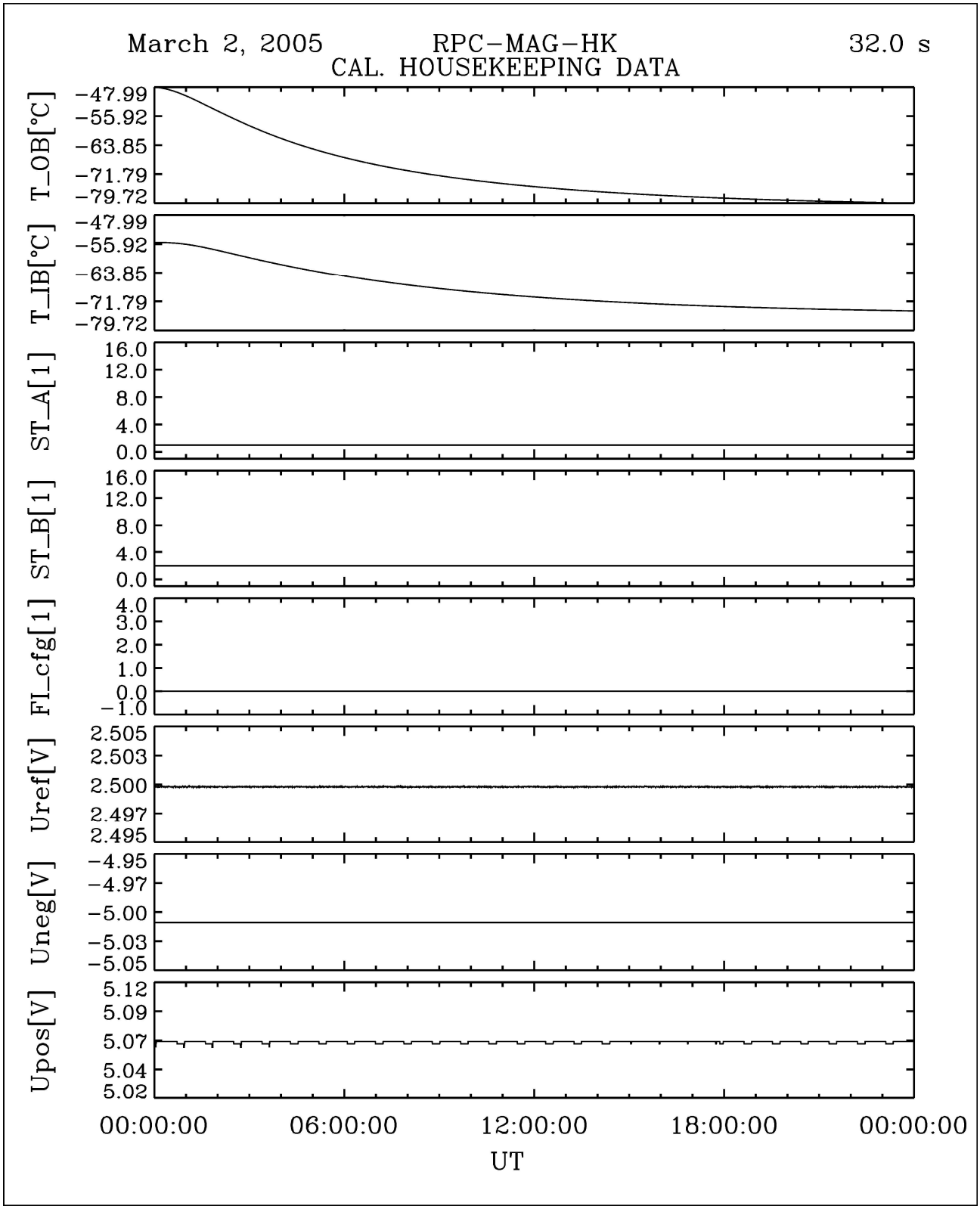

Figure 12: File: RPCMAG050302T0000_CLA_HK_P0000_2400

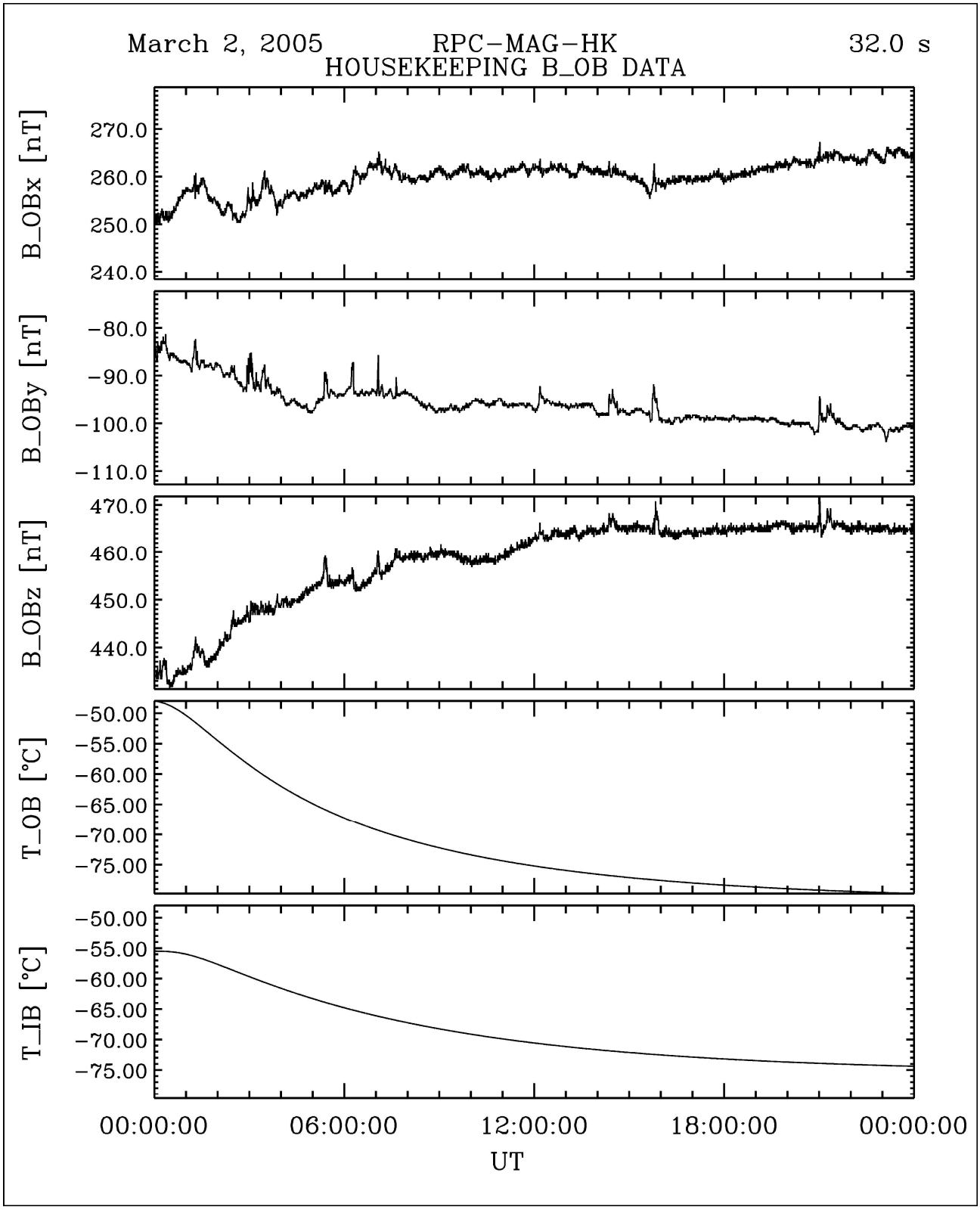

Figure 13: File: RPCMAG050302T0000_CLA_HK_B_P0000_2400

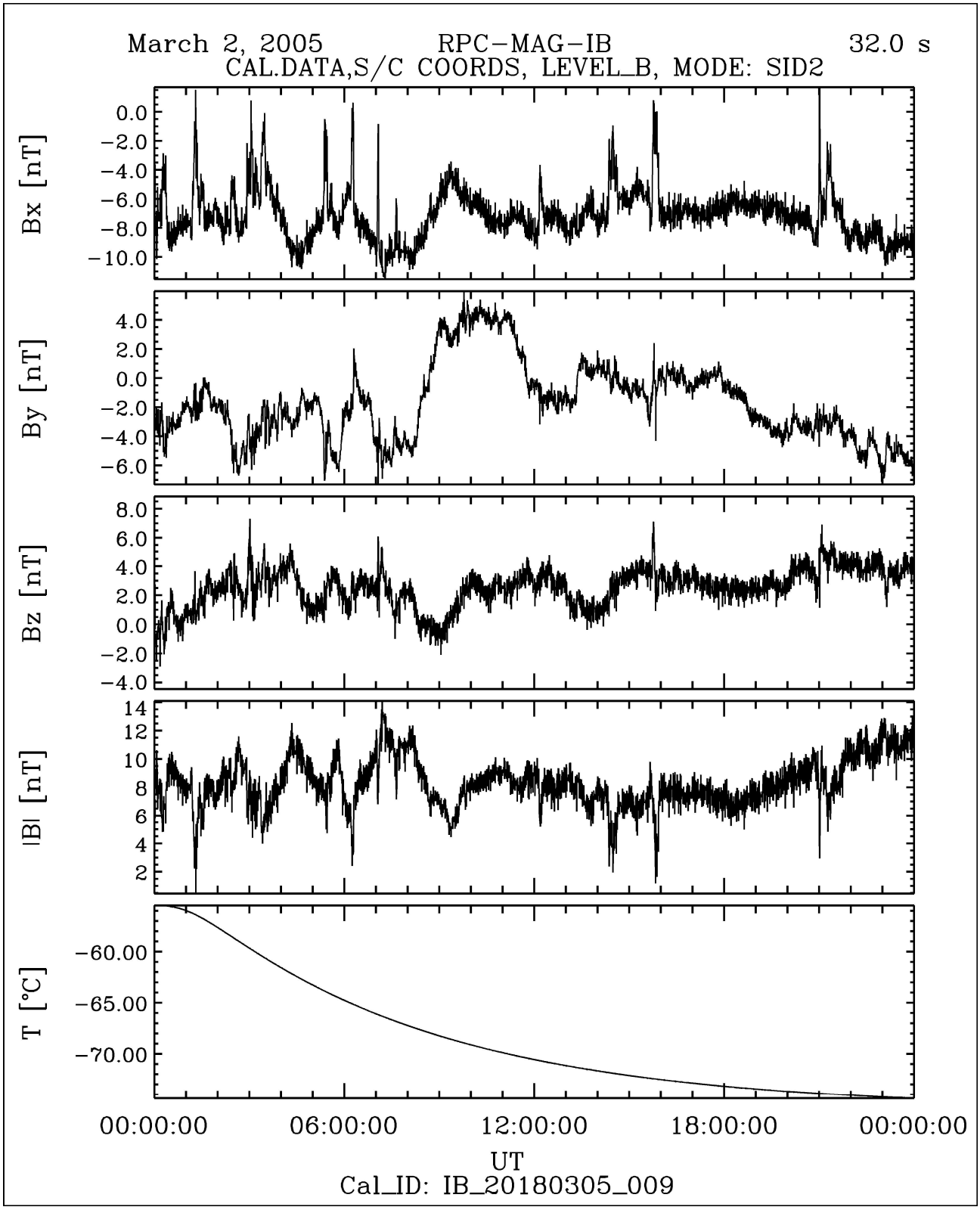

Figure 14: File: RPCMAG050302T0000_CLB_IB_M2_T0000_2400_009

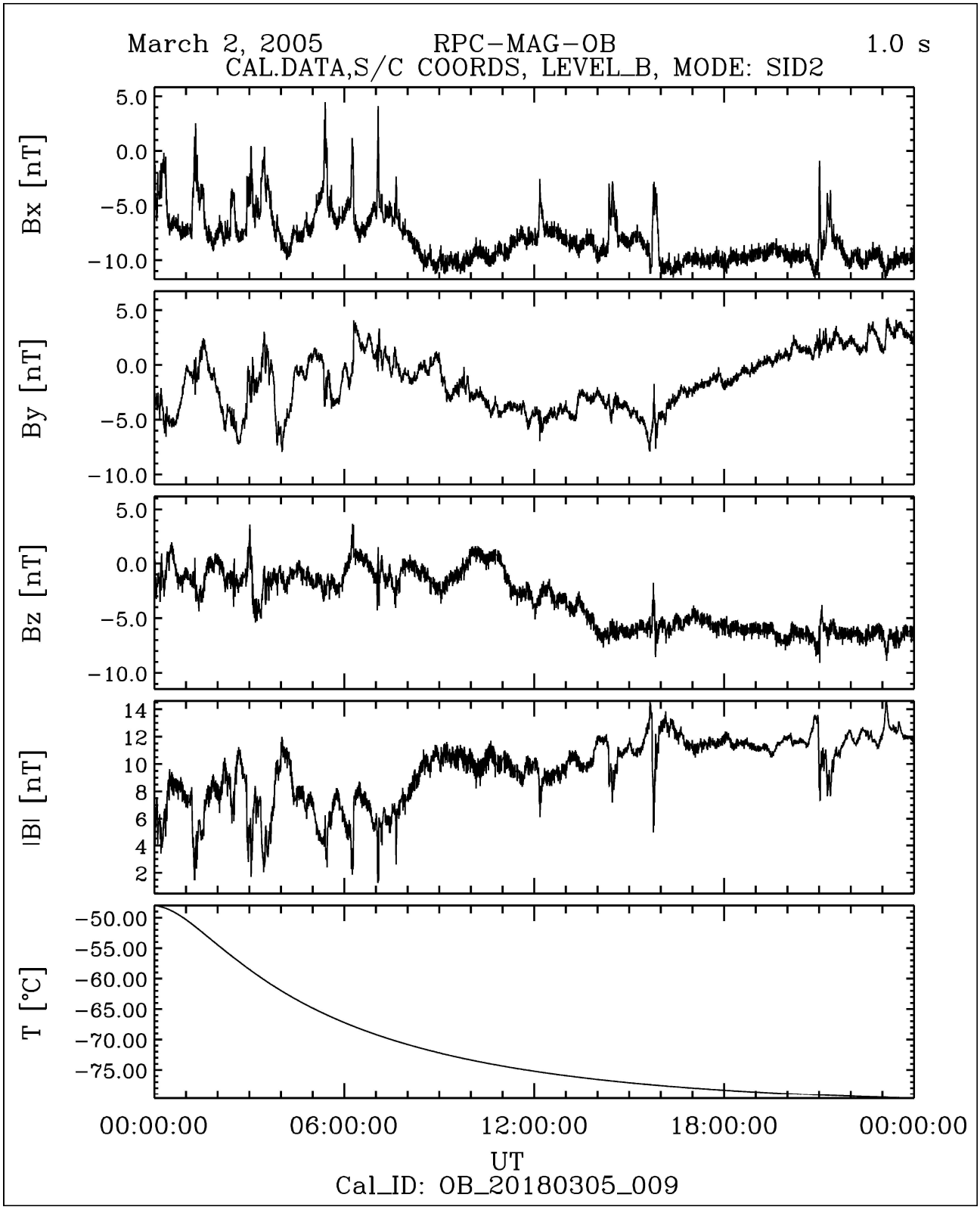

Figure 15: File: RPCMAG050302T0000_CLB_OB_M2_T0000_2400_009

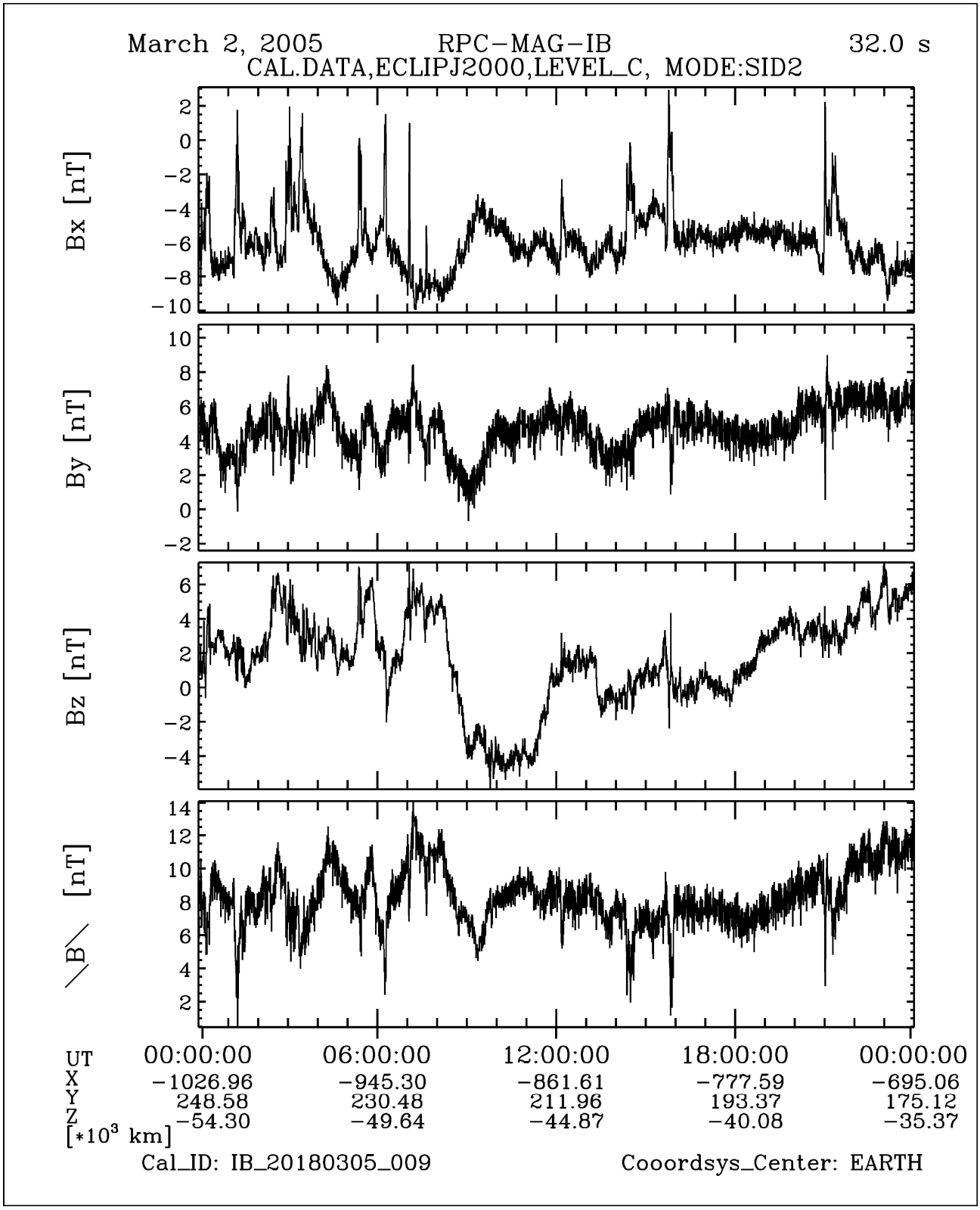

Figure 16: File: RPCMAG050302T0000_CLC_IB_M2_T0000_2400_009

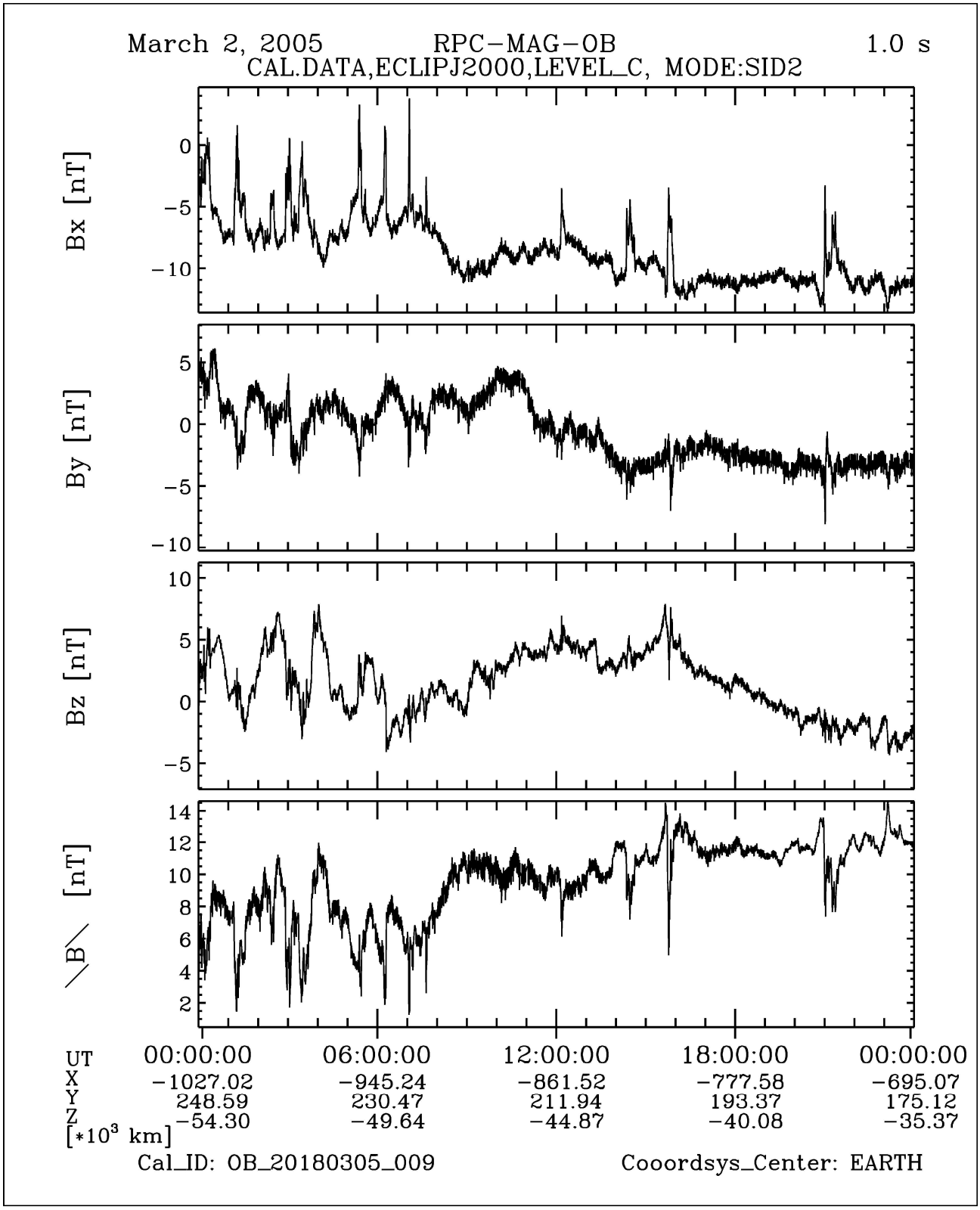

Figure 17: File: RPCMAG050302T0000_CLC_OB_M2_T0000_2400_009

3.4 March 03, 2005:

3.4.1 Actions

MAG stayed in SID 2. No problems occurred. Since today orbit data are available in Earth-centered coordinates.

3.4.2 Plots of Calibrated Data

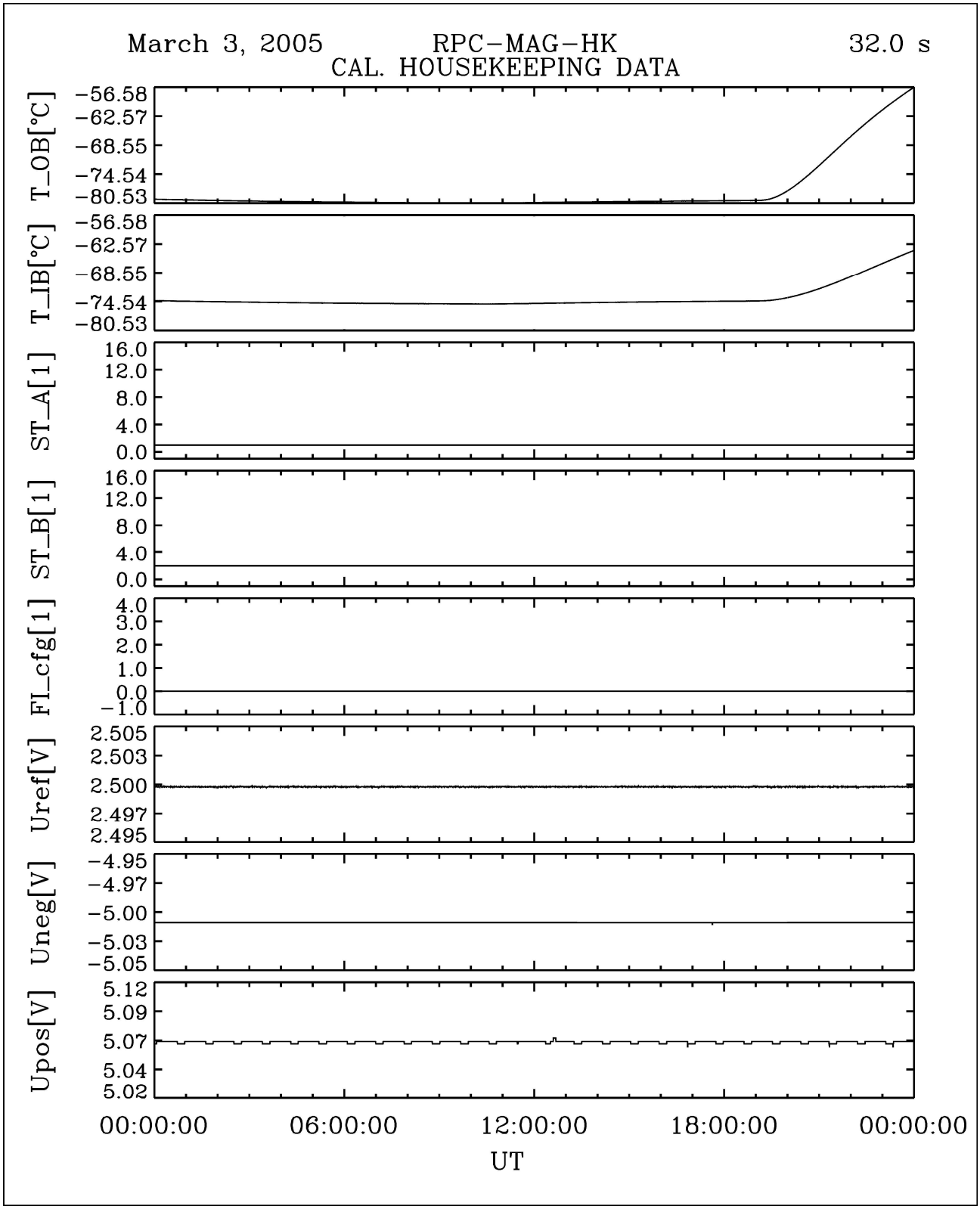

Figure 18: File: RPCMAG050303T0000_CLA_HK_P0000_2400

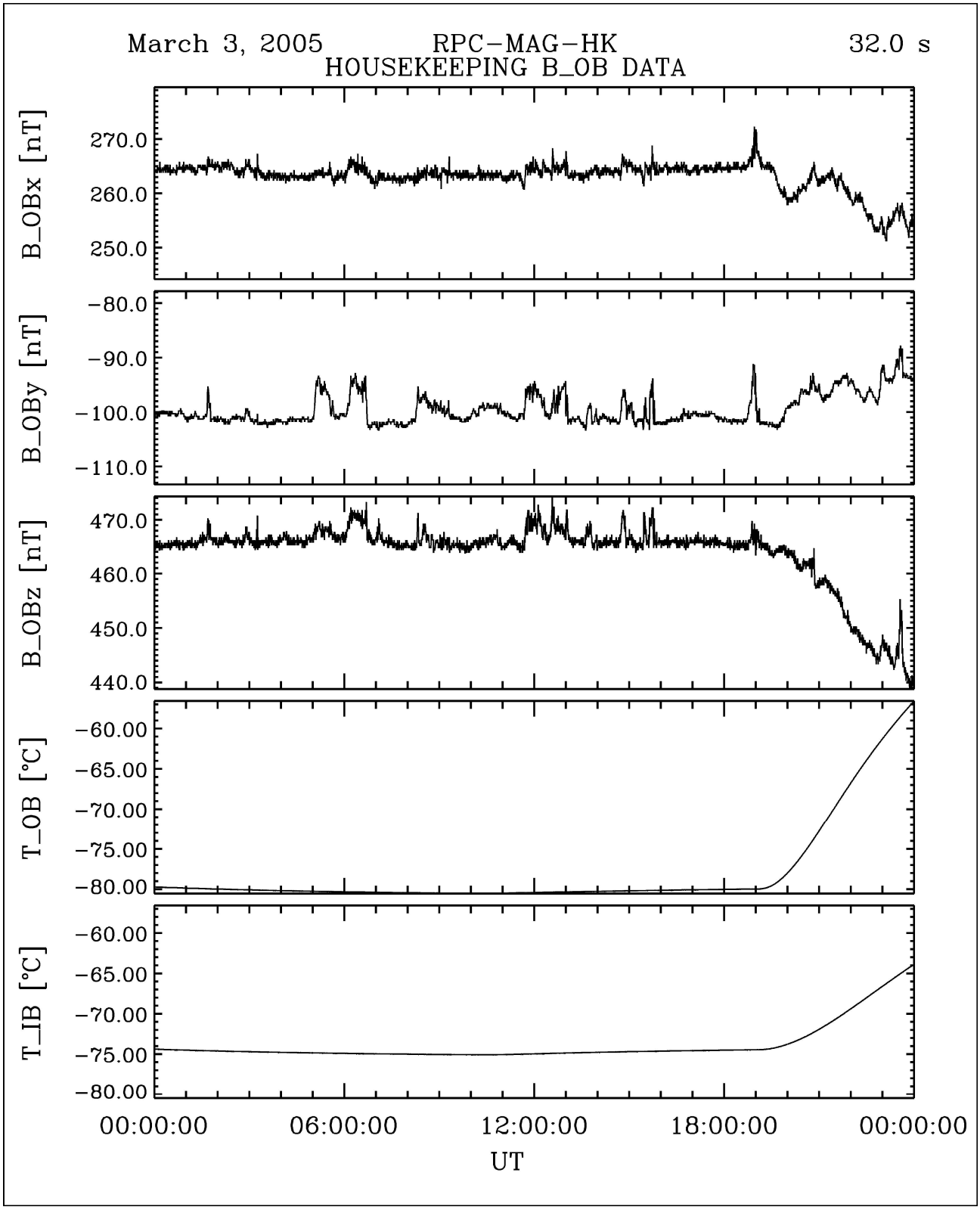

Figure 19: File: RPCMAG050303T0000_CLA_HK_B_P0000_2400

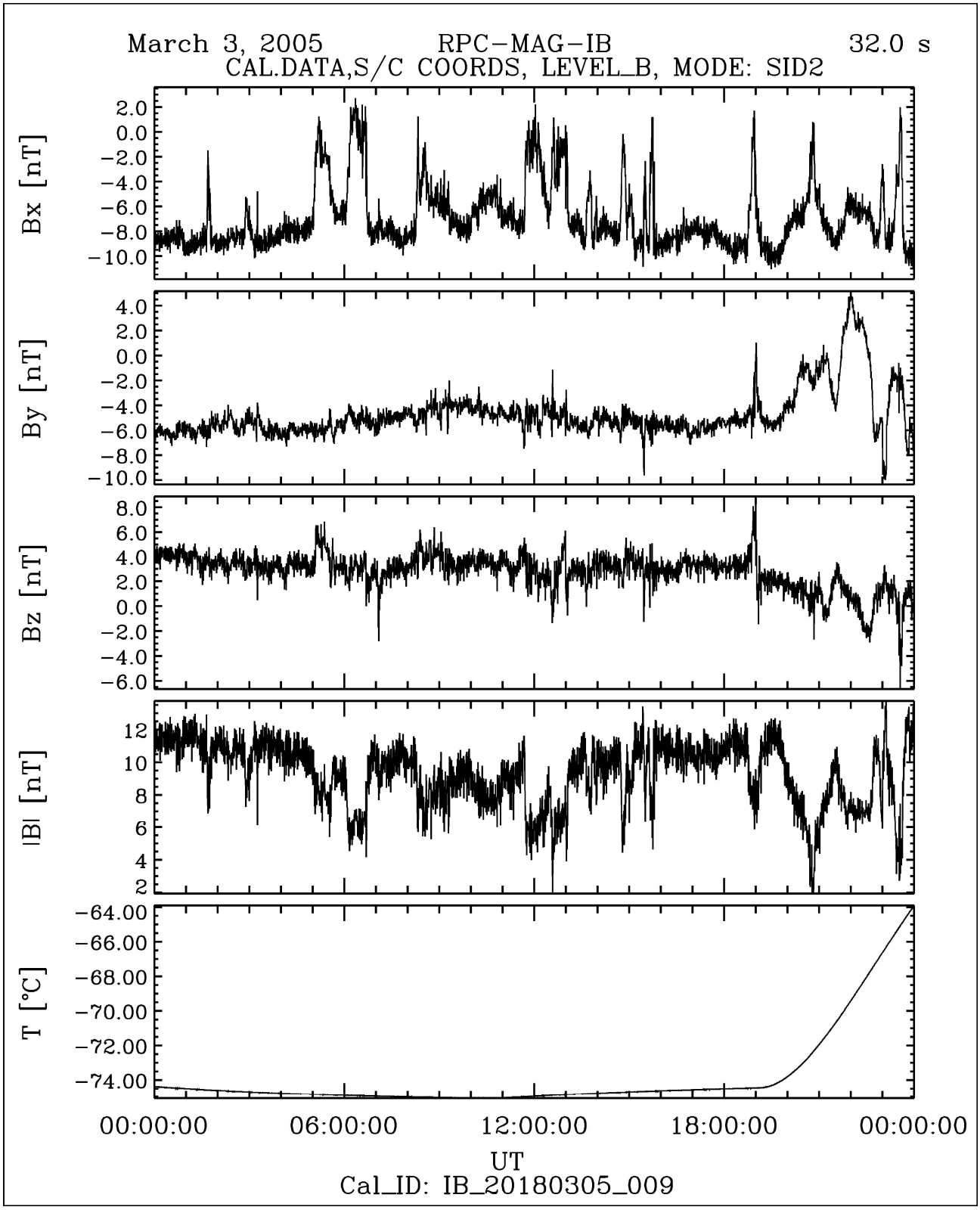

Figure 20: File: RPCMAG050303T0000_CLB_IB_M2_T0000_2400_009

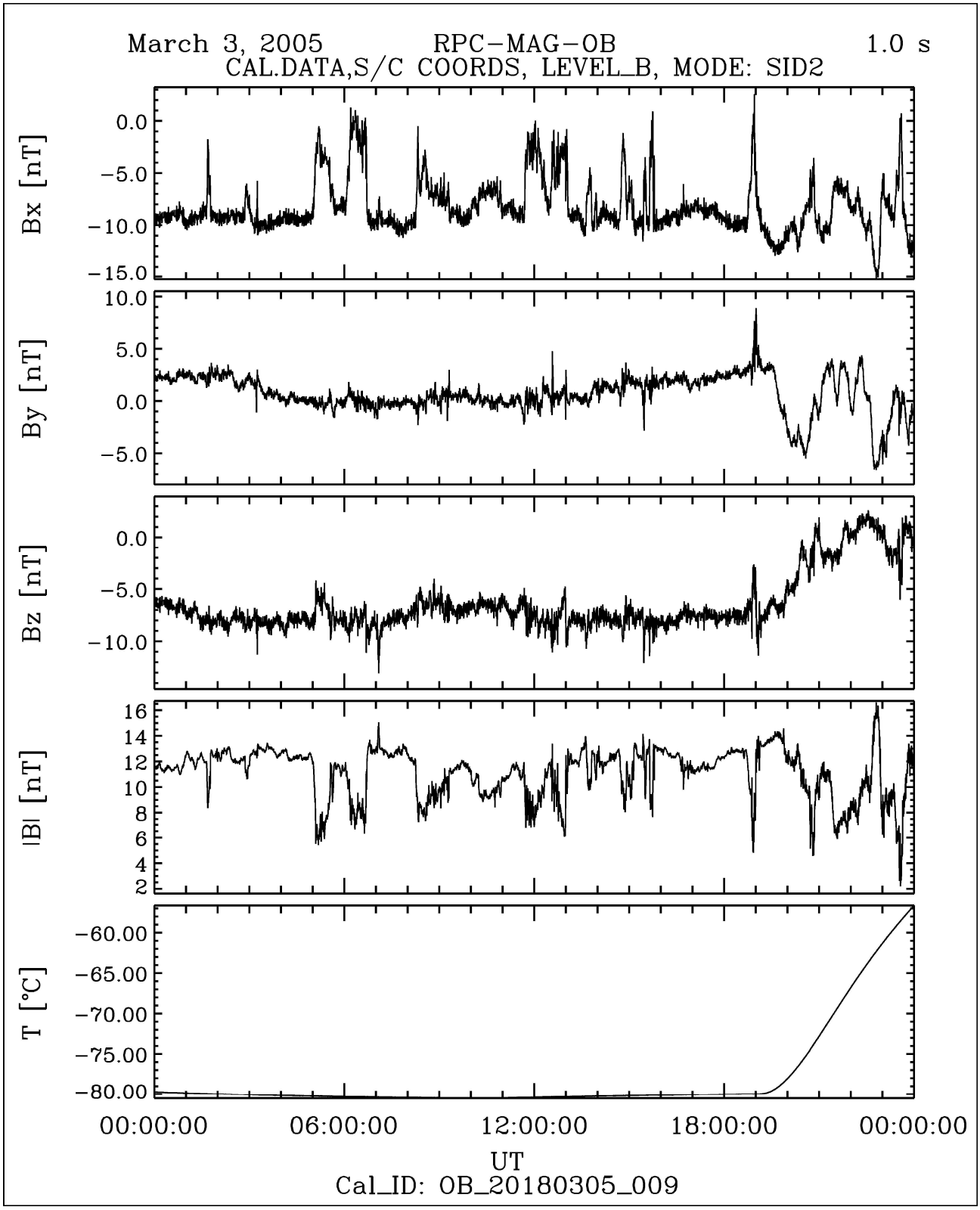

Figure 21: File: RPCMAG050303T0000_CLB_OB_M2_T0000_2400_009

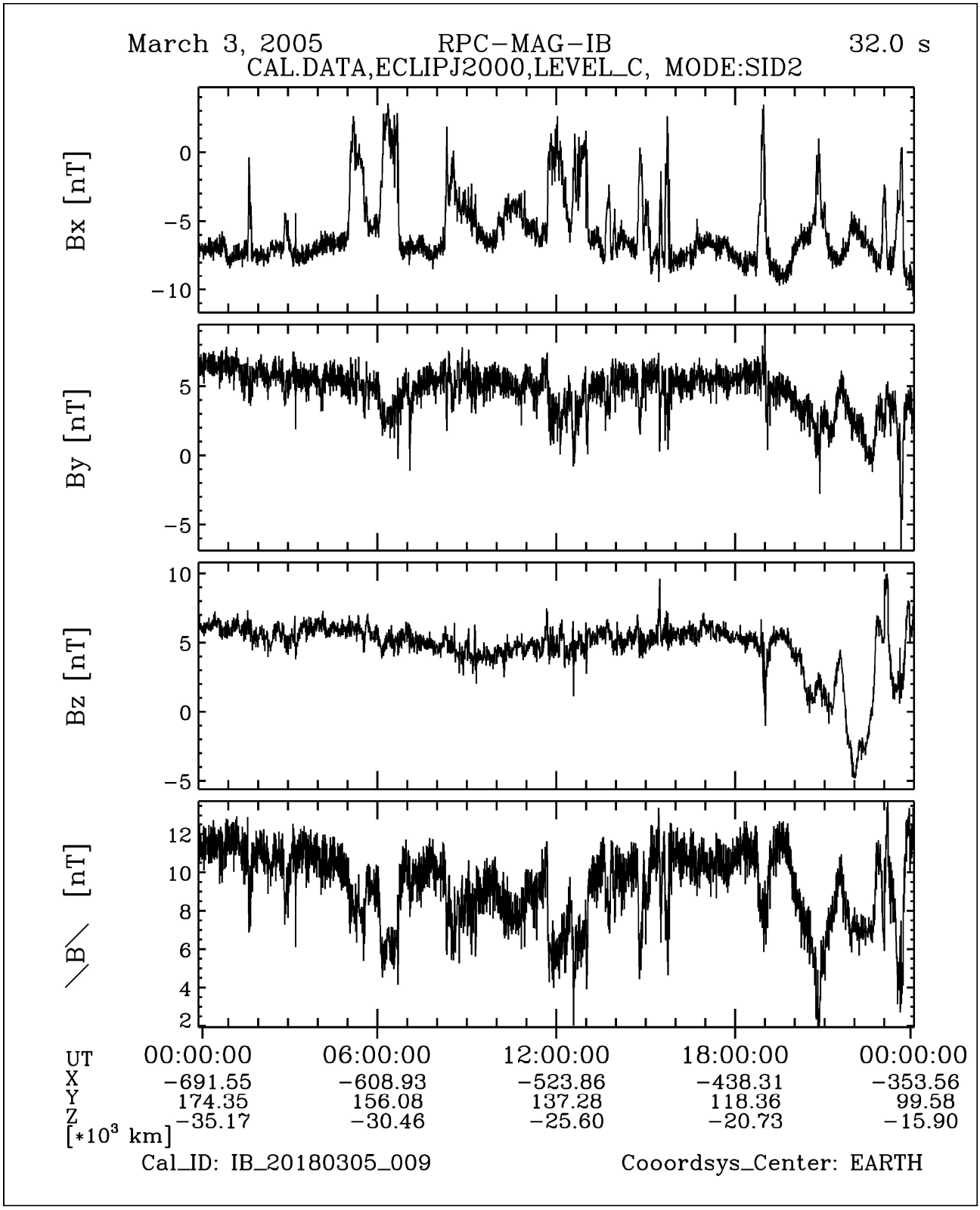

Figure 22: File: RPCMAG050303T0000_CLC_IB_M2_T0000_2400_009

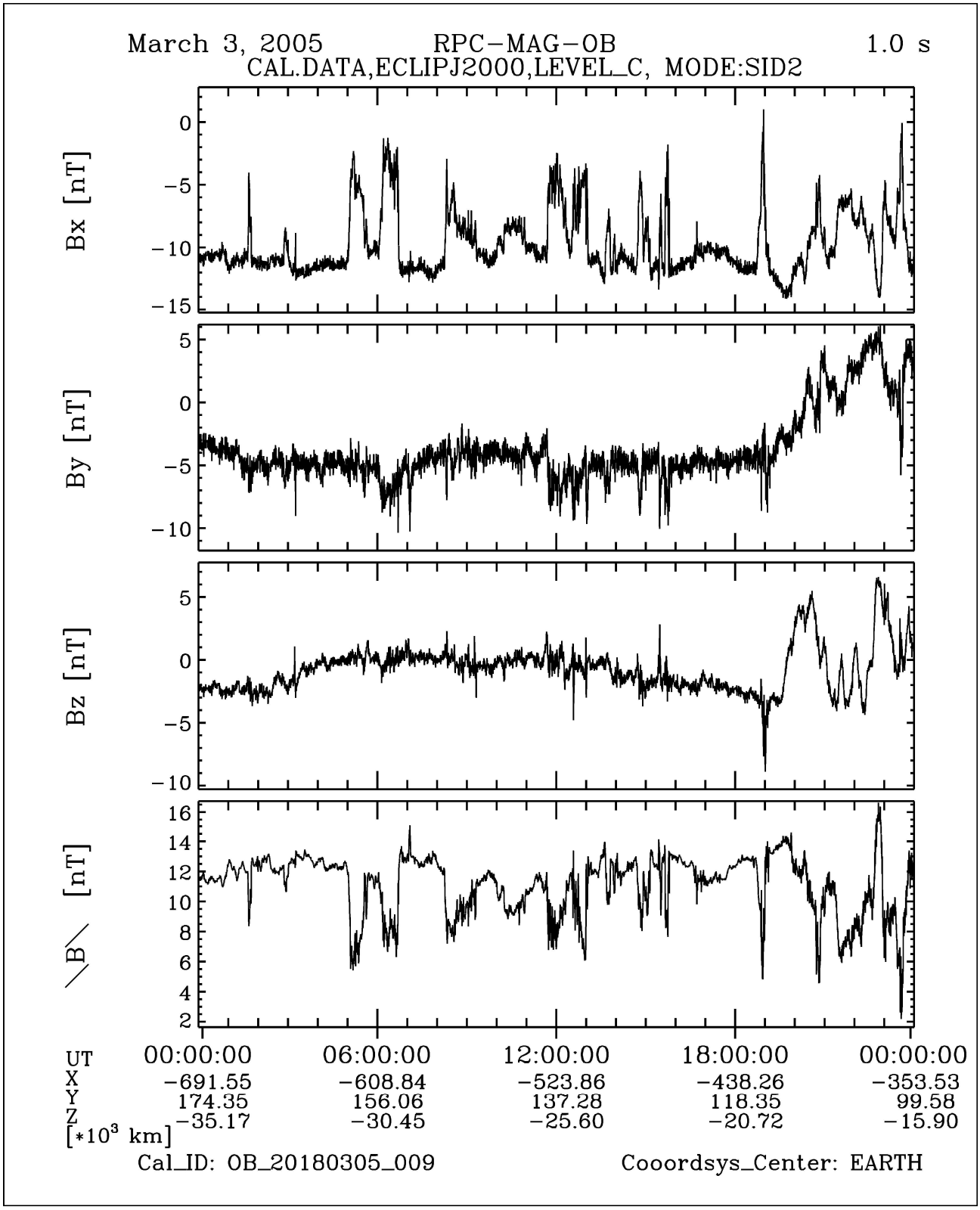

Figure 23: File: RPCMAG050303T0000_CLC_OB_M2_T0000_2400_009

3.5 March 04, 2005:

3.5.1 Actions

MAG stayed in SID 2. No problems occurred. The closest approach (CA) happened at 22:09.

3.5.2 Plots of Calibrated Data

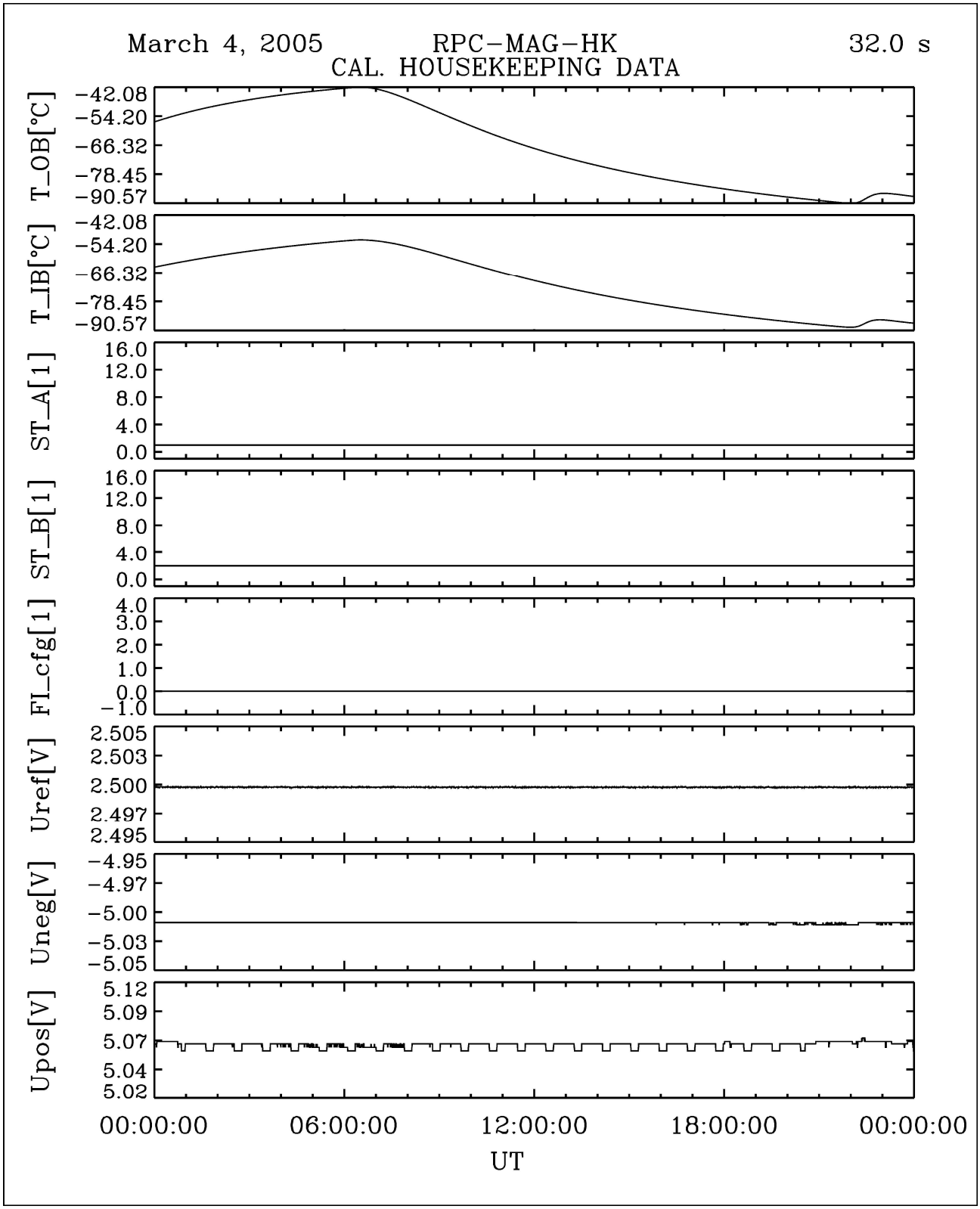

Figure 24: File: RPCMAG050304T0000_CLA_HK_P0000_2400

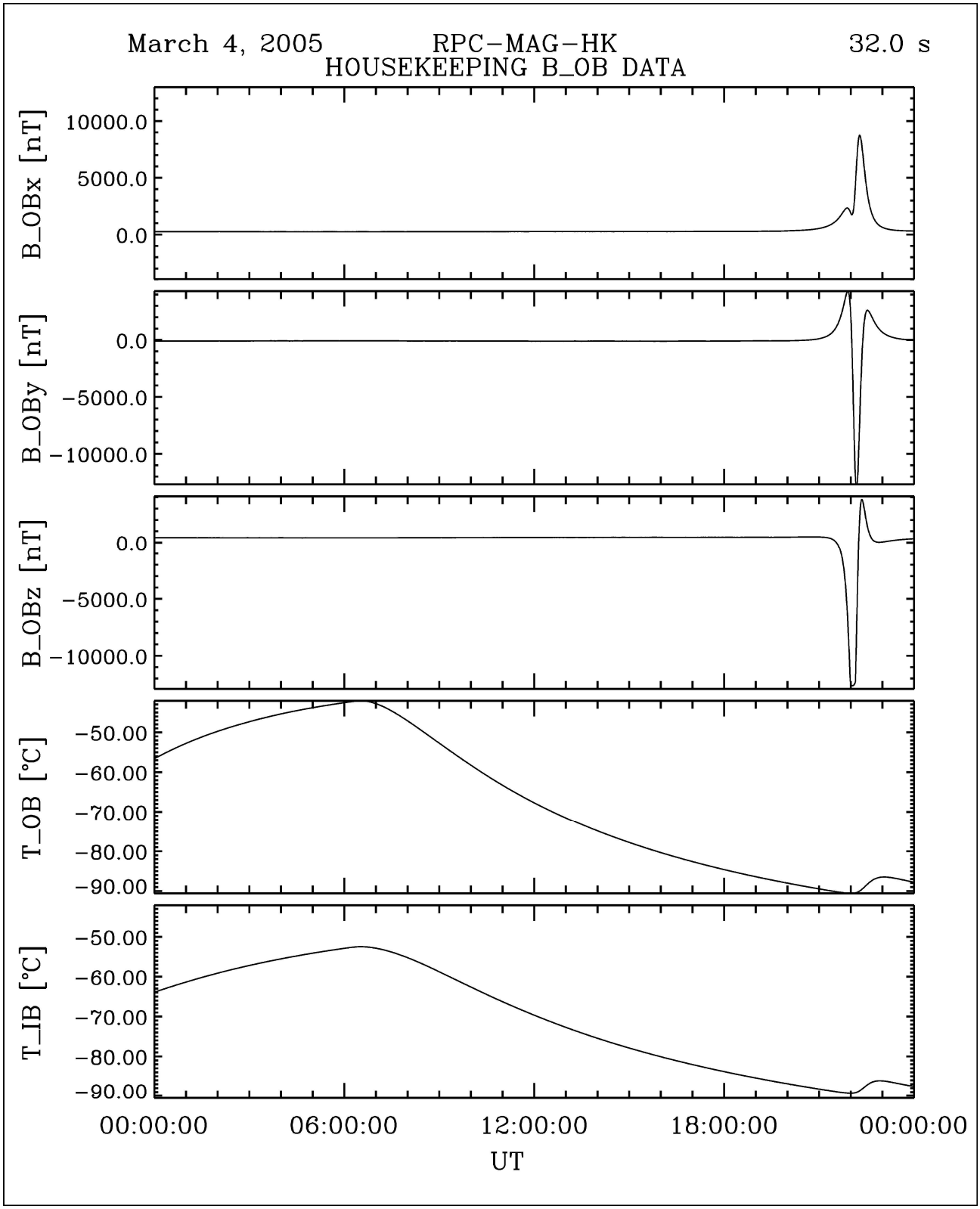

Figure 25: File: RPCMAG050304T0000_CLA_HK_B_P0000_2400

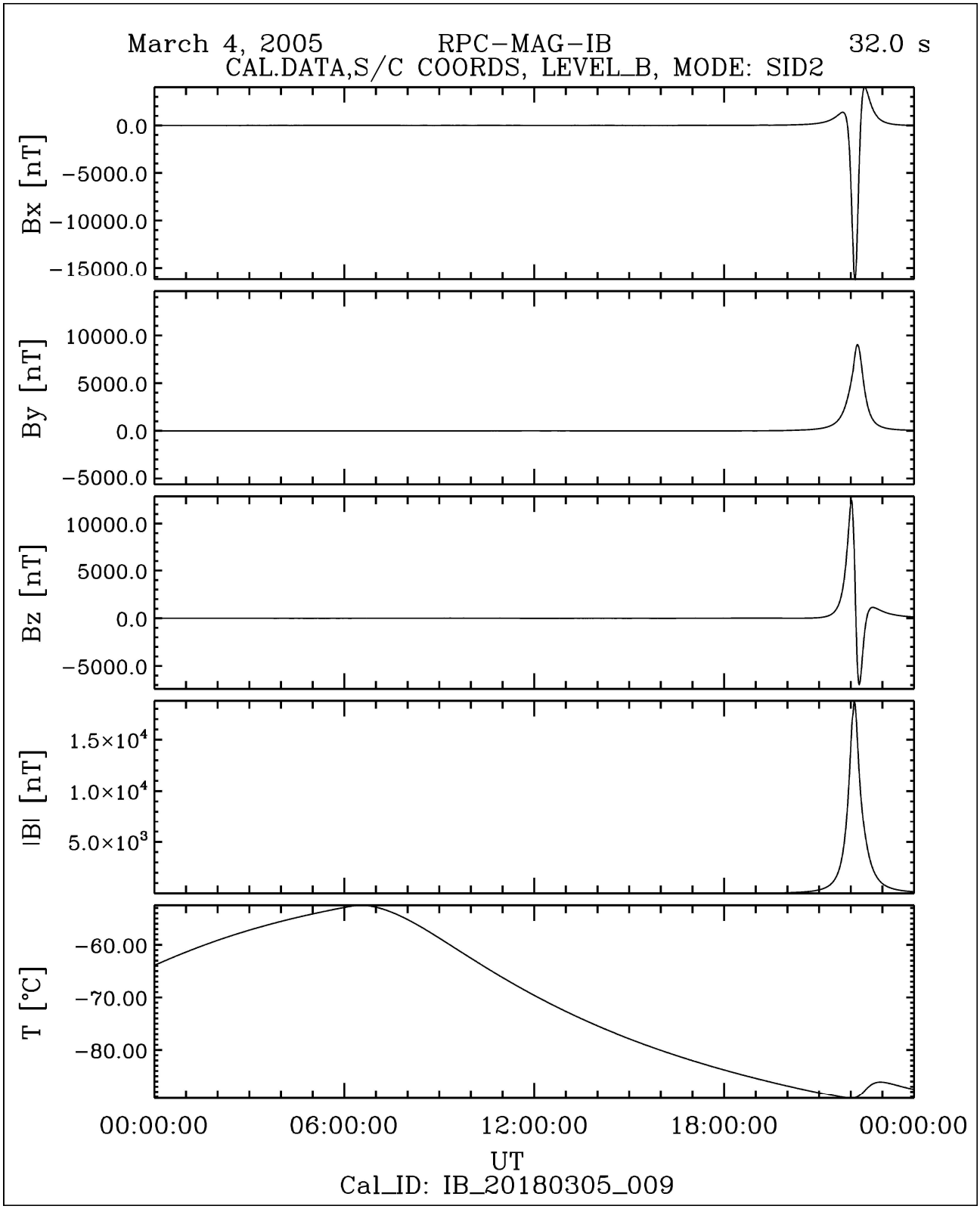

Figure 26: File: RPCMAG050304T0000_CLB_IB_M2_T0000_2400_009

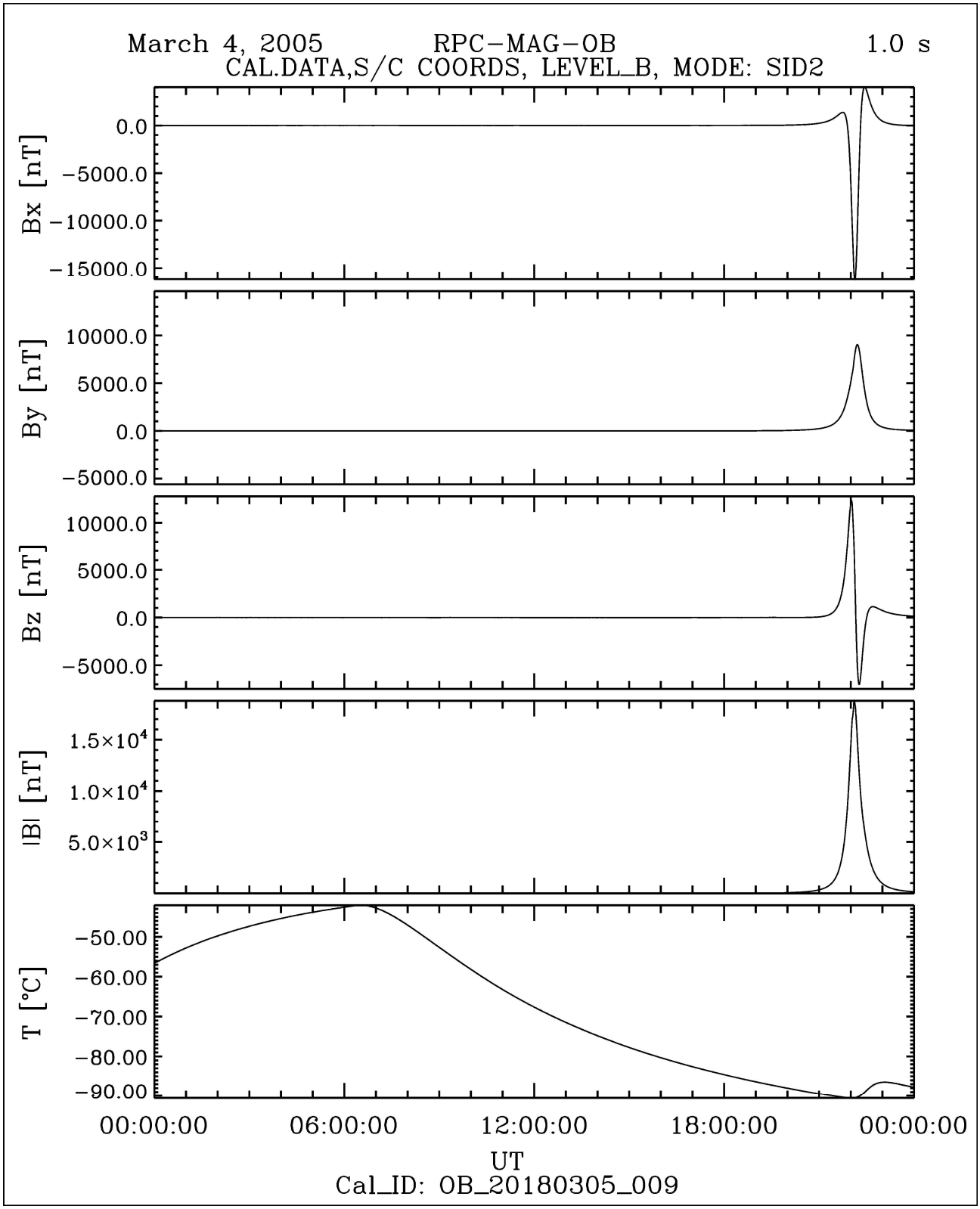

Figure 27: File: RPCMAG050304T0000_CLB_OB_M2_T0000_2400_009

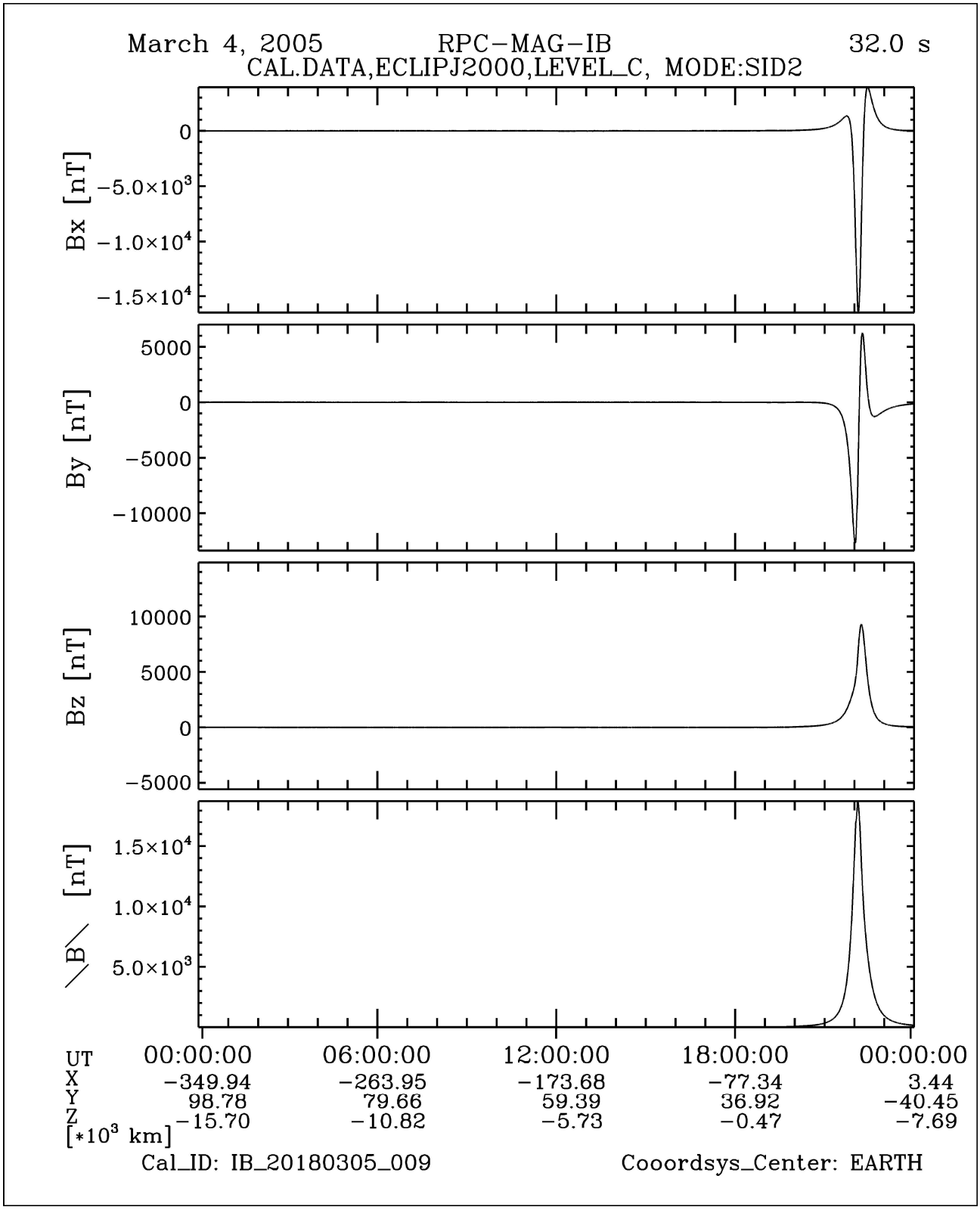

Figure 28: File: RPCMAG050304T0000_CLC_IB_M2_T0000_2400_009

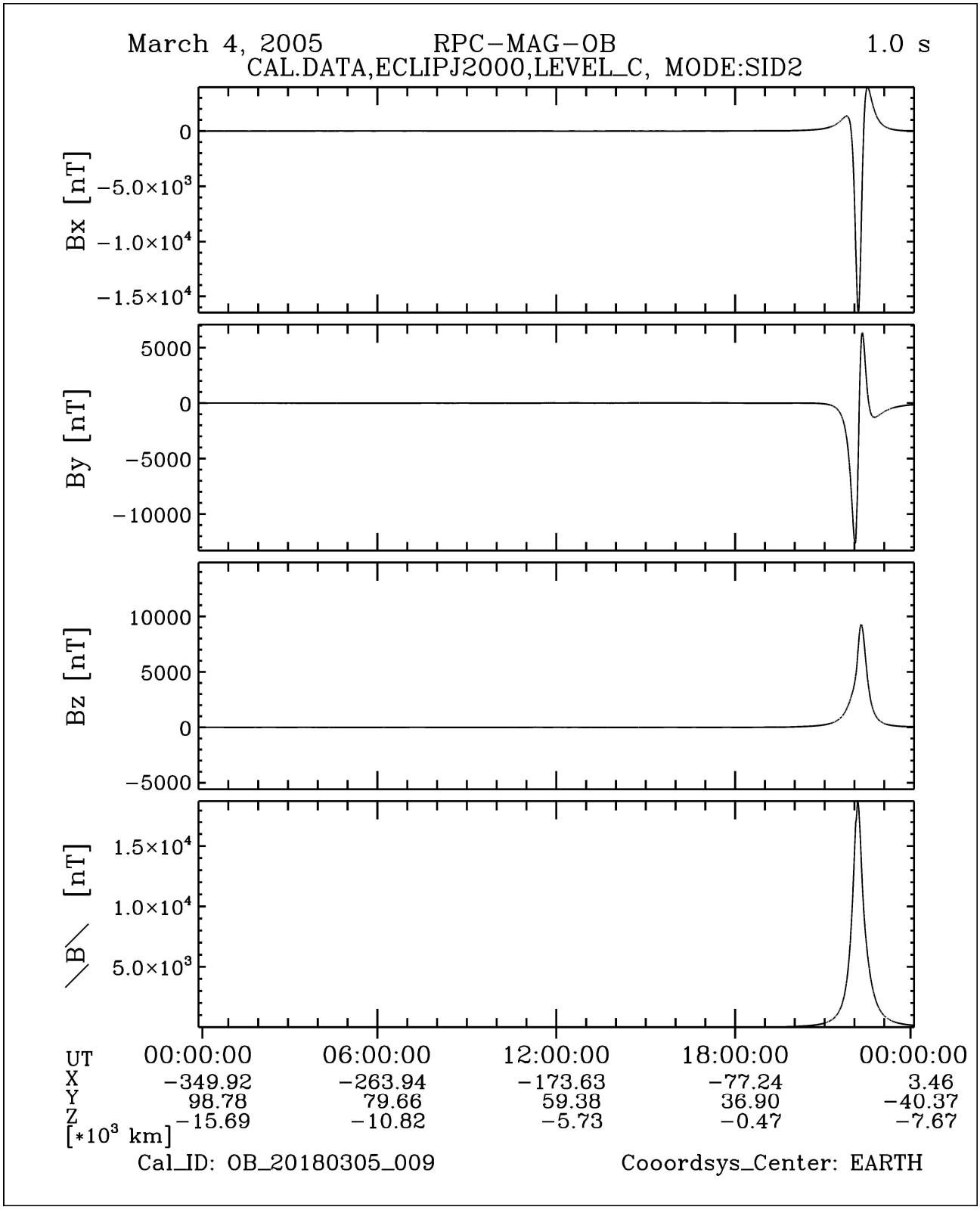

Figure 29: File: RPCMAG050304T0000_CLC_OB_M2_T0000_2400_009

3.6 March 05, 2005:

3.6.1 Actions

MAG stayed nominally in SID 2. At 00:03:25 16 bad vectors occurred on the OB data. The IB data remained in good condition. Besides these minor events no problems arose.

3.6.2 Plots of Calibrated Data

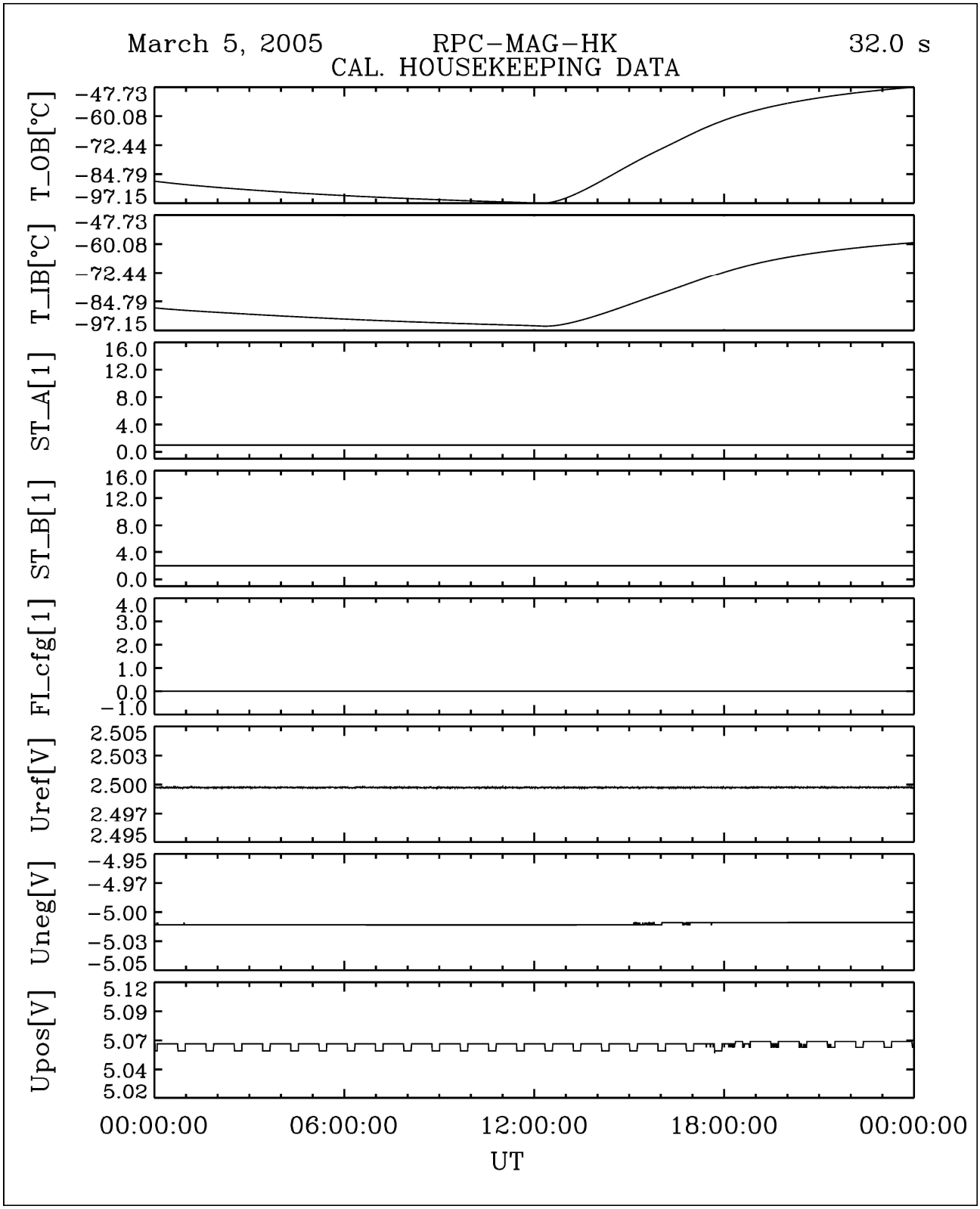

Figure 30: File: RPCMAG050305T0000_CLA_HK_P0000_2400

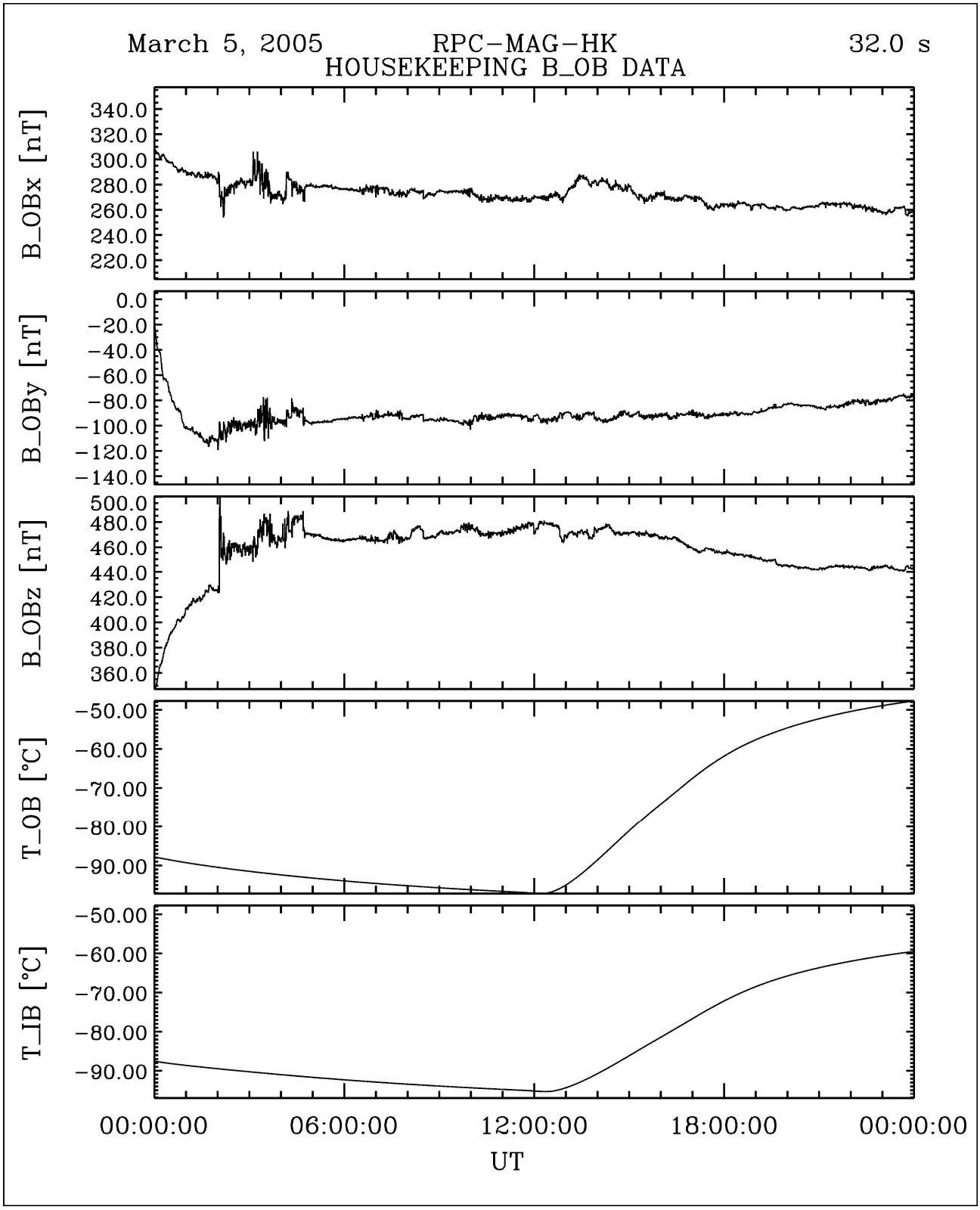

Figure 31: File: RPCMAG050305T0000_CLA_HK_B_P0000_2400

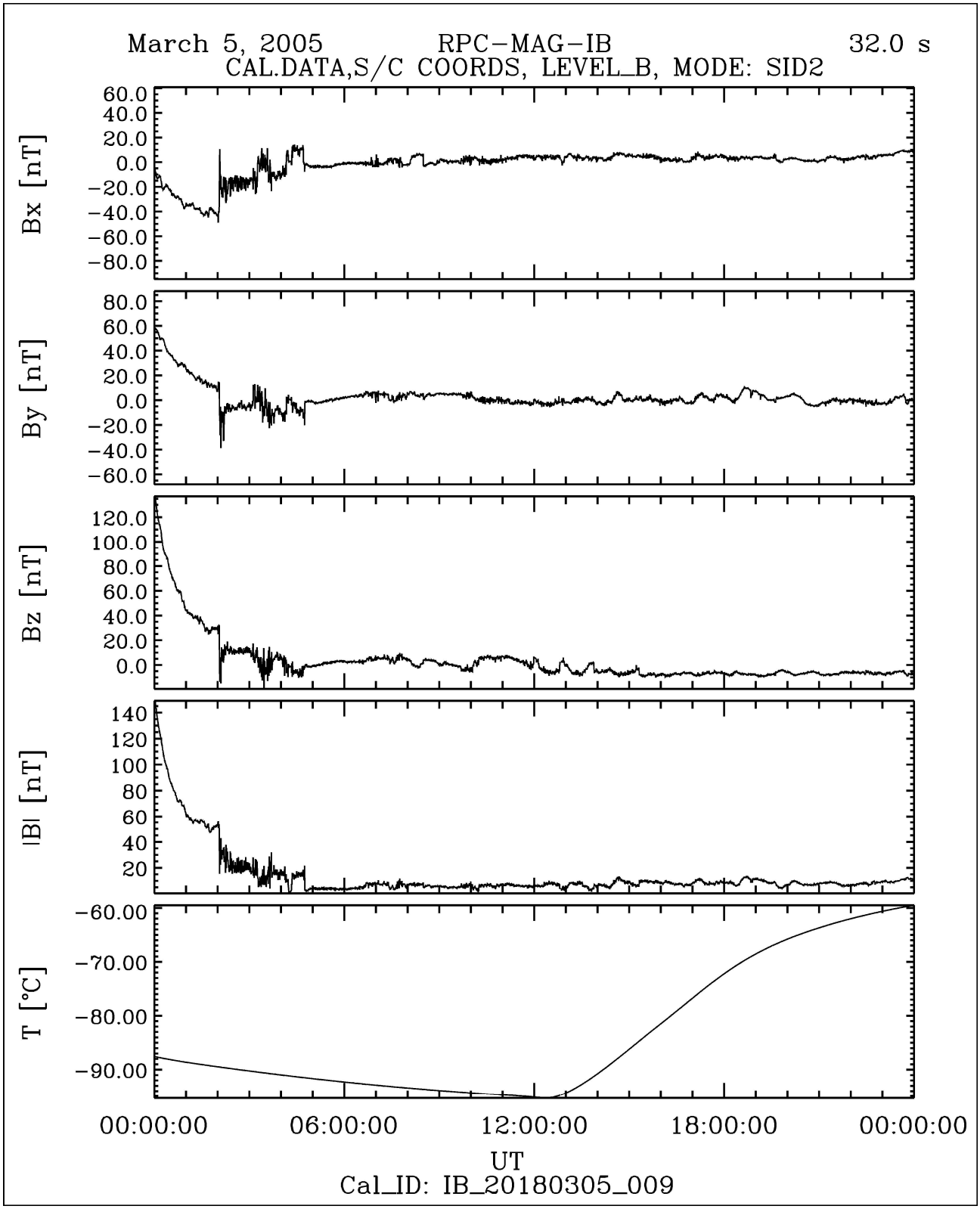

Figure 32: File: RPCMAG050305T0000_CLB_IB_M2_T0000_2400_009

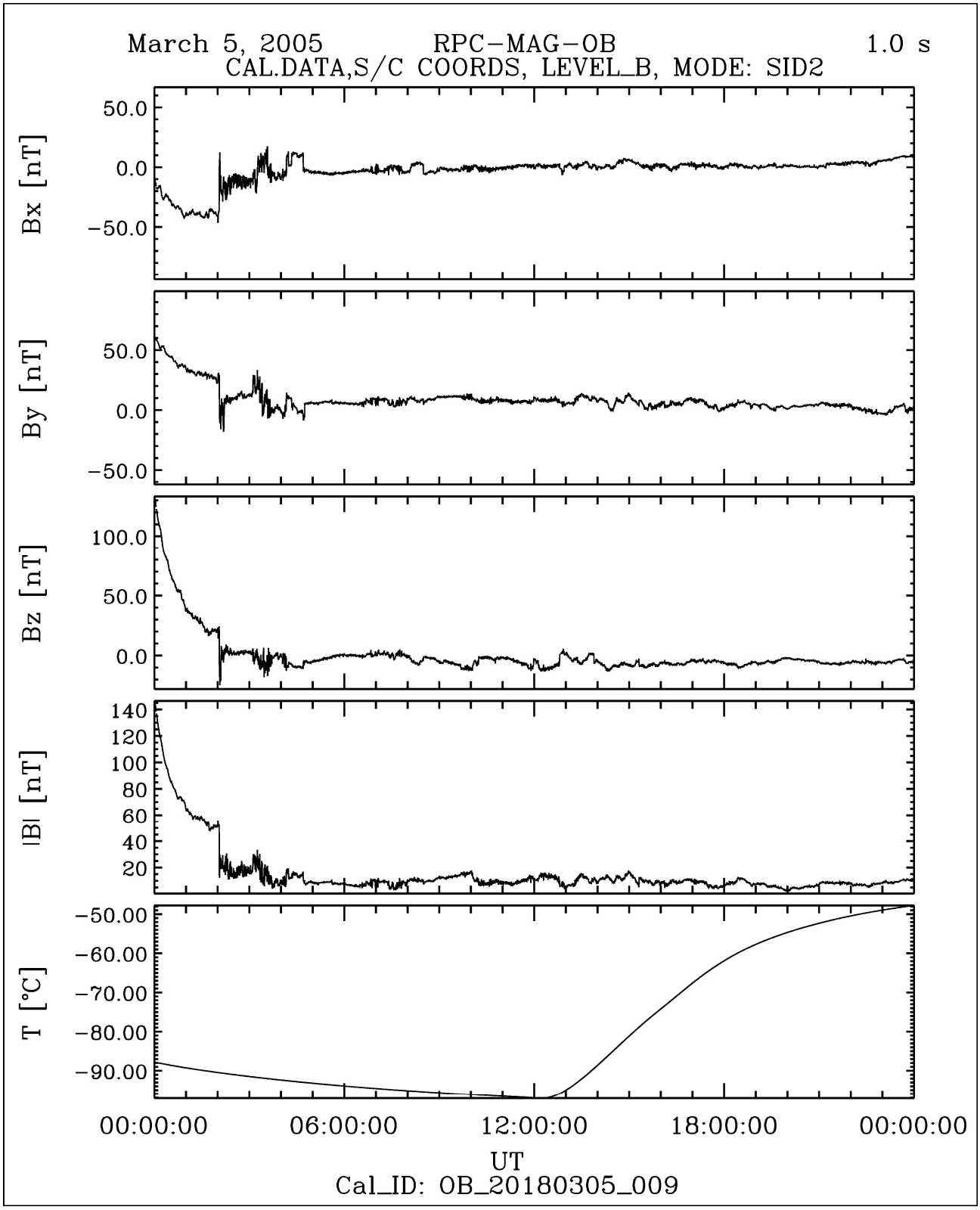

Figure 33: File: RPCMAG050305T0000_CLB_OB_M2_T0000_2400_009

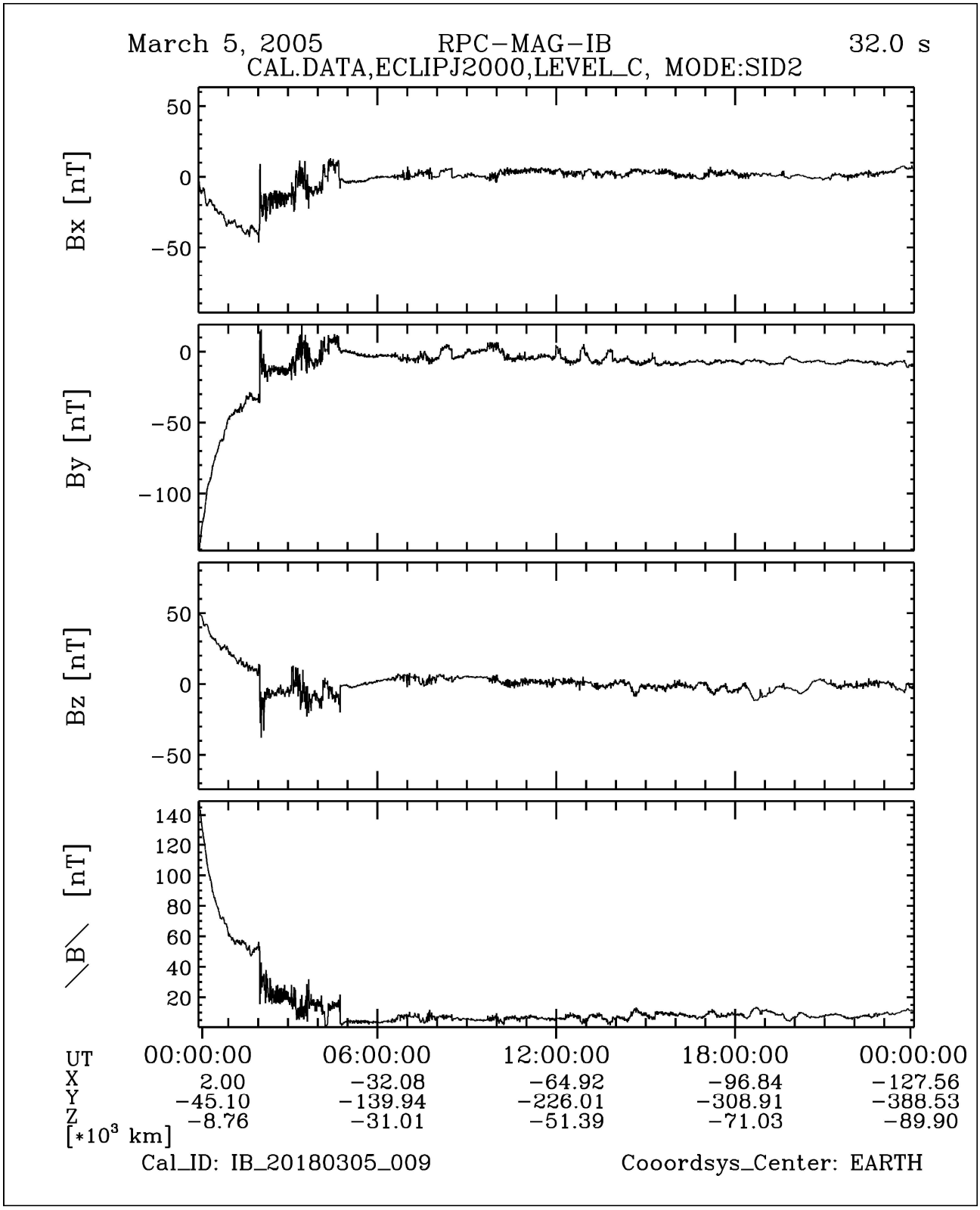

Figure 34: File: RPCMAG050305T0000_CLC_IB_M2_T0000_2400_009

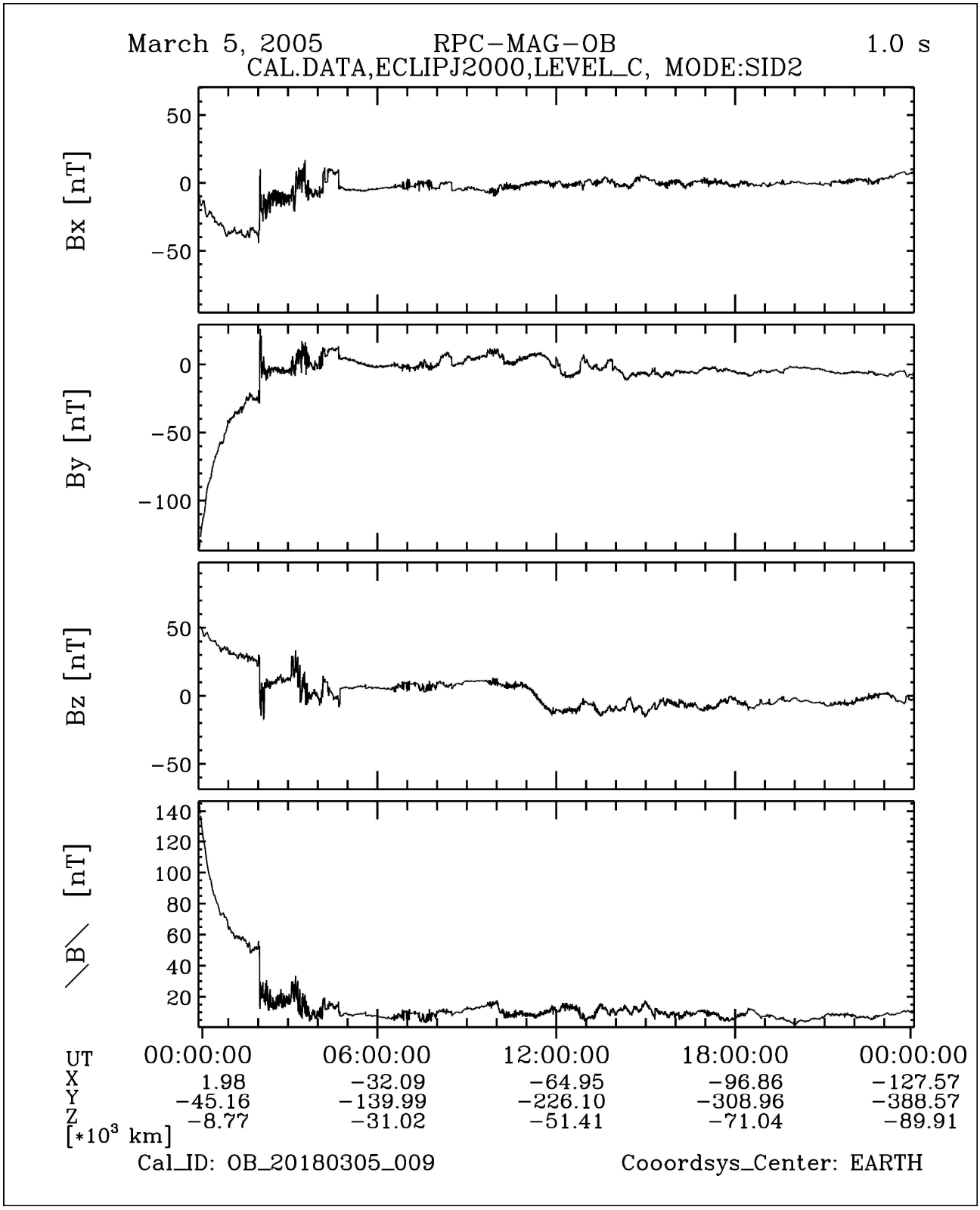

Figure 35: File: RPCMAG050305T0000_CLC_OB_M2_T0000_2400_009

3.7 March 06, 2005:

3.7.1 Actions

MAG stayed in SID 2. No problems occurred.

3.7.2 Plots of Calibrated Data

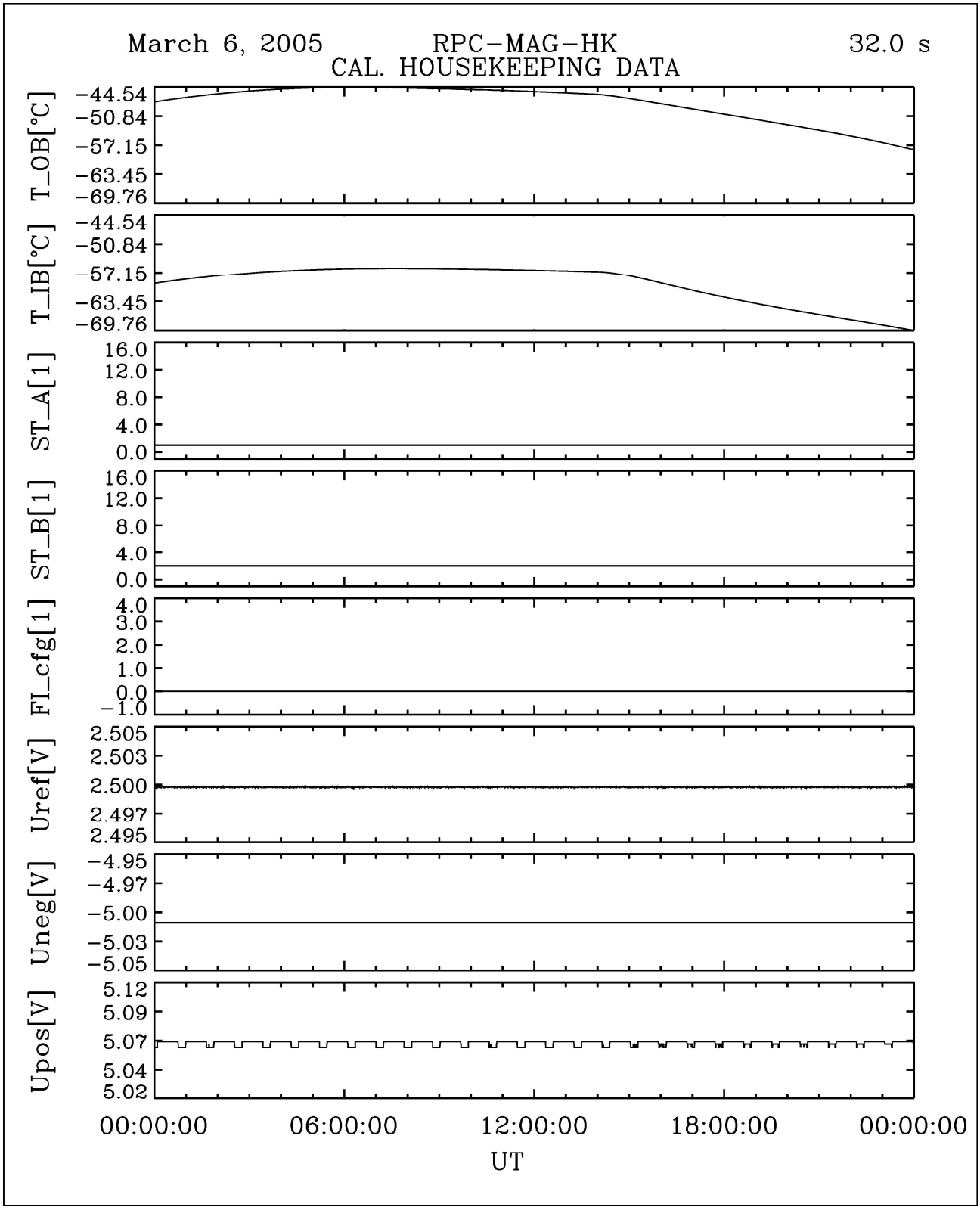

Figure 36: File: RPCMAG050306T0000_CLA_HK_P0000_2400

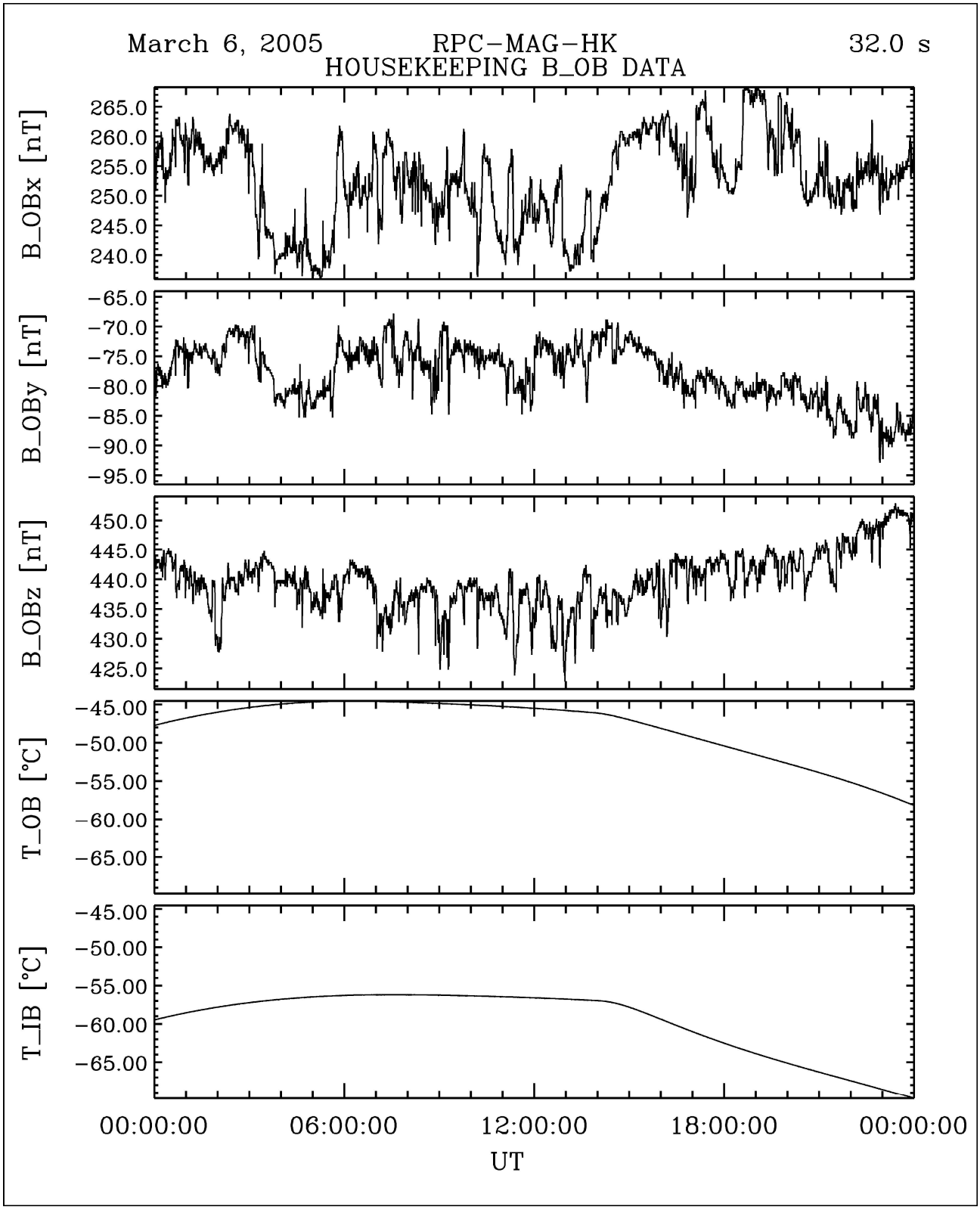

Figure 37: File: RPCMAG050306T0000_CLA_HK_B_P0000_2400

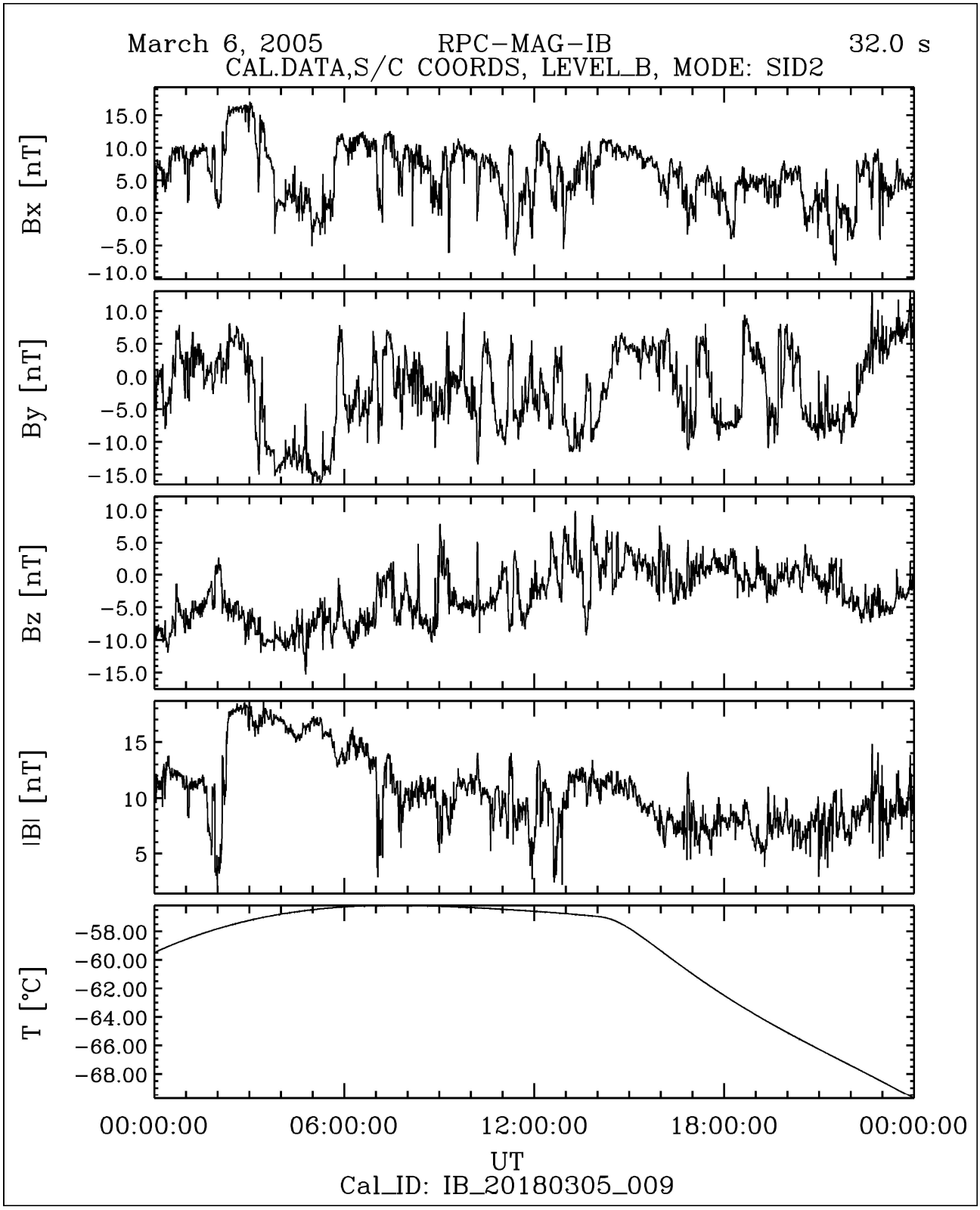

Figure 38: File: RPCMAG050306T0000_CLB_IB_M2_T0000_2400_009

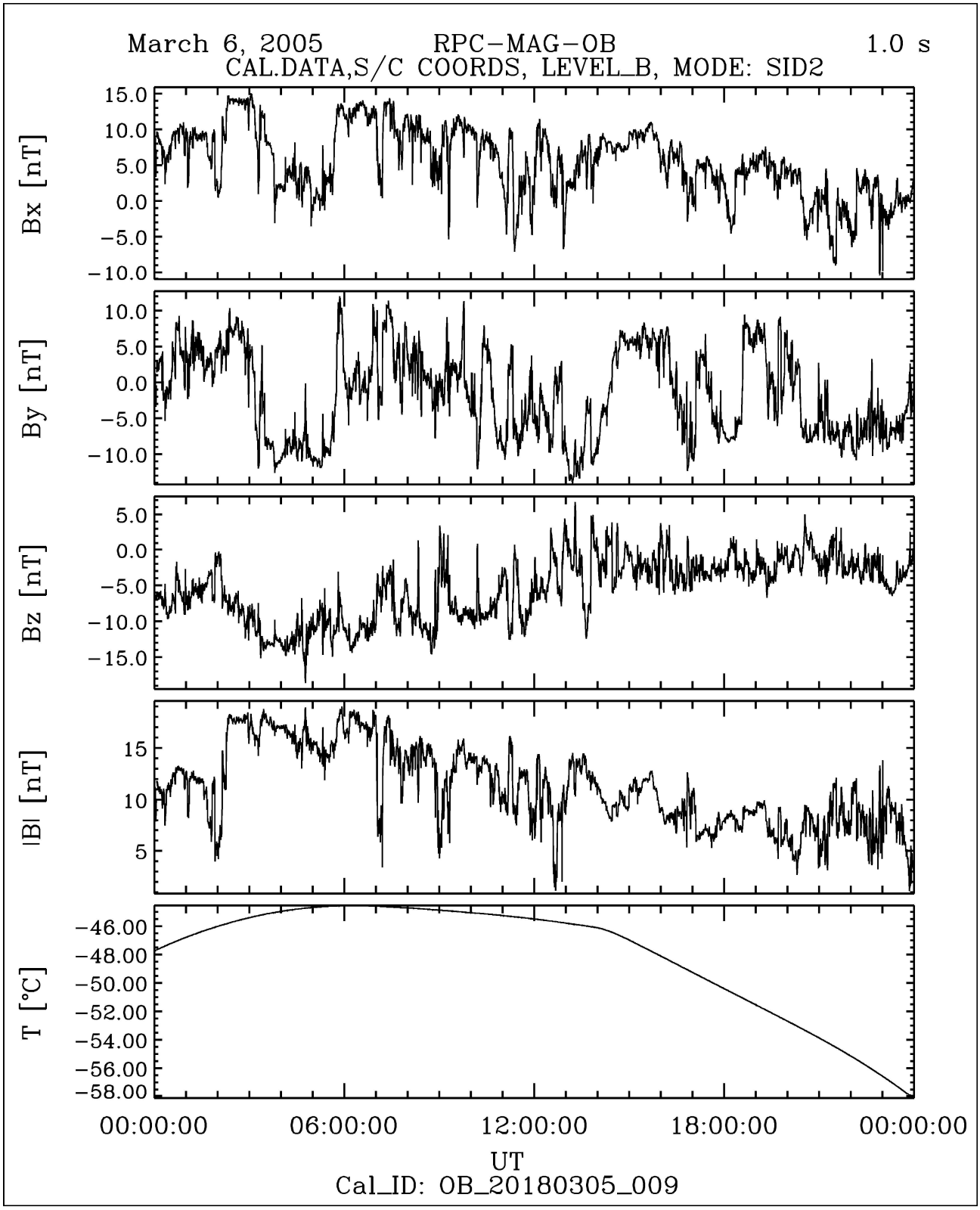

Figure 39: File: RPCMAG050306T0000_CLB_OB_M2_T0000_2400_009

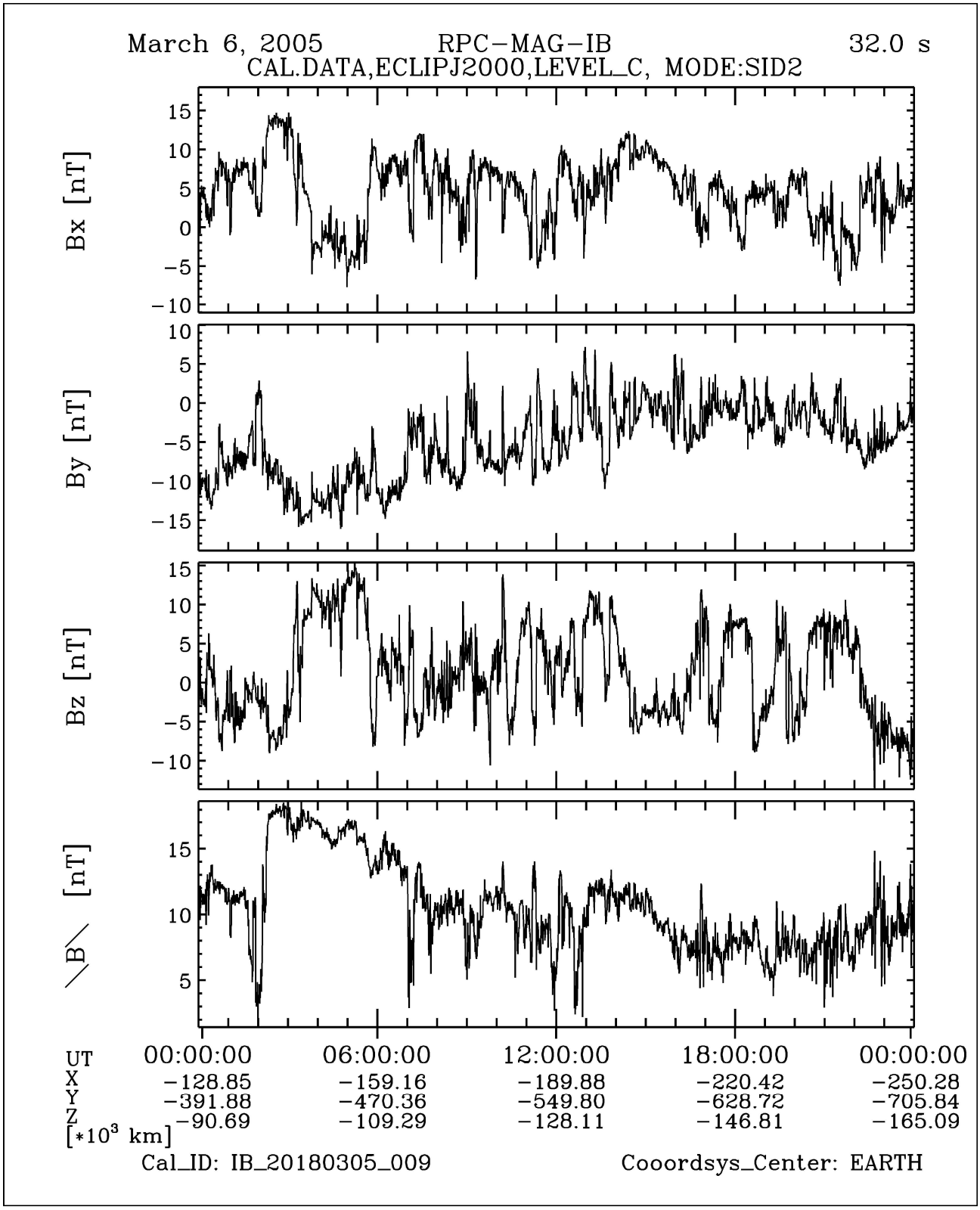

Figure 40: File: RPCMAG050306T0000_CLC_IB_M2_T0000_2400_009

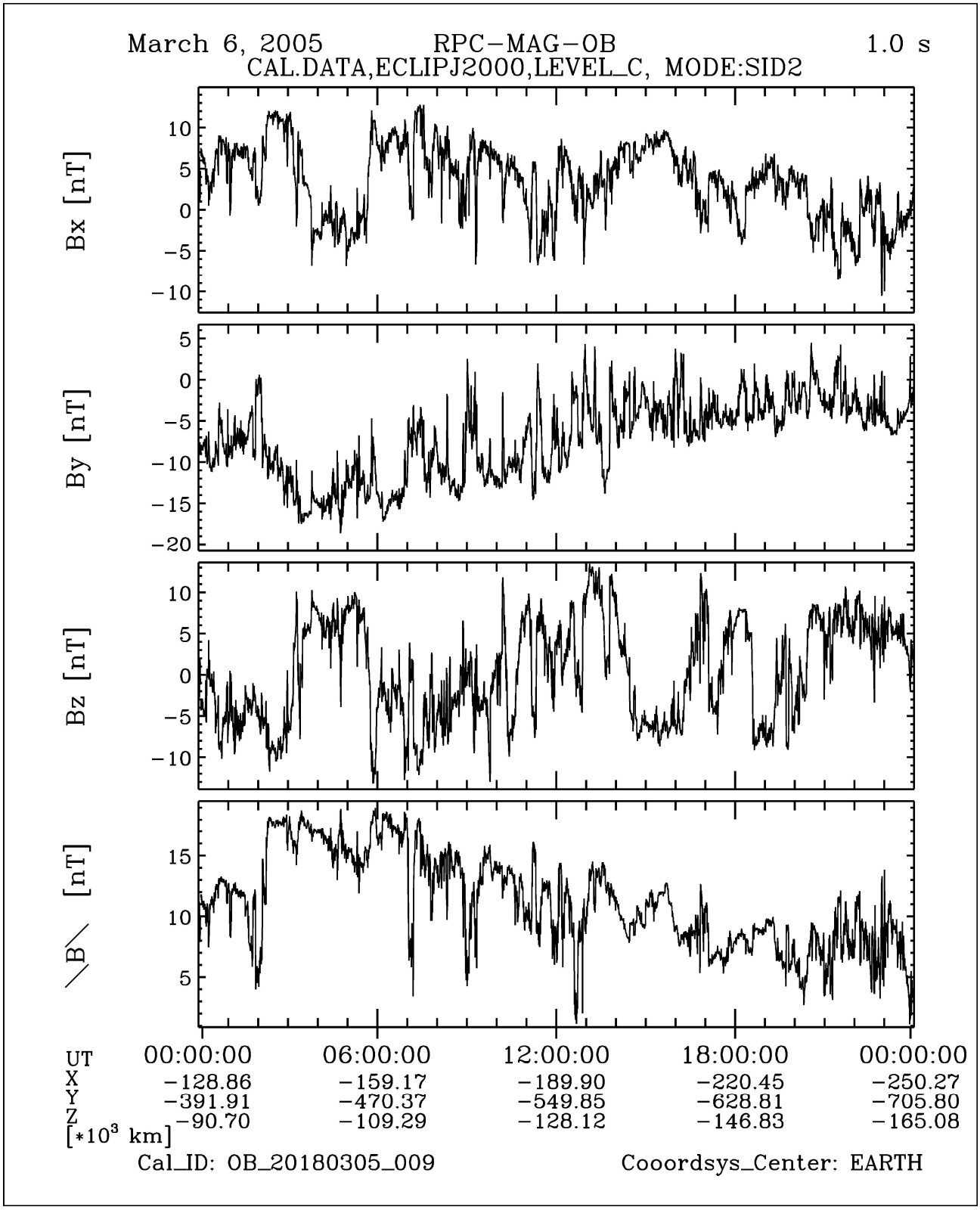

Figure 41: File: RPCMAG050306T0000_CLC_OB_M2_T0000_2400_009

3.8 March 07, 2005:

3.8.1 Actions

MAG stayed in SID 2 until 23:55. Then RPC was switched off. No problems occurred.

3.8.2 Plots of Calibrated Data

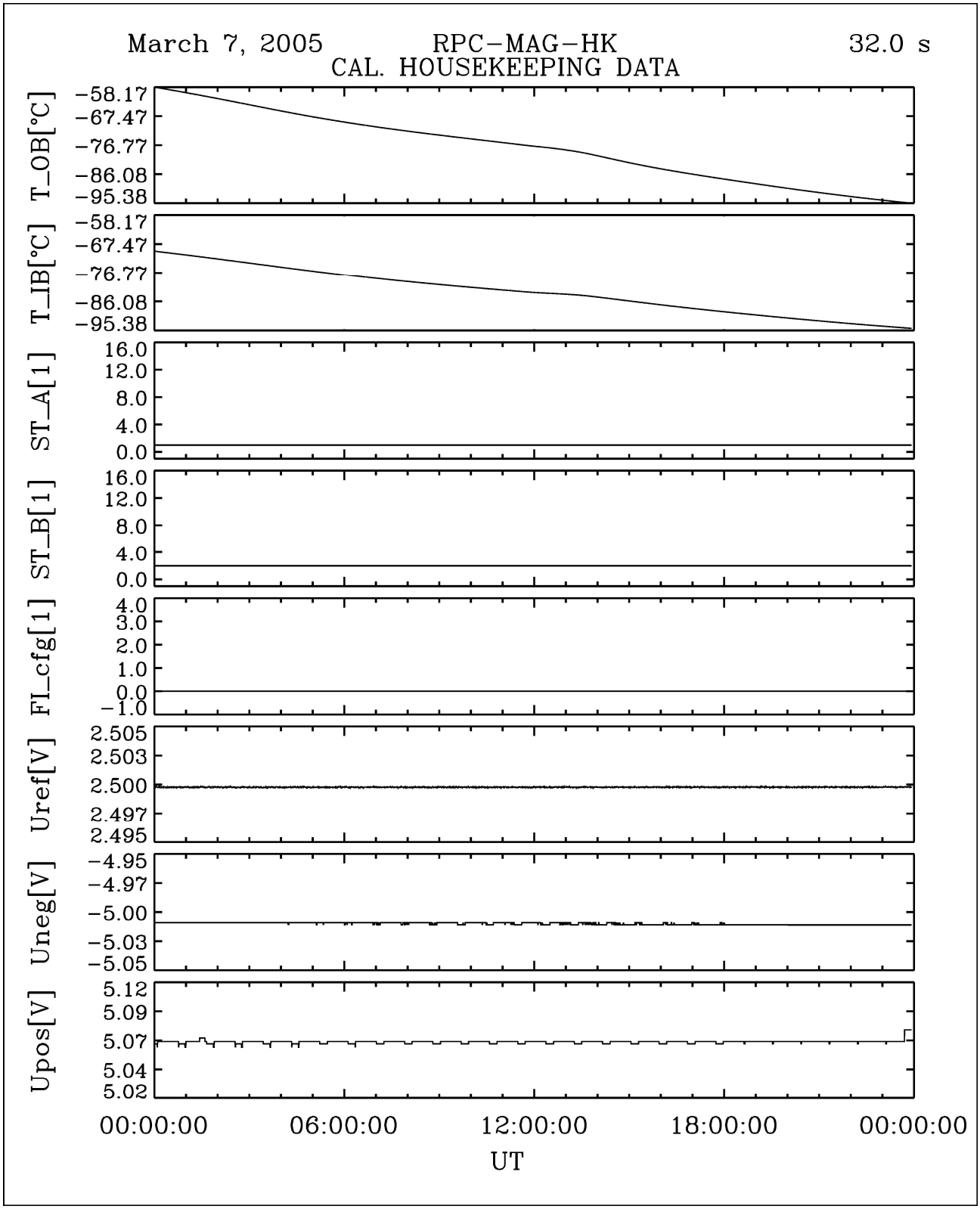

Figure 42: File: RPCMAG050307T0000_CLA_HK_P0000_2400

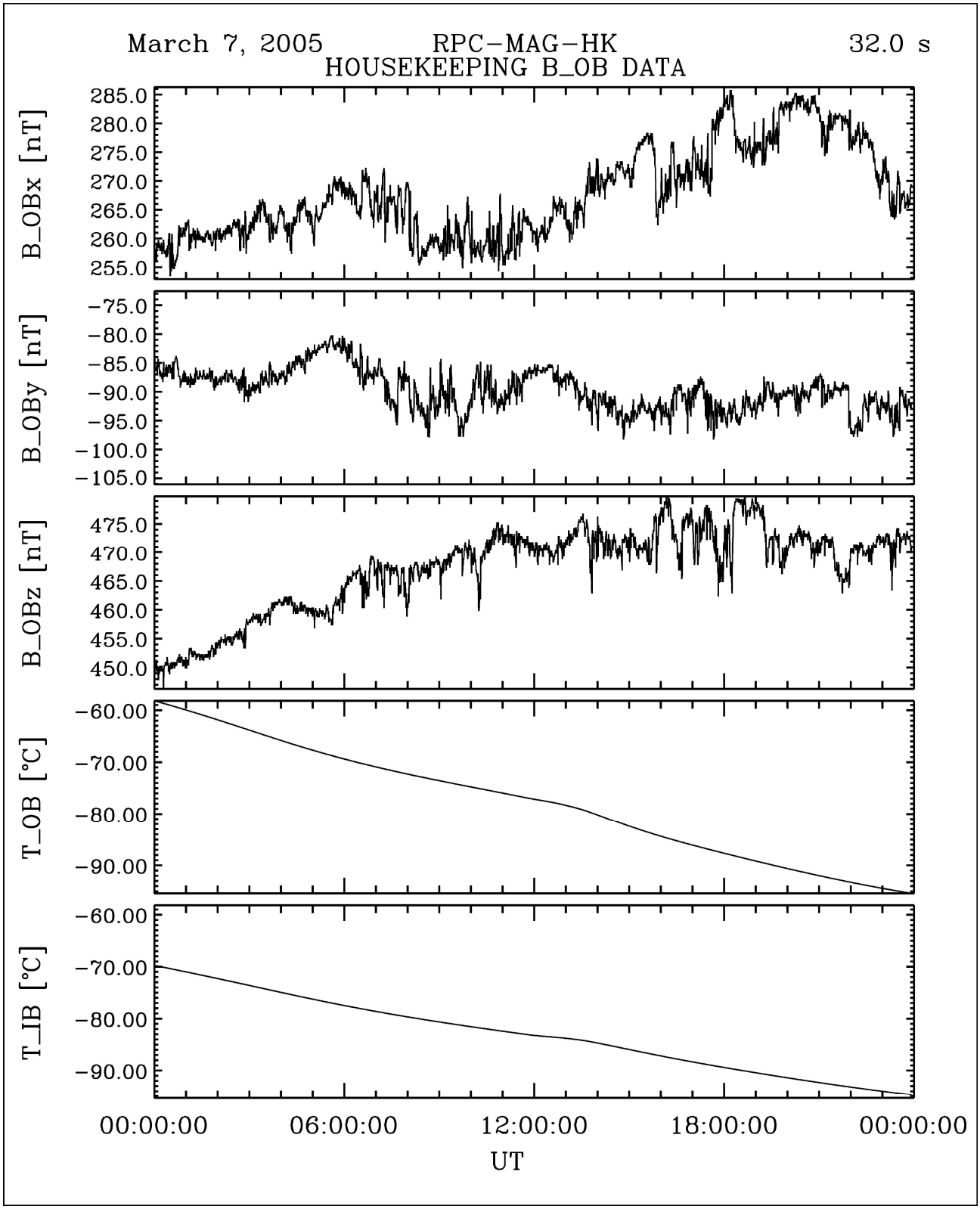

Figure 43: File: RPCMAG050307T0000_CLA_HK_B_P0000_2400

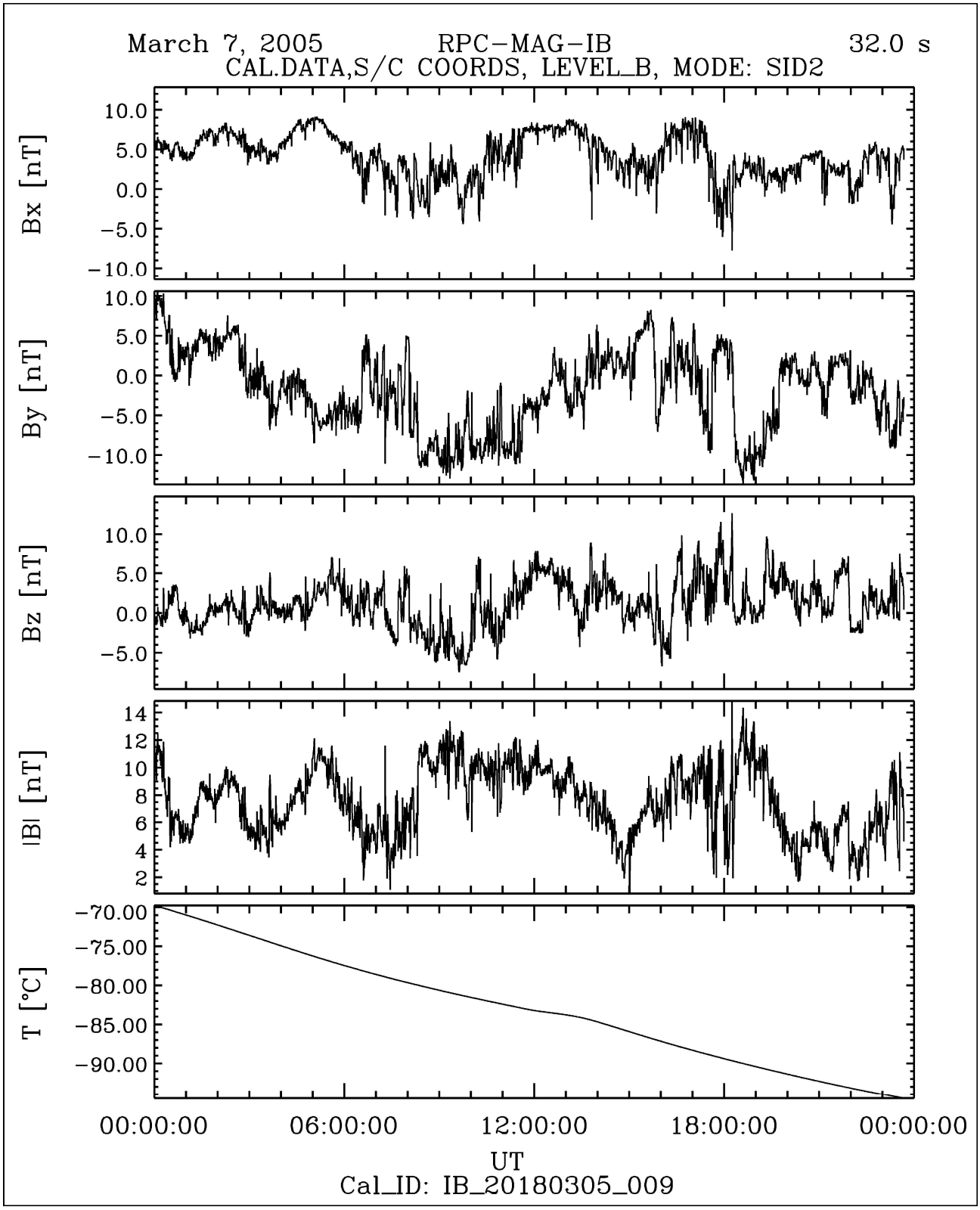

Figure 44: File: RPCMAG050307T0000_CLB_IB_M2_T0000_2400_009

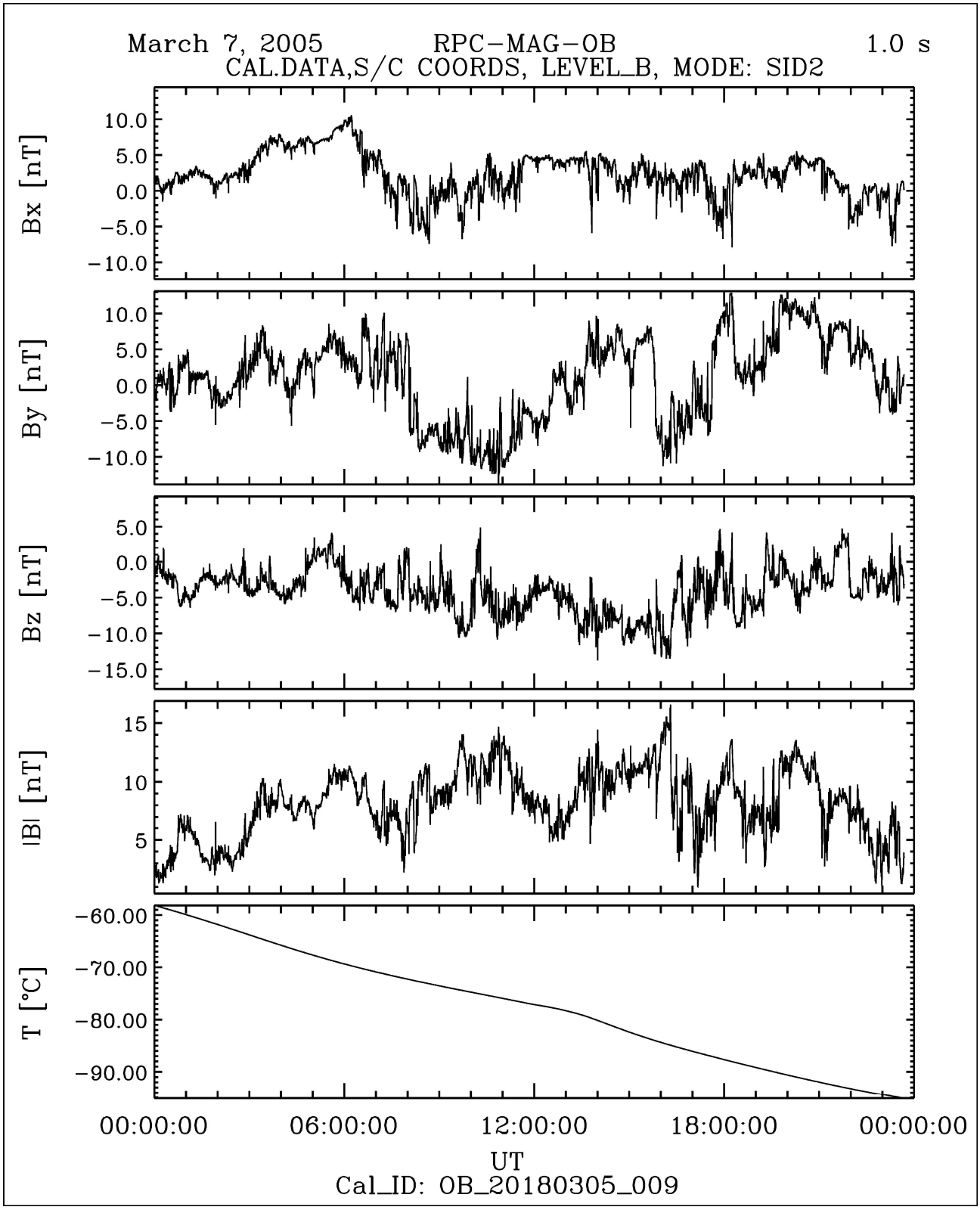

Figure 45: File: RPCMAG050307T0000_CLB_OB_M2_T0000_2400_009

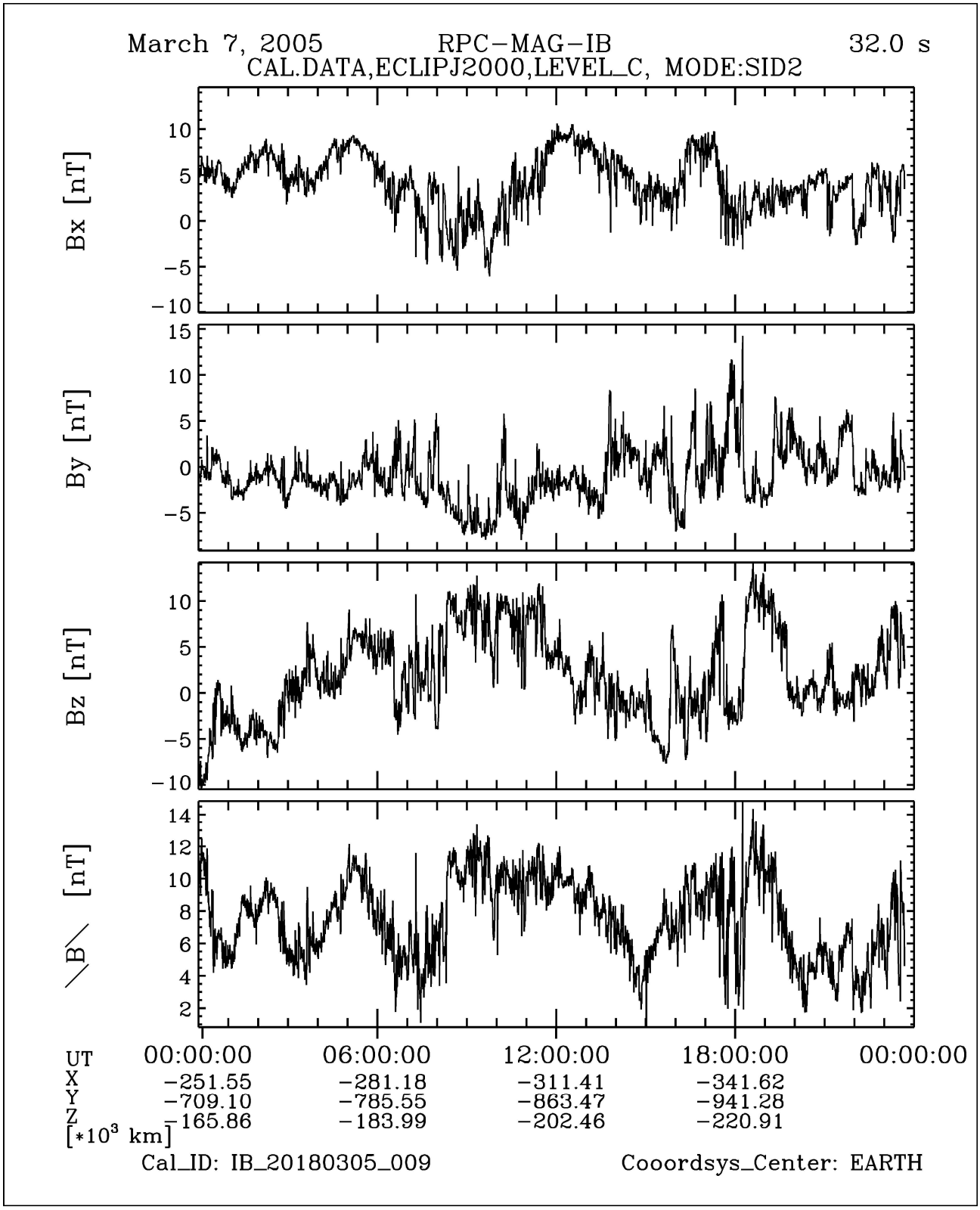

Figure 46: File: RPCMAG050307T0000_CLC_IB_M2_T0000_2400_009

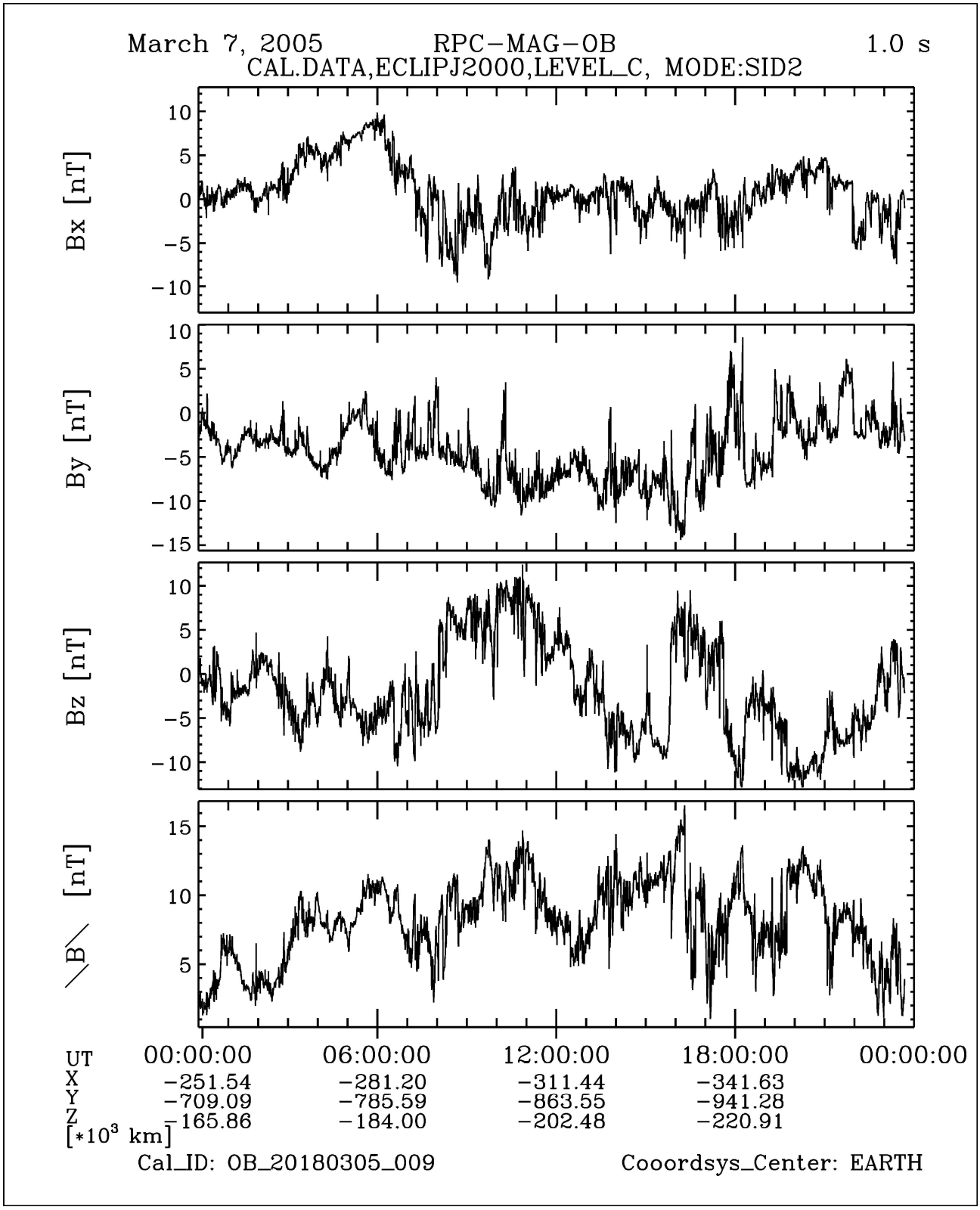

Figure 47: File: RPCMAG050307T0000_CLC_OB_M2_T0000_2400_009

4 Comparison between OB and IB: The Influence of the Sensor Temperature to the Data Quality

In this section we compare the measured data of the OB Sensor with the IB ones. The investigation is done with 1 s averaged LEVEL_F data (s/c coordinates) for various days.

Figure 48 shows the magnetic field data and the sensor temperatures of March 3. The differences for the same day are plotted in Figure 49. The data for March 5, and March 6 have been plotted in Figures 52 – 55.

One can clearly see, that the OB and IB data match very well at times where the both sensors feel the same temperature *variation*. When the temperature changes are different, then the magnetic field data diverge as well. We do see this effect still a littel bit although the 009 temperature calibration model has been applied. Using the former calibration models caused much higher deviations. On short time scales, however, different heat capacities and micro physical hysteresis effects of the sensors core material may cause this behavior and cannot be avoided completely.

From this analysis we can derive a "Data Quality Indicator" based on the temperature difference between OB and IB. The data quality is expected to be good if this difference is constant. If it varies with time, however, the data quality will most likely be poor.

Remark:
The "bursts" in the differences at certain times are most likely caused by the non perfect time matching of the differences of 1 s OB data and averaged 32 s IB data.

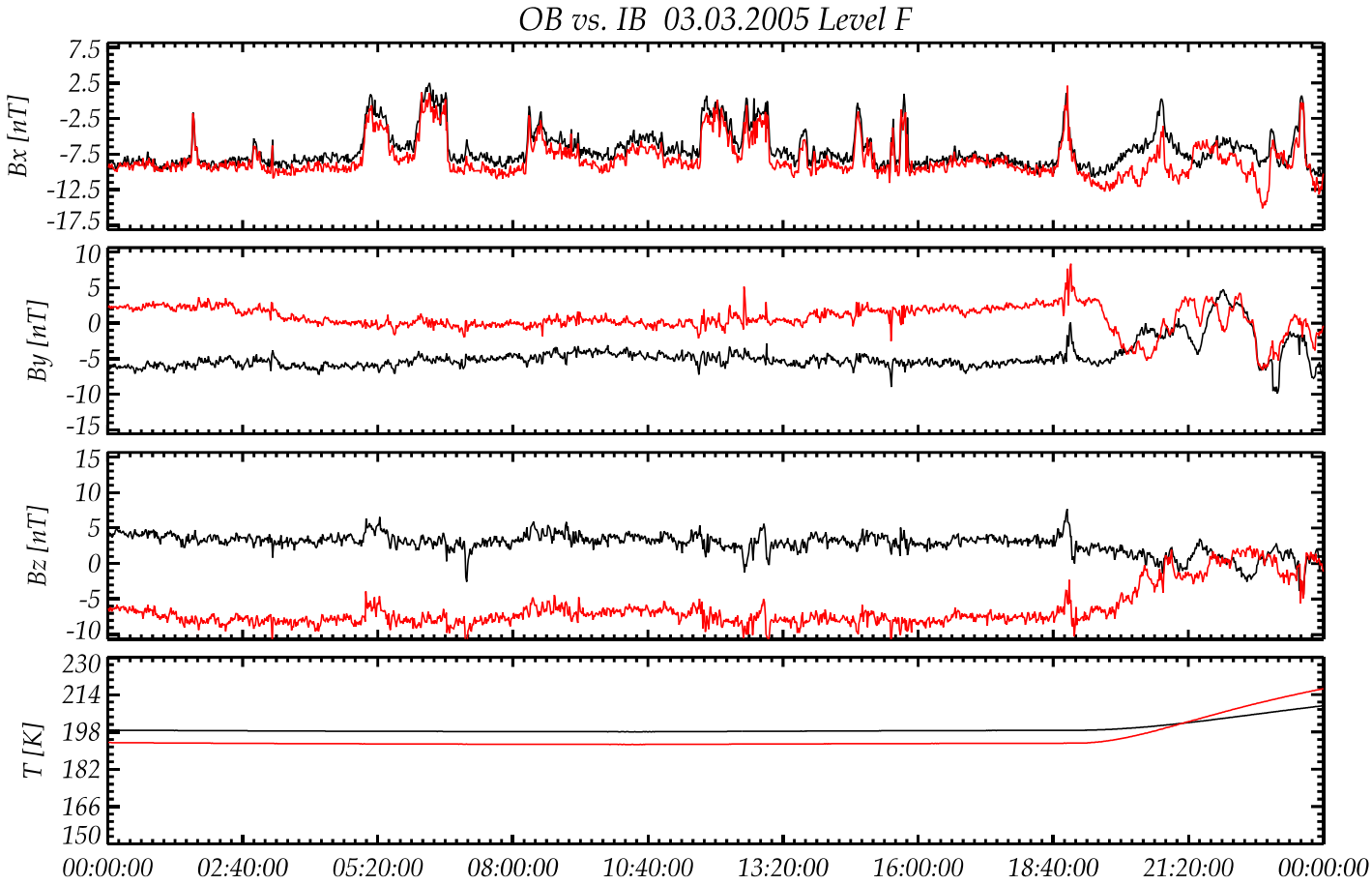

Figure 48: OB(black) versus IB(red): Data of March 3, 2005

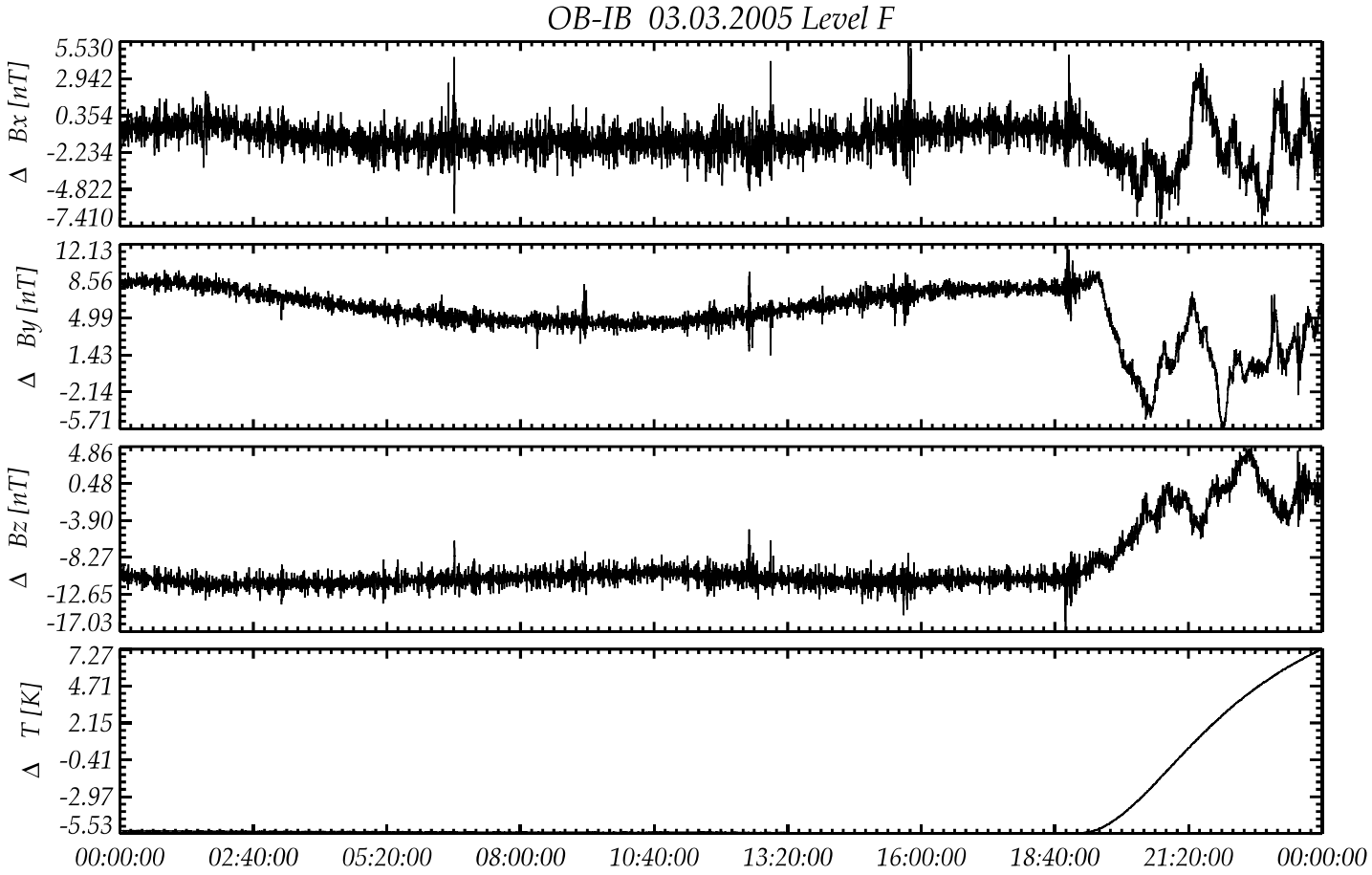

Figure 49: OB-IB: Data of March 3, 2005, Differences

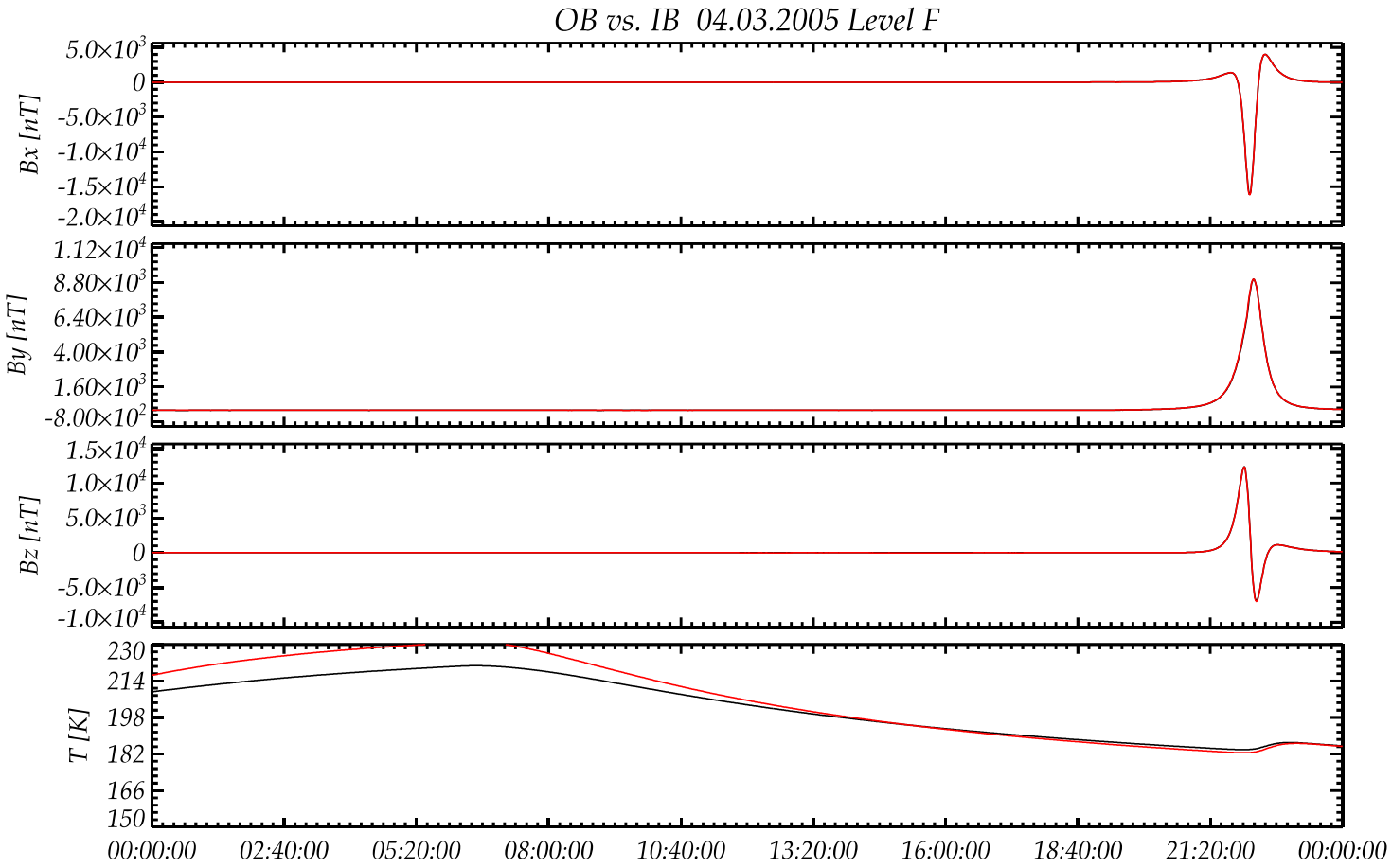

Figure 50: OB(black) versus IB(red): Data of March 4, 2005

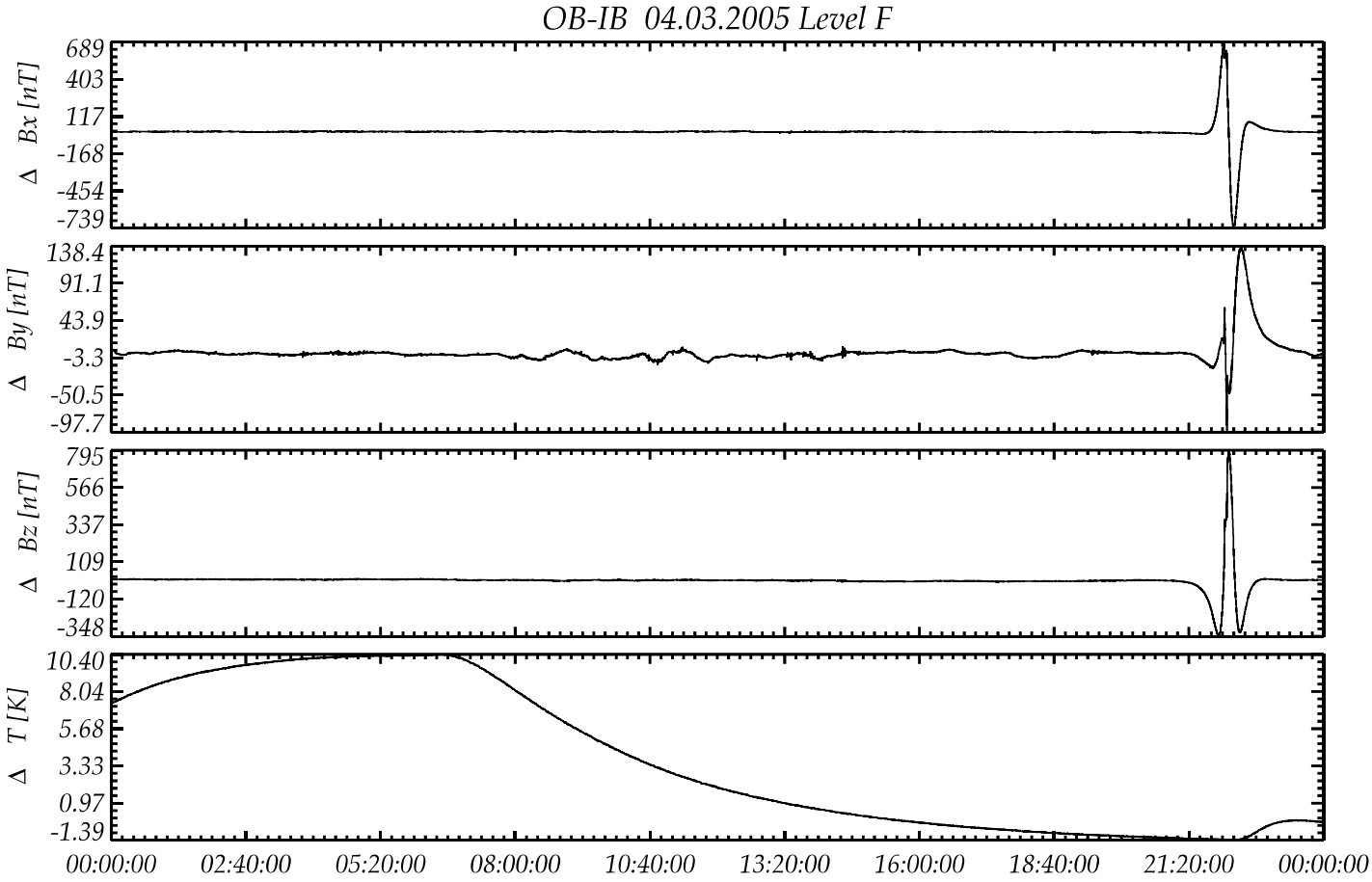

Figure 51: OB-IB: Data of March 4, 2005, Differences

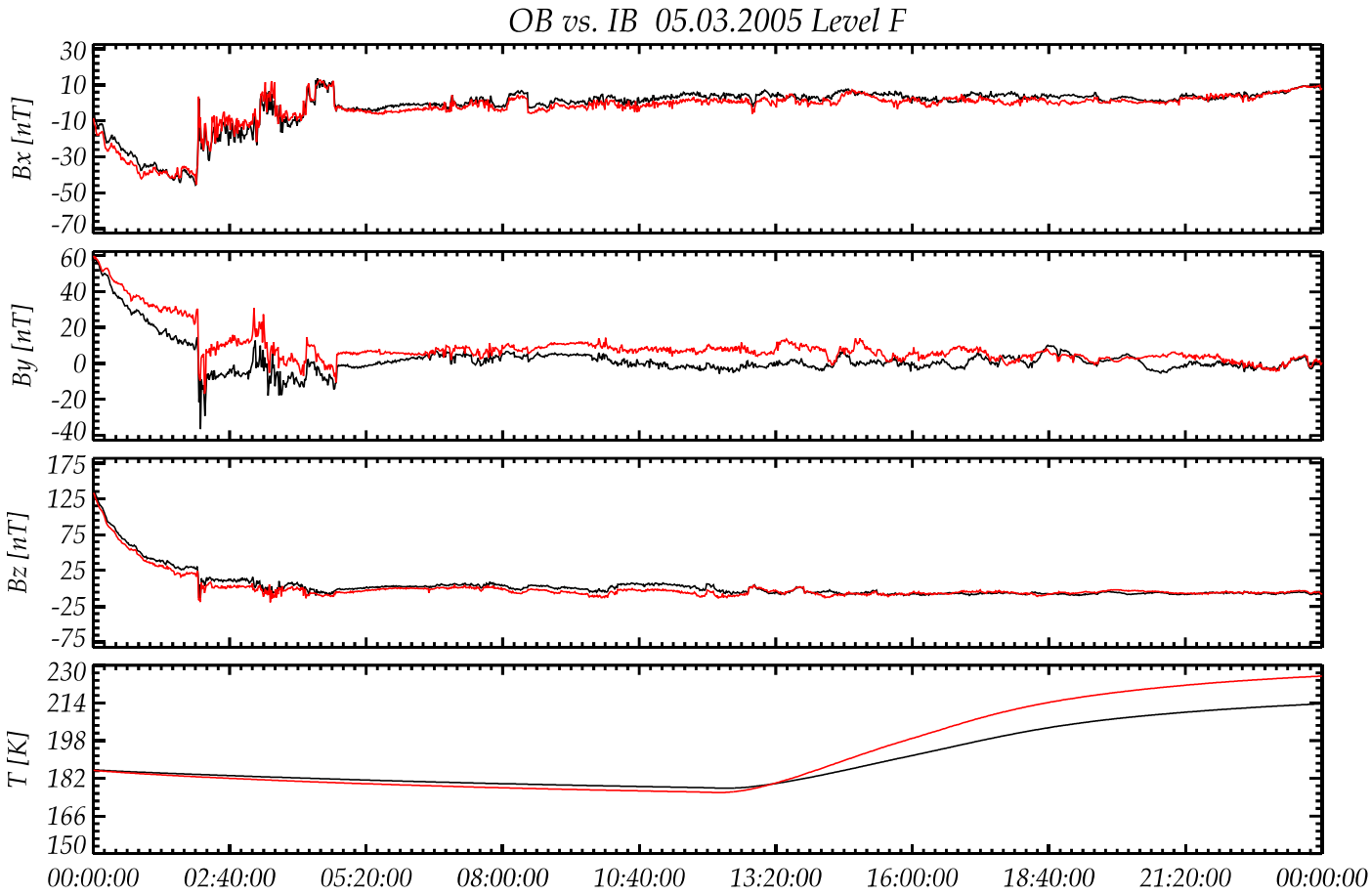

Figure 52: OB(black) versus IB(red): Data of March 5, 2005

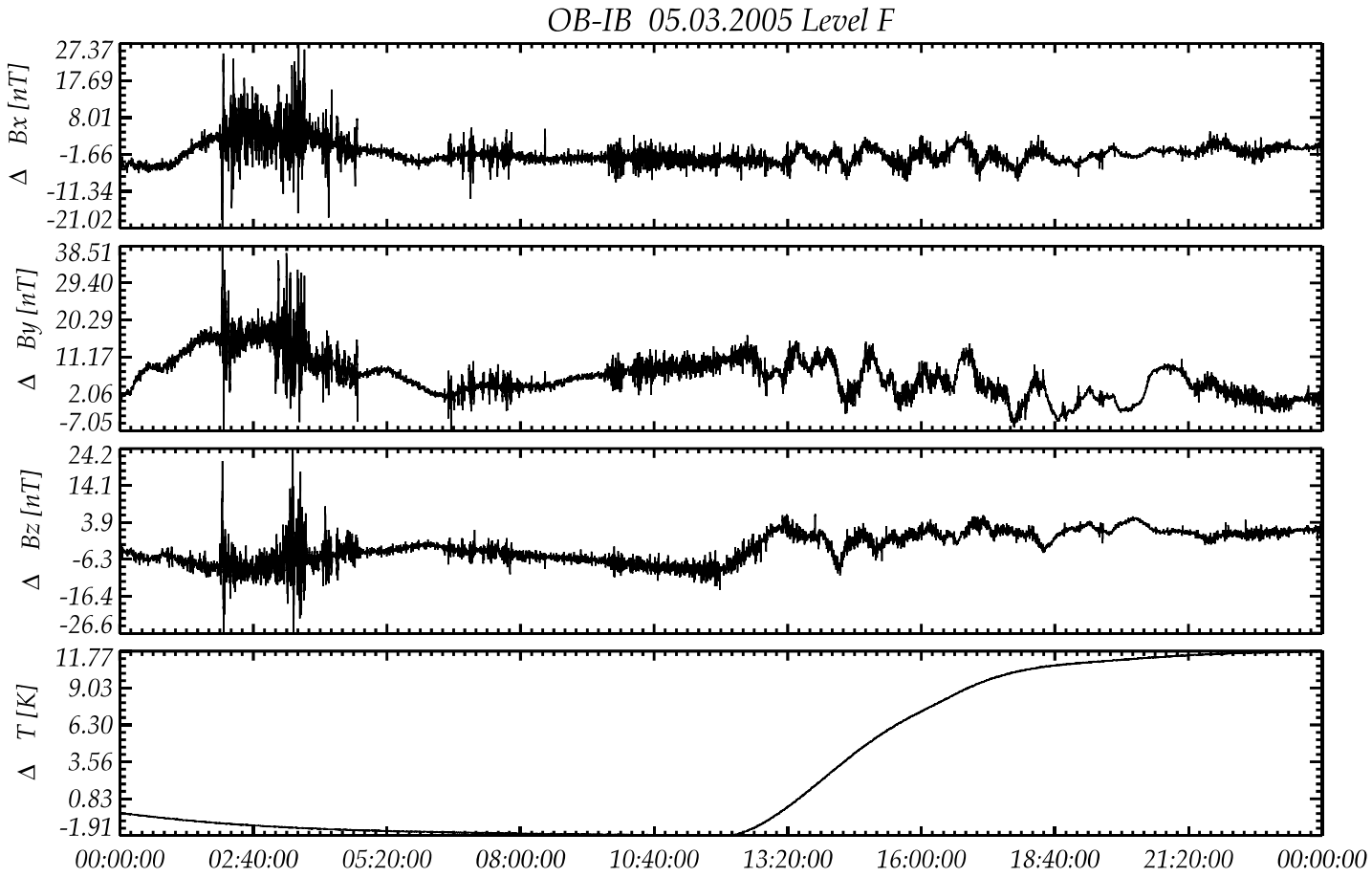

Figure 53: OB-IB: Data of March 5, 2005, Differences

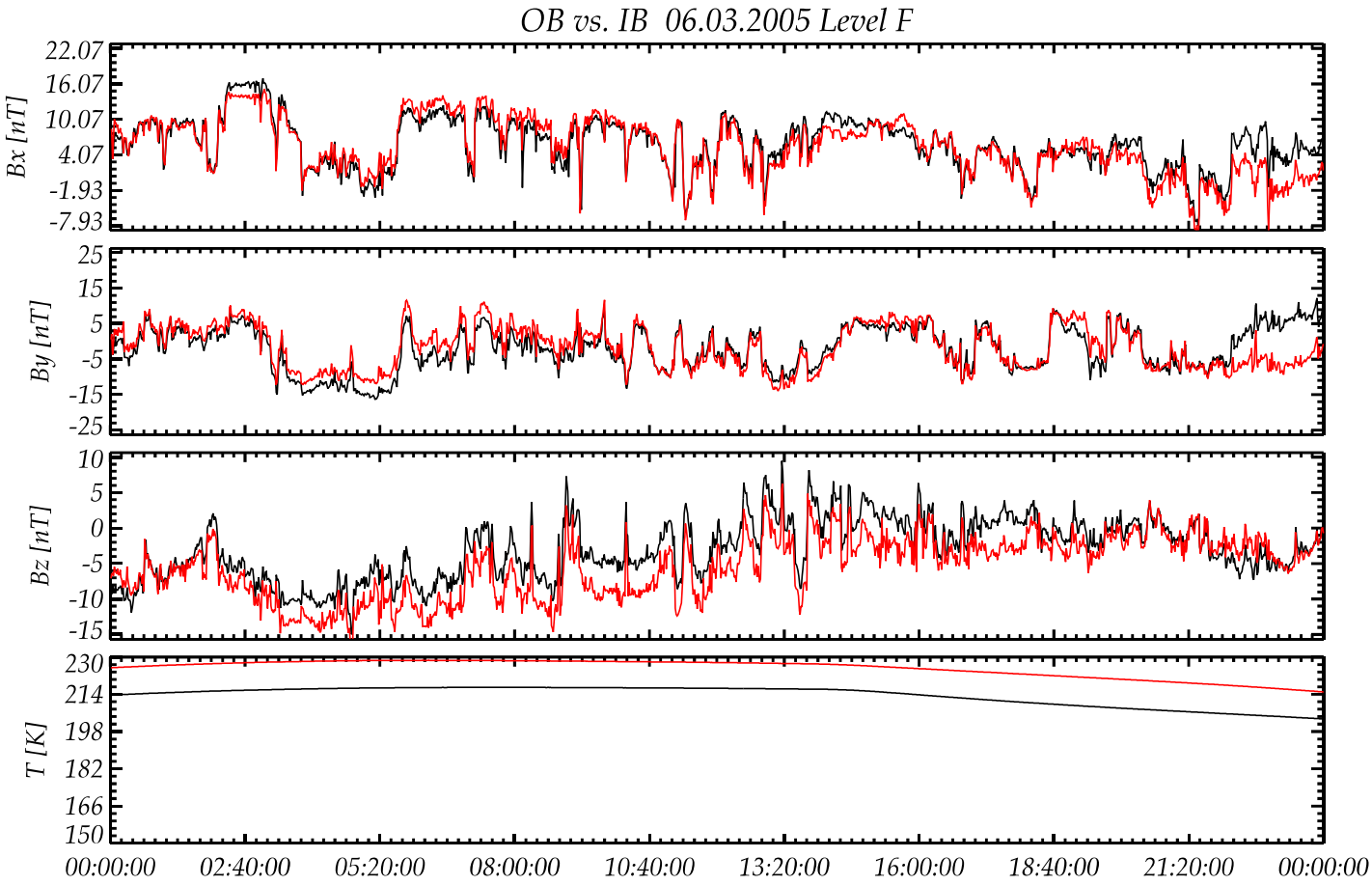

Figure 54: OB(black) versus IB(red): Data of March 6, 2005

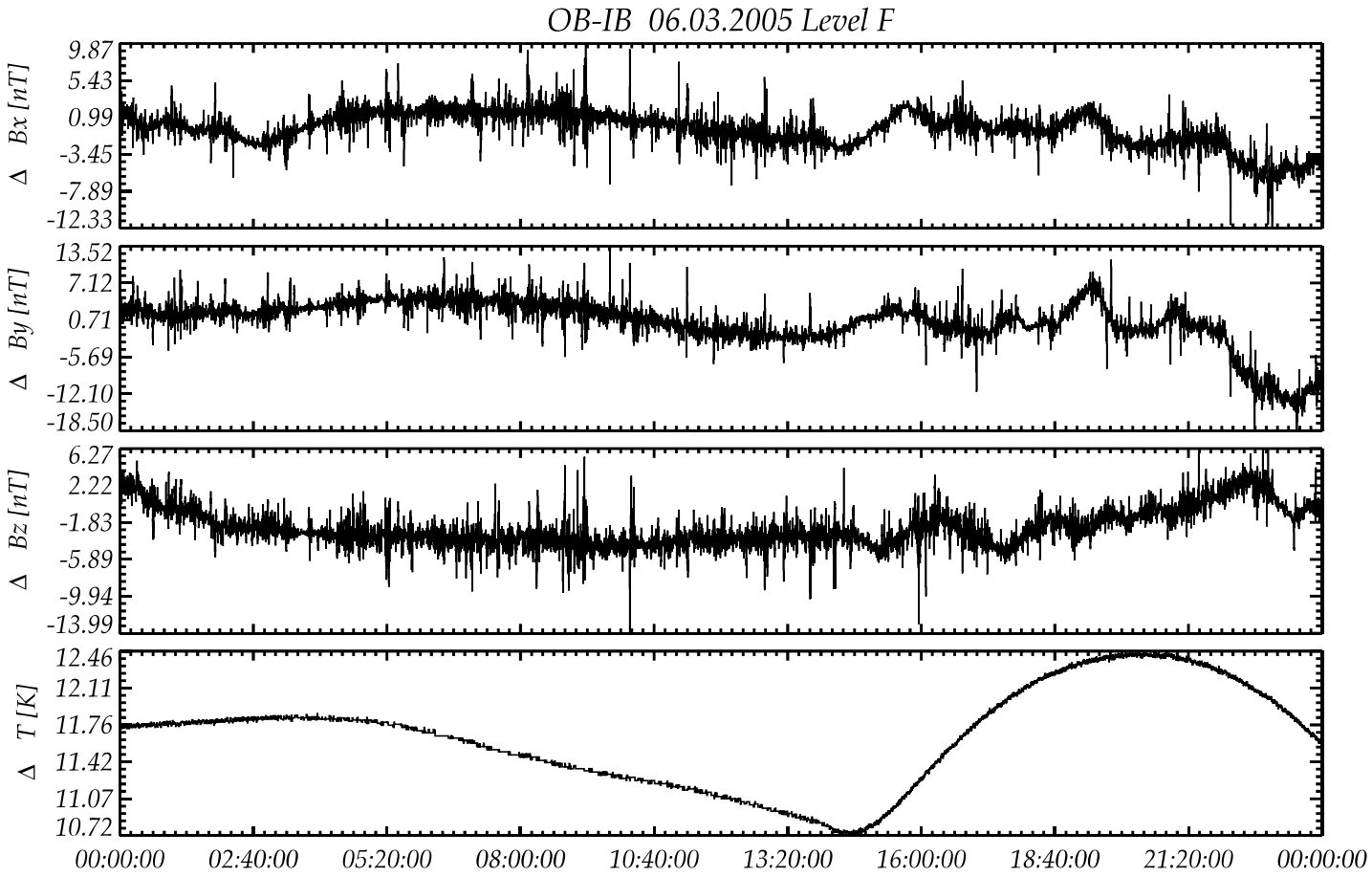

Figure 55: OB-IB: Data of March 6, 2005, Differences

5 Comparison of the MAG data with the POMME Model

In this section we compare the RPCMAG data with a theoretical Earth field model. As model the so called POMME2-model (**Po**tsdam **M**agnetic **M**odel of the **E**arth) developed by the Geo–Forschungs–Zentrum (GFZ) Potsdam is used. This model is based on CHAMP and OERSTED data and includes the following geophysical features:

- Time varying core field
- Ring current (DST)
- Time averaged magnetospheric field
- Secular variations
- Taking into account Main field & Crust field model MF4
  (MF4 Model : crust field model, based on spherical harmonic analysis up to degree 90)

The comparison will be done for the total field and as well for the single components for a time intervall of ± 30 min around Closest Approach (CA).

5.1 Comparison with the OB–Sensor

Figure 56 shows the modulus of the OB sensor in the most upper panels and the total field calculated by the POMME model in the second panel. On this large scale the difference are negligible. The computed difference in the bottom panels, however reveals an error of about ± 10 nT for the most times[1] It is remarkable, that there is bump in the RPCMAG data for about 4 min just before CA (S/C passed from the Gulf of Mexico via Mexico to the Pacific ocean). There is no external explanation for this bump. We guess that there are movable parts on ROSETTA. In the following investigation we will exclude this specific time interval.

[1] At a first analysis in 2005 there were differences up to a few hundred nanotesla which initiated a detailed investigation. The result was that we used wrong time tags caused by shifts in the digital filter onboard ROSETTA. This delay of about 8.37s in normalmode was successfully corrected and lead to perfect data.

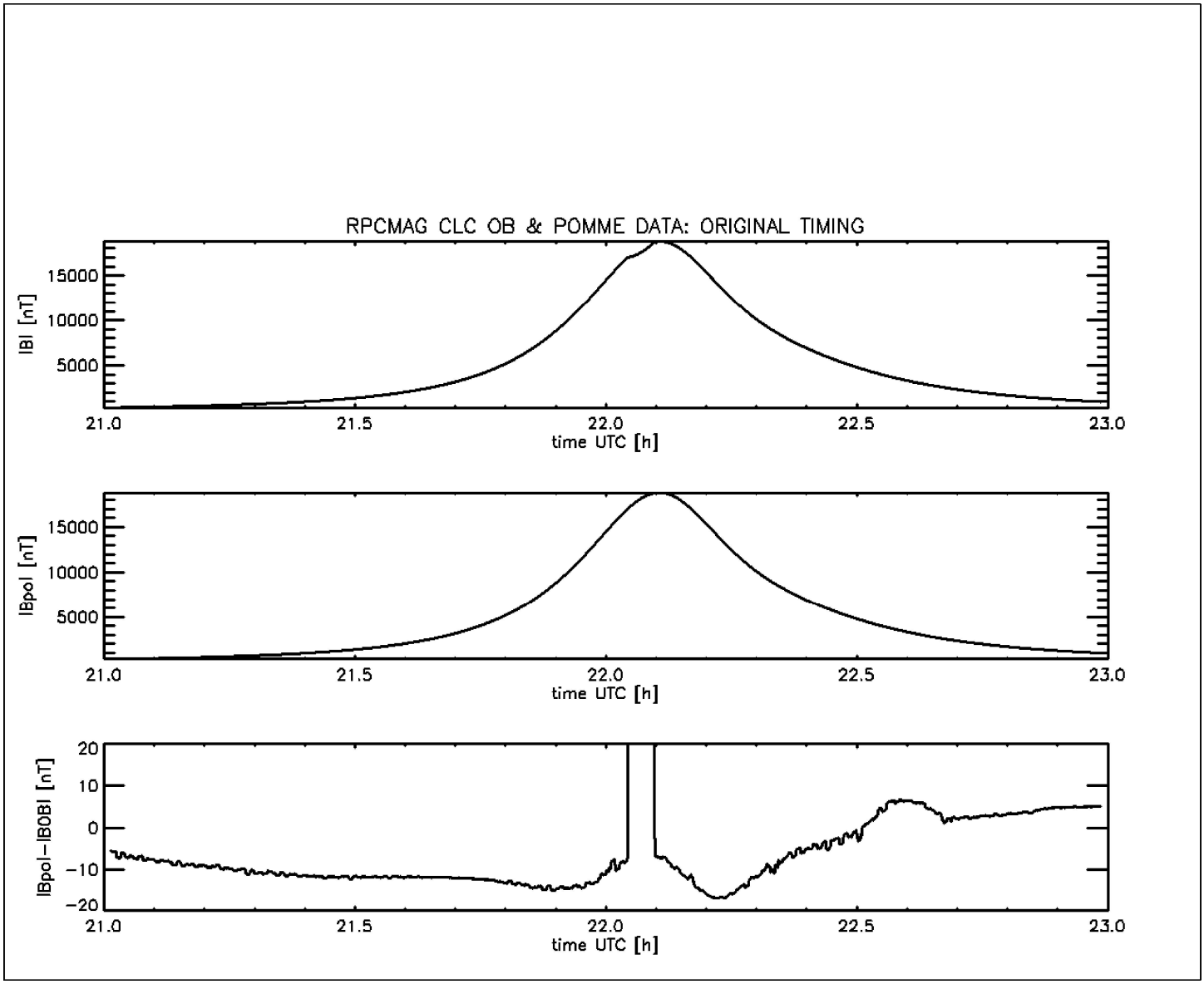

Figure 56: POMME versus OB: Total field, original timing

Although the residua were in the expected order we tried to minimize the difference by shifting the RPCMAG data in time domain. This was done using a minimization routine, minimizing the variance of the difference of both time series by shifting one time series in time domain. The result, shown in Figure 57, was that the OB data have to be shifted by -0.2 s against the POMME data. The calculated shift did not gain much improvement as expected, because the optimal shift was already implemented after the digital filter delay time correction. This check was however a good check for the impact of the correction.

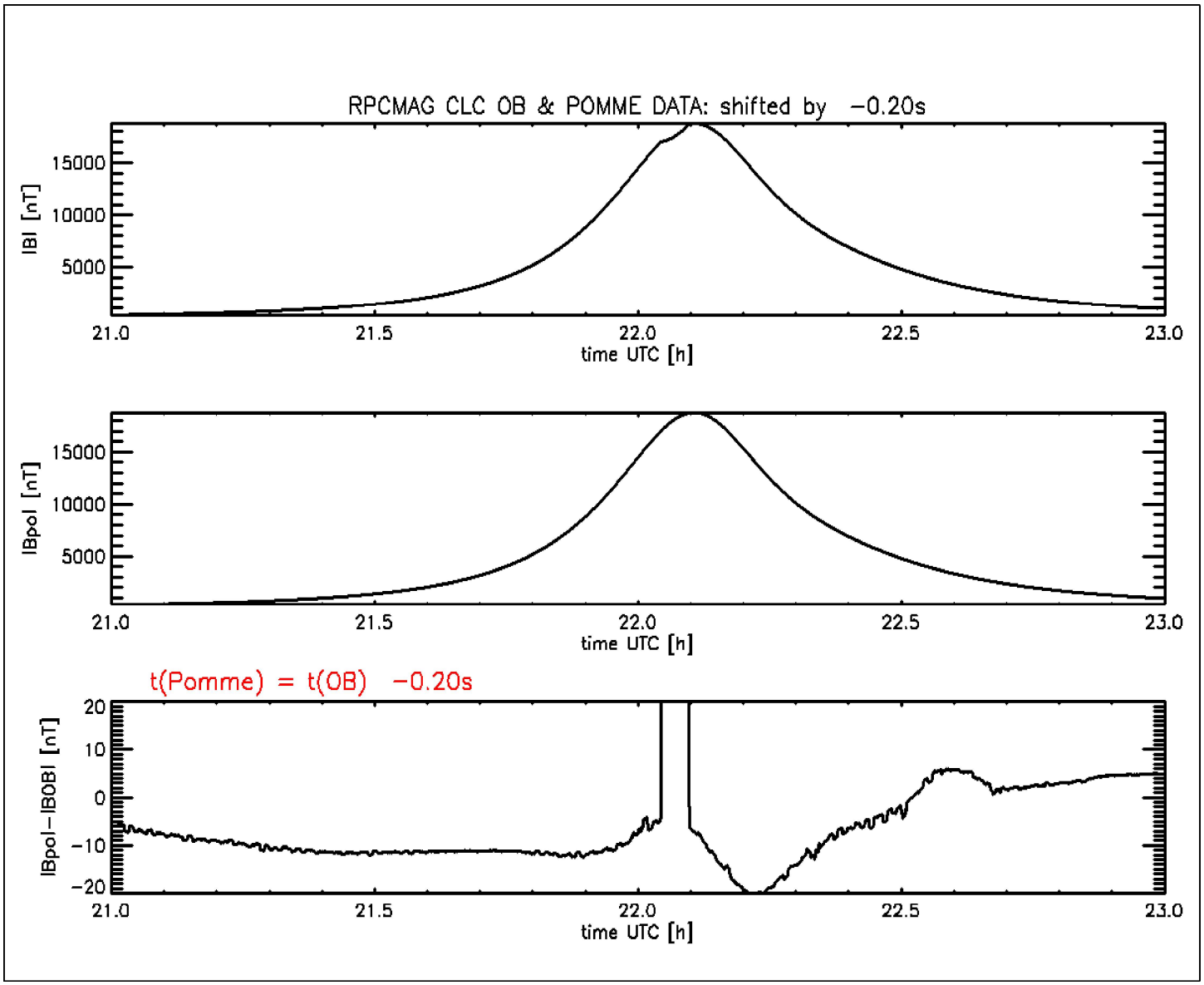

Figure 57: POMME versus OB: Total field, shifted timing

A comparison of the components of the OB sensor and POMME is displayed in Figure 58 for the original timing. At a first view this looks quite good as well. The differences of the model and the measurements are plotted in Figure 59 for the original timing and in Figure 60 for the time shifted data.

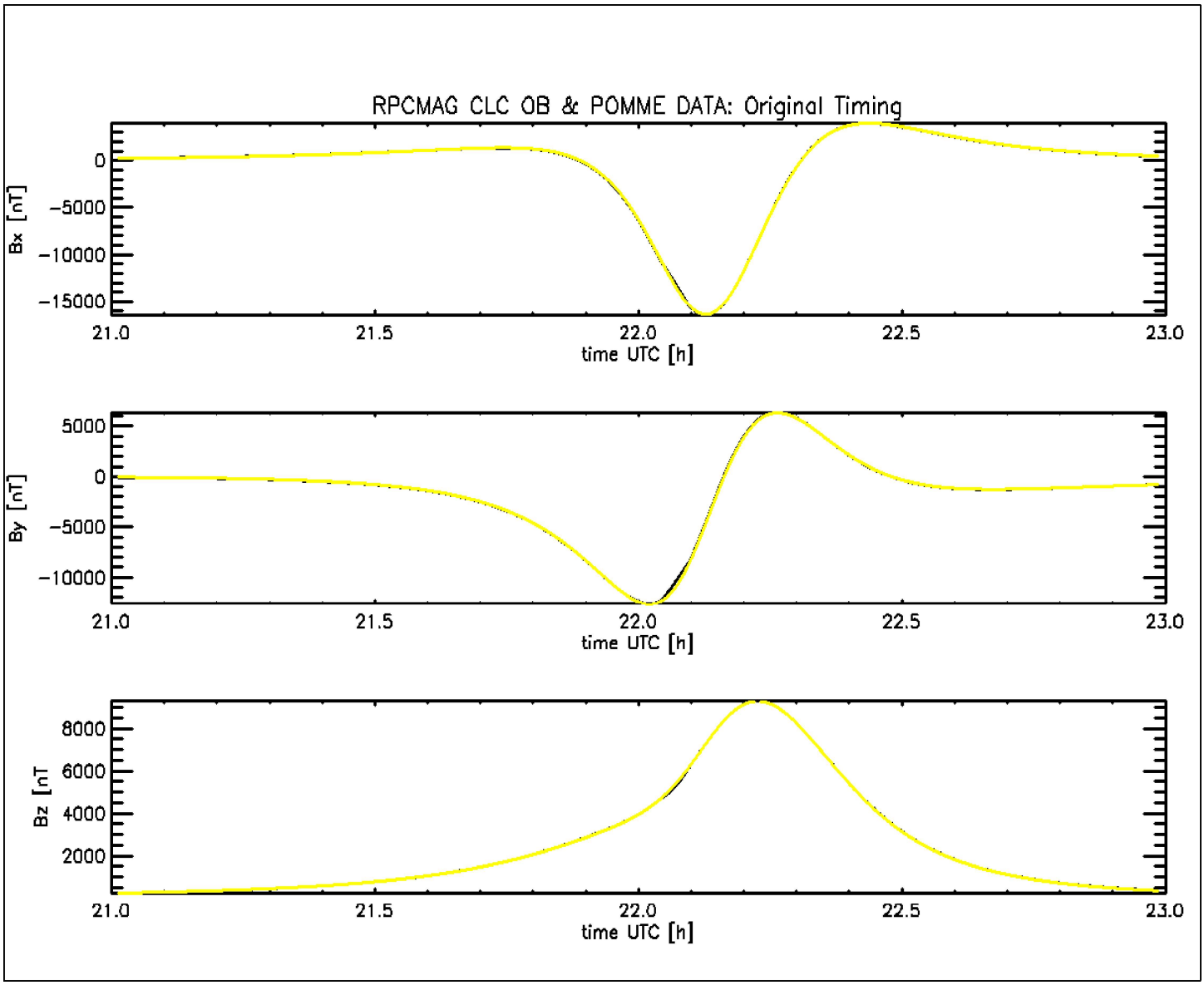

Figure 58: POMME versus OB: Components, original timing

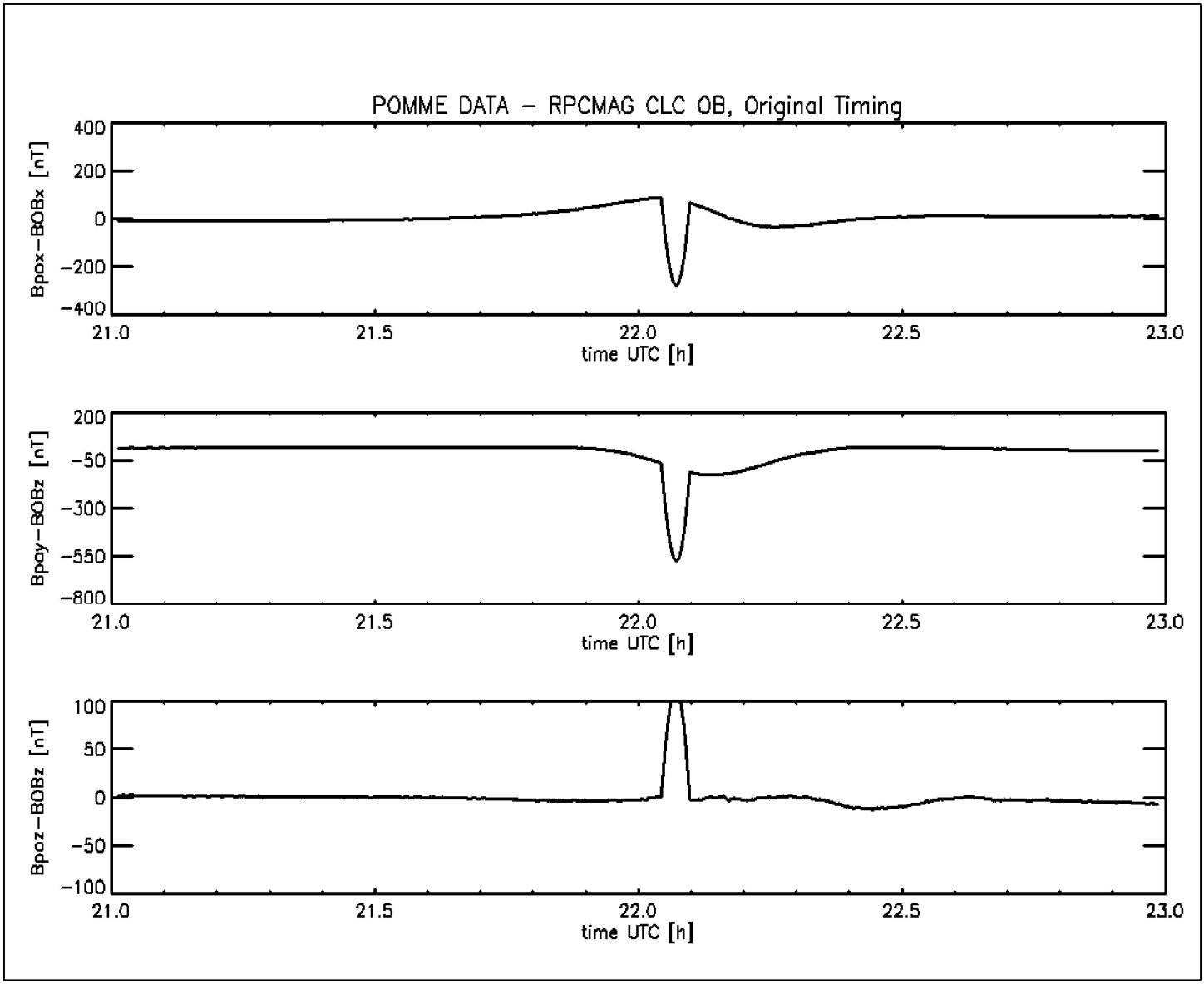

Figure 59: POMME versus OB: Differences of the Components, original timing

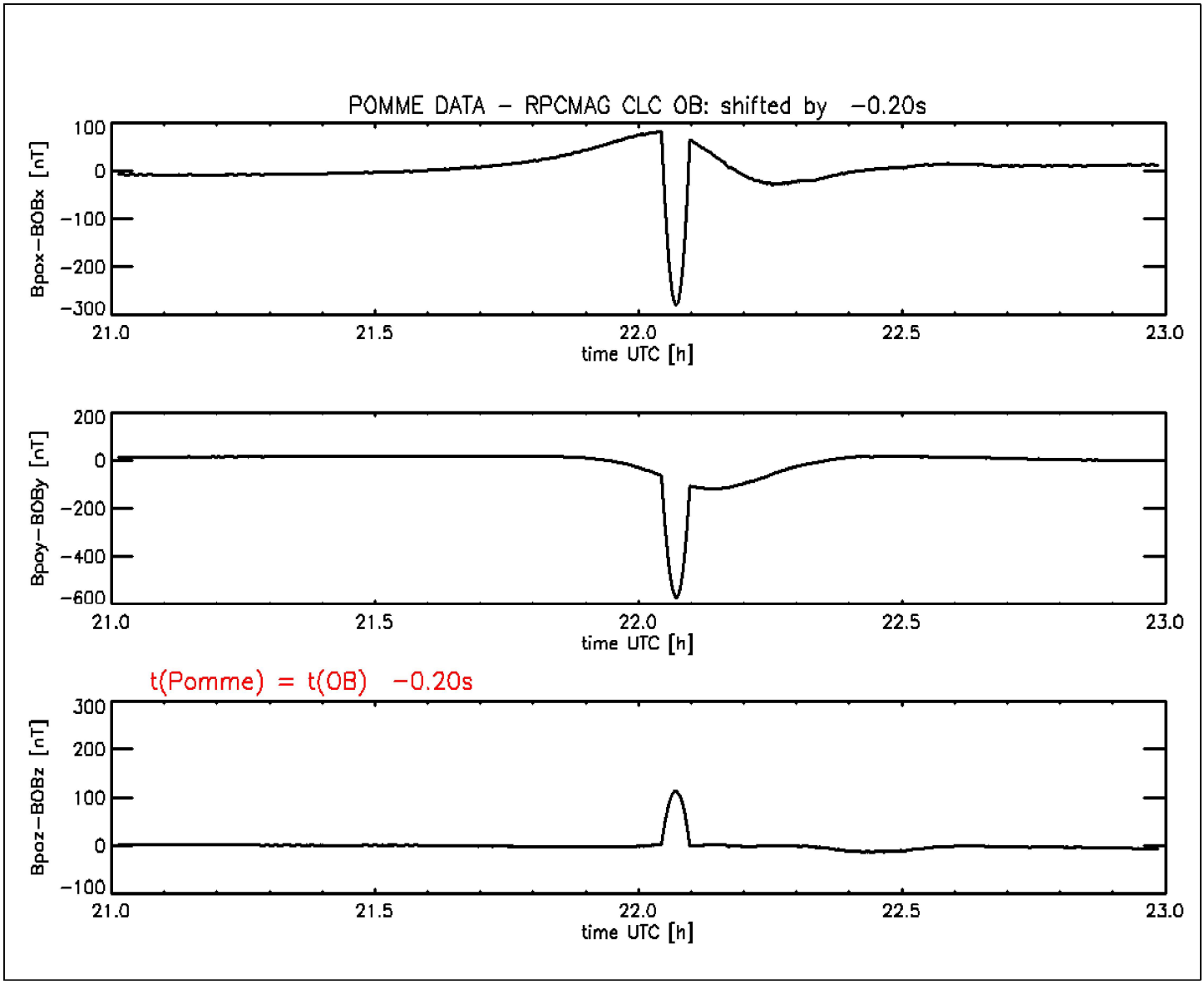

Figure 60: POMME versus OB: Differences of the Components, shifted timing

For the components we get residua in the order of ± 70 nT. The time shifted data show – as expected – nearly the same behaviour.

Analyzing the structure of the deviation the idea arose that the result could be improved by rotation of the sensor reference frame. It could be that the actual orientation of the sensor does not perfectly coincide with the nominal build–in orientation.
To check this the RPCMAG data were feeded into an algorithm that minimizes the variance of the difference between measured and model data by applying three suitable rotations about the main axes. As output the three desired rotation angles are obtained.
The result of the procedure is displayed in Figure 61. This shows impressively that rotations of maximal 0.35° will reduce the error down to ±15 nT.

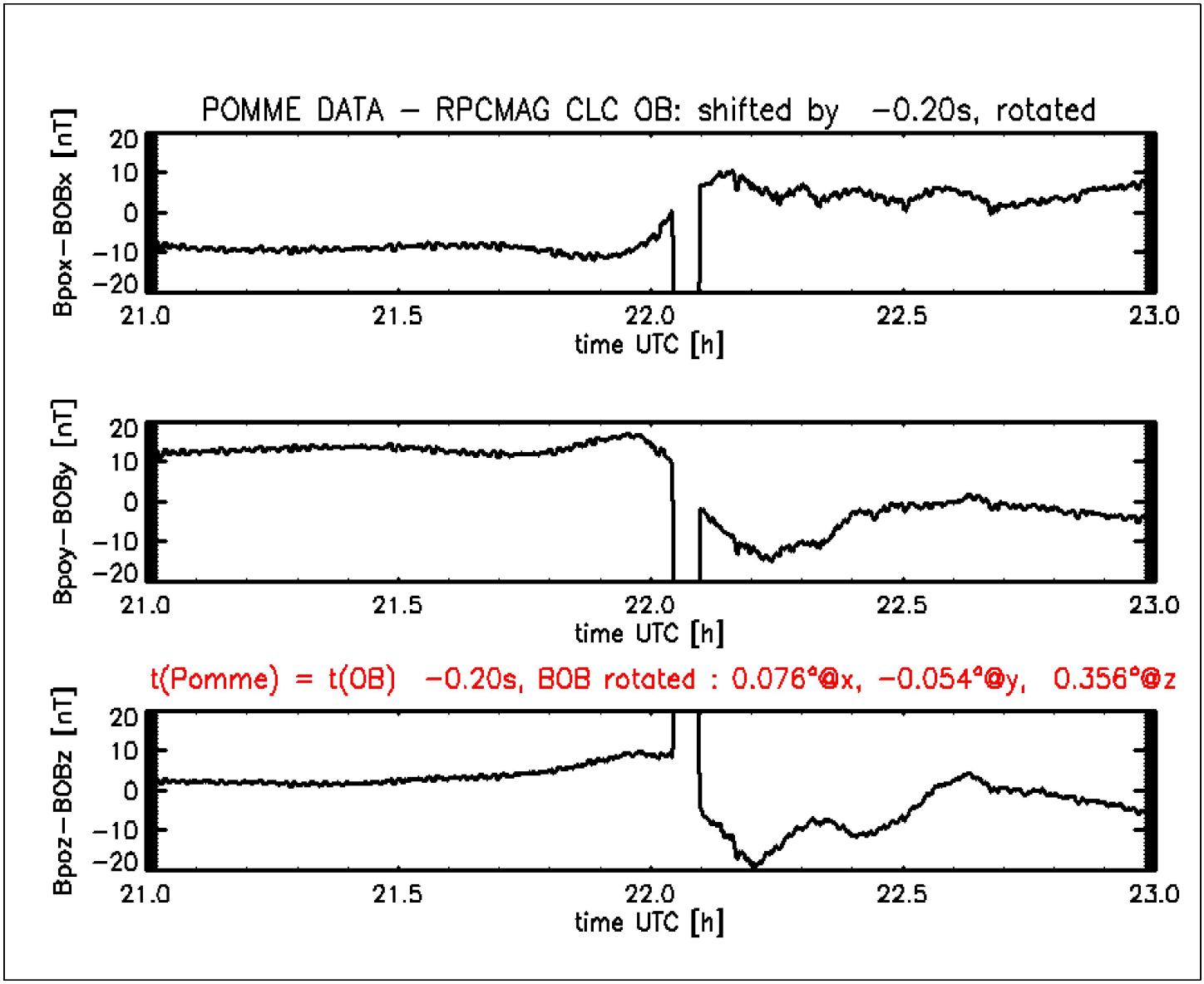

Figure 61: POMME versus OB: Differences of the Components, shifted timing, rotated URF

5.2 Comparison with the IB–Sensor

The same investigation as for the OB has been performed for the IB sensor.

Figure 62 shows the modulus of the IB sensor in the most upper panels and the total field calculated by the POMME model in the second panel. On this large scale the difference are negligible. The computed difference in the bottom panels, however reveals an error of about $\pm$ 5 nT for the most times. Also here we observe a bump in the data for about 4 min just before CA (S/C passed from the Gulf of Mexico via Mexico to the Pacific ocean). There is no external explanation for this bump. We guess that there are movable parts on ROSETTA. In the following investigation we will exclude this specific time interval.

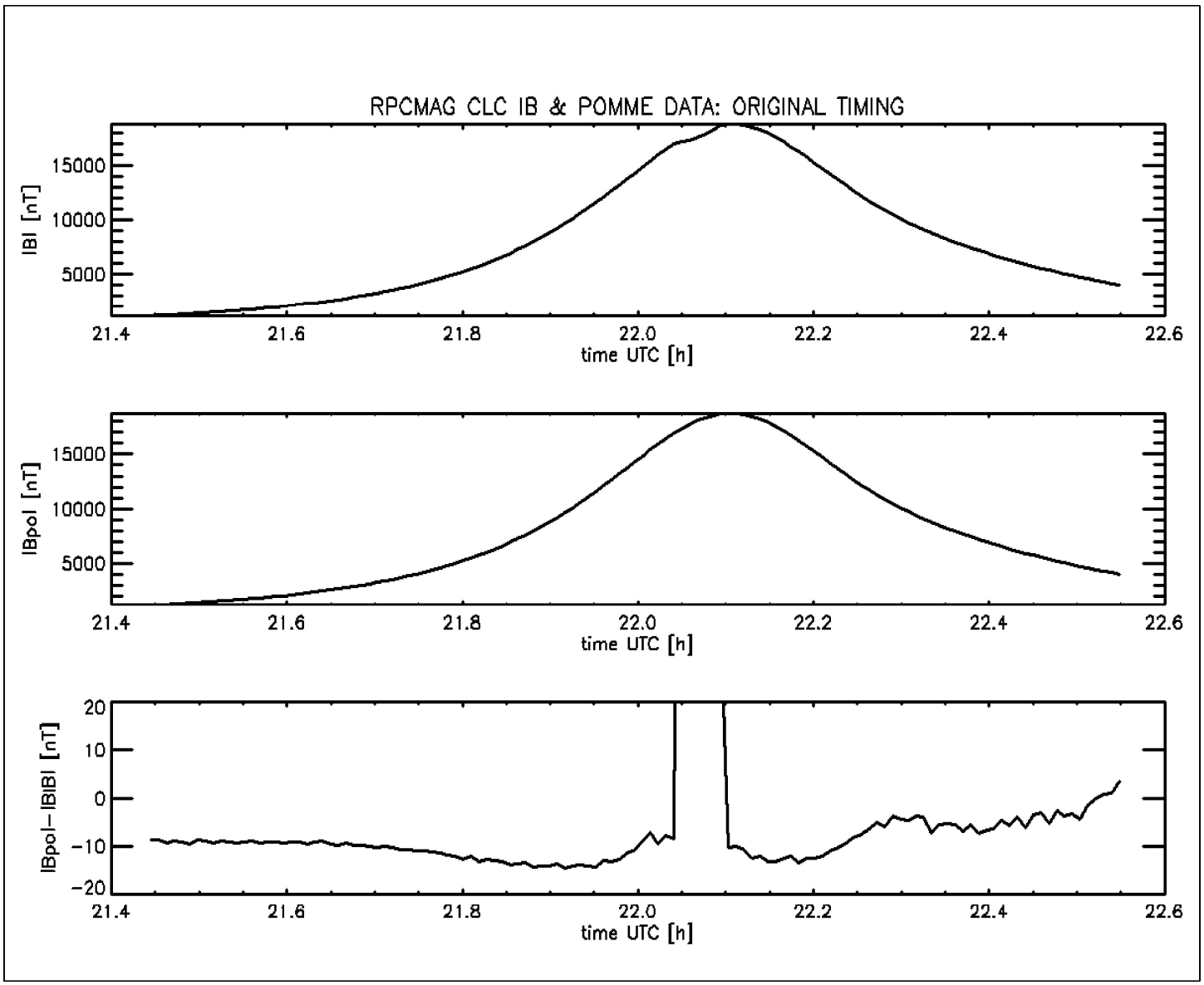

Figure 62: POMME versus IB: Total field, original timing

Also here we tried to shift the data in time to minimize the difference between POMME data and measured data. But as expected the that are already time tagged correctly. The applied shift due to filter delays is -35.62 s for the IB data in normalmode.

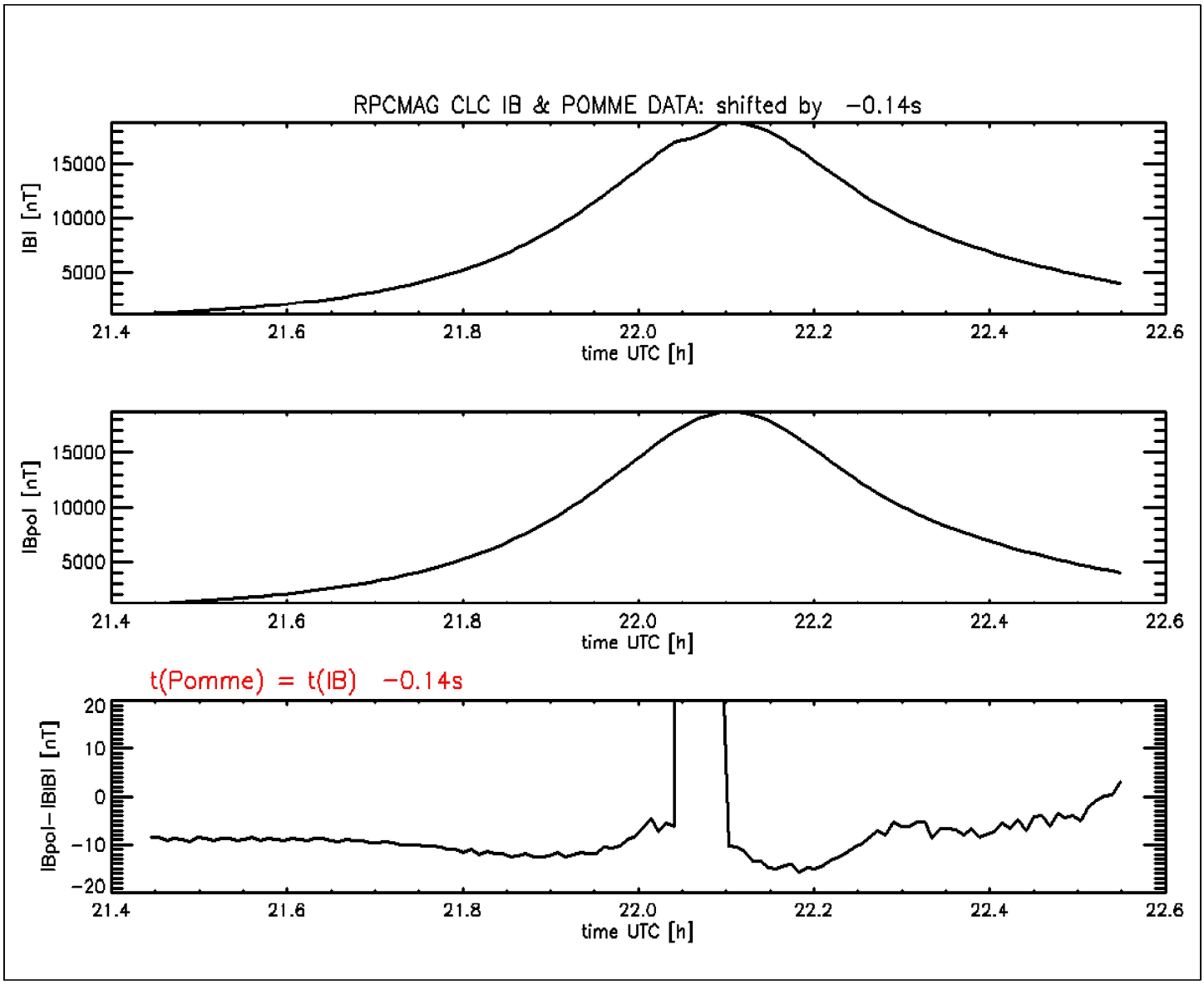

Figure 63: POMME versus IB: Total field, shifted timing

A comparison of the components of the IB sensor and POMME is displayed in Figure 64 for the original timing. At a first view this looks quite good as well. The differences of the model and the measurements are plotted in Figure 65 for the original timing and in Figure 66 for the time shifted data.

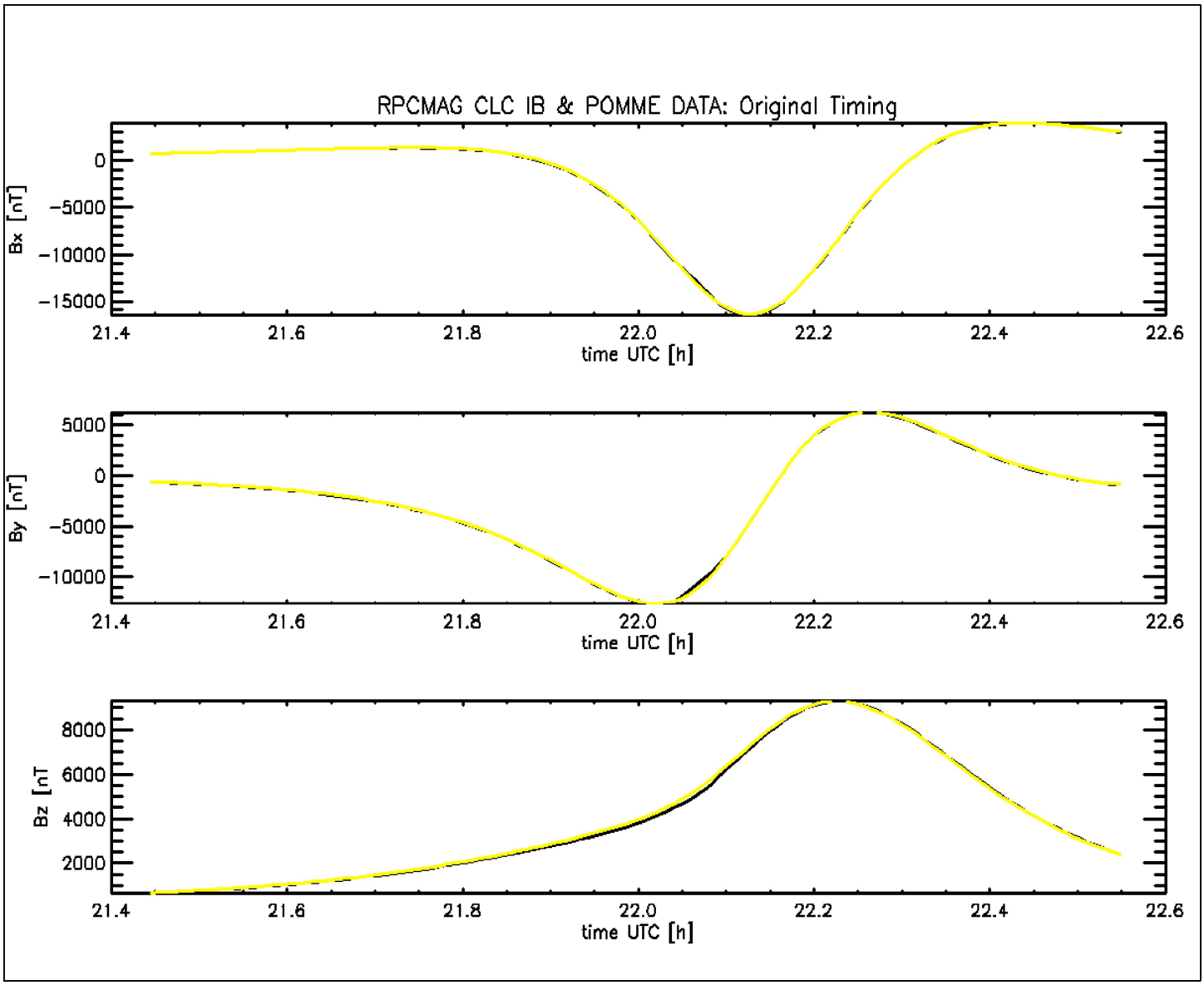

Figure 64: POMME versus IB: Components, original timing

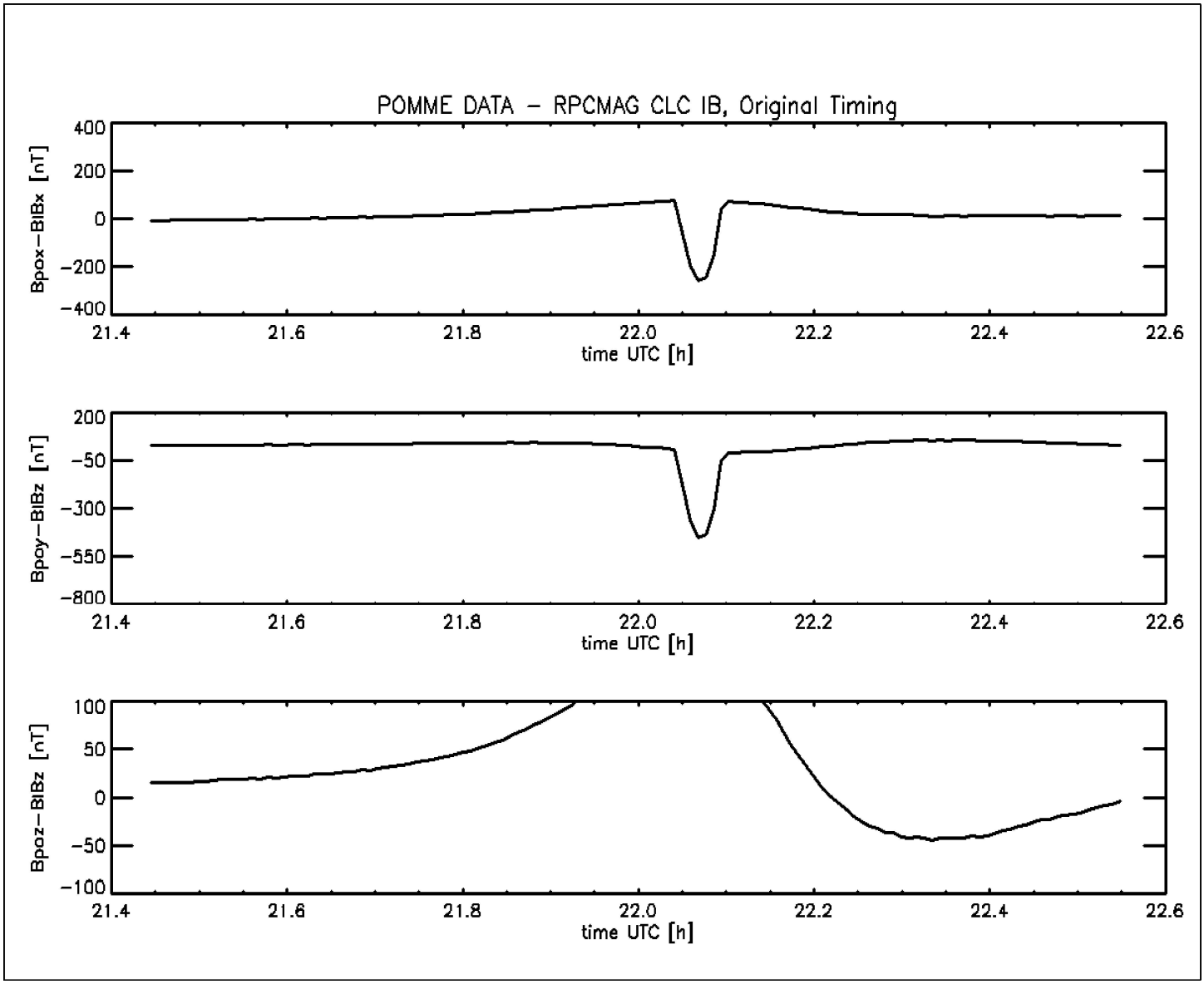

Figure 65: POMME versus IB: Differences of the Components, original timing

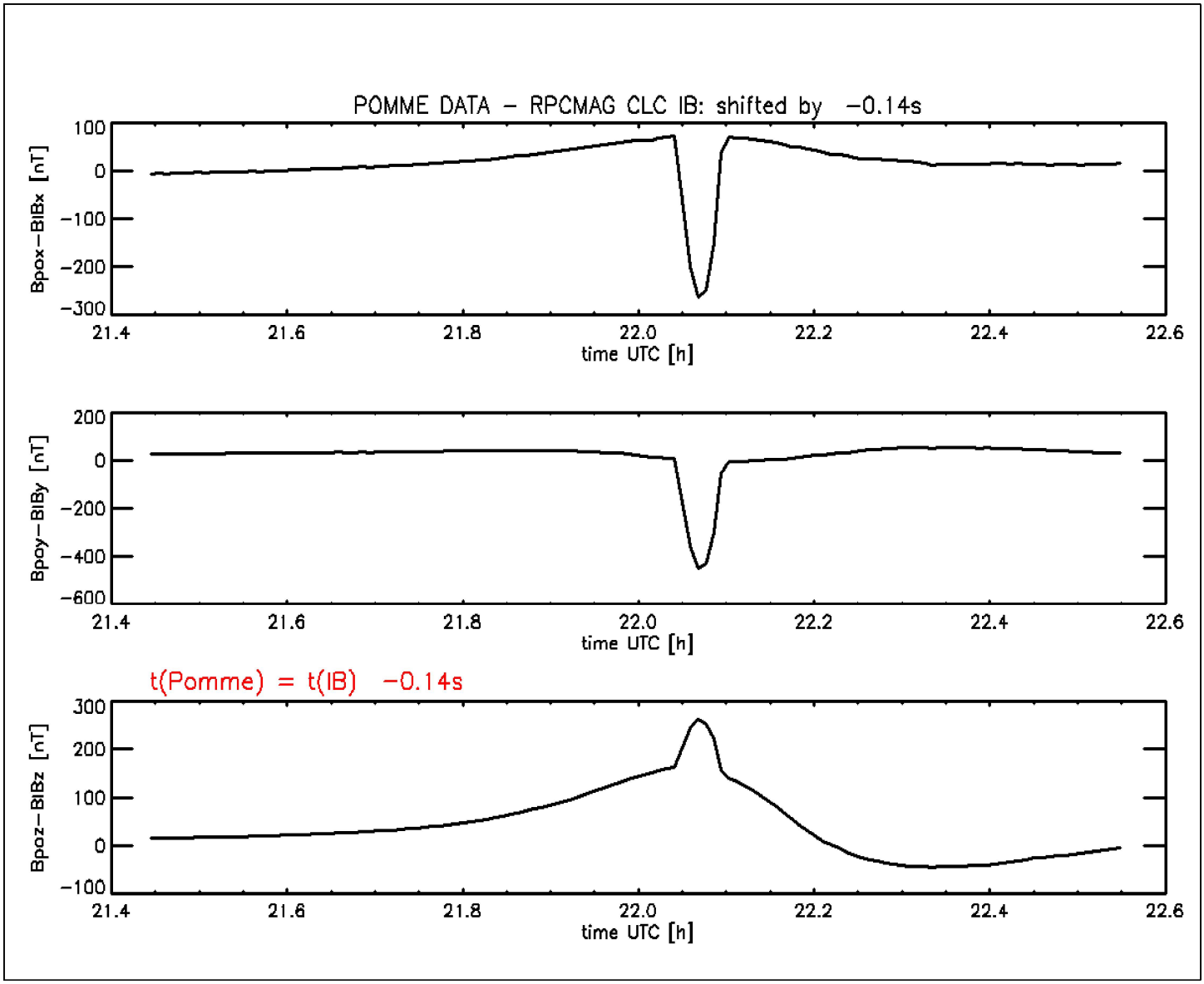

Figure 66: POMME versus IB: Differences of the Components, shifted timing

We get residua in the order of ± 80 nT. Analyzing the structure of the deviation the idea arose that the result could be improved drastically by rotation of the sensor reference frame. It could be that the actual orientation of the sensor does not perfectly coincide with the nominal build–in orientation.
To check this the RPCMAG data were feeded into an algorithm that minimizes the variance of the difference between measured and model data by applying three suitable rotations about the main axes. As output the three desired rotation angles are obtained.
The result of the procedure is displayed in Figure 67. This shows impressively that rotations of maximal 0.45° will reduce the error down to ±15 nT also for the IB sensor.

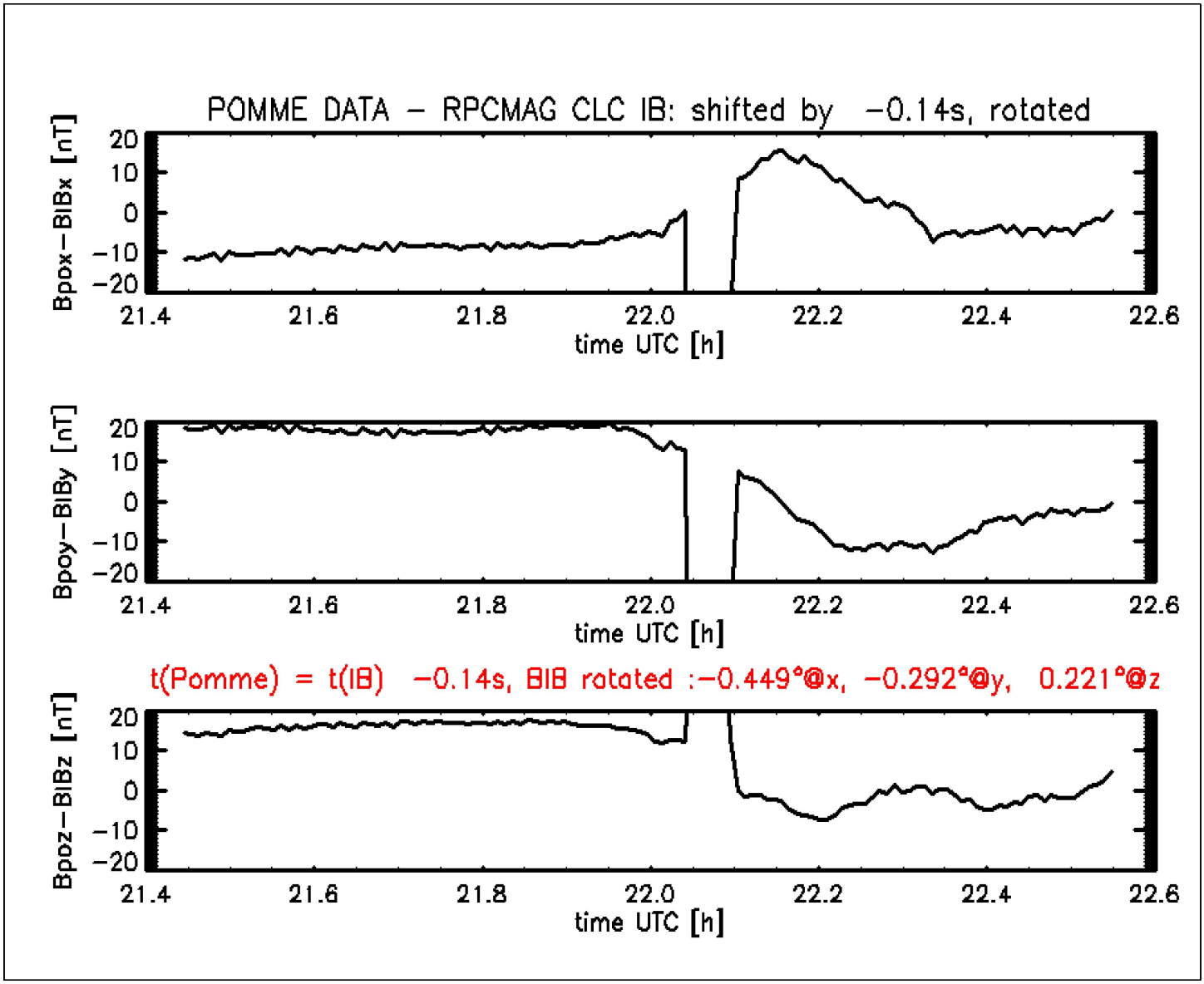

Figure 67: POMME versus IB: Differences of the Components, shifted timing, rotated URF

6 Comparison of the MAG with WIND data

This section show the result of a comparison between the RPCMAG OB data and the magnetic field data measured by the WIND satellite (positioned near the Lagrange Point L_1). The comparison has been executed for March 6, 2005. On this day the Wind Satellite was about 237 R_E = 1514768 km away from the Earth. Assuming a reasonable solar wind speed of 537 km/s there should be a time lag of 47 min between WIND data and RPCMAG data. Exactly this time delay has to be taken into account to obtain the best coincidence between both time series. The related correlation coefficient is 0.89.
The plots shows a good accordance for OB as for IB as well for the complete day.

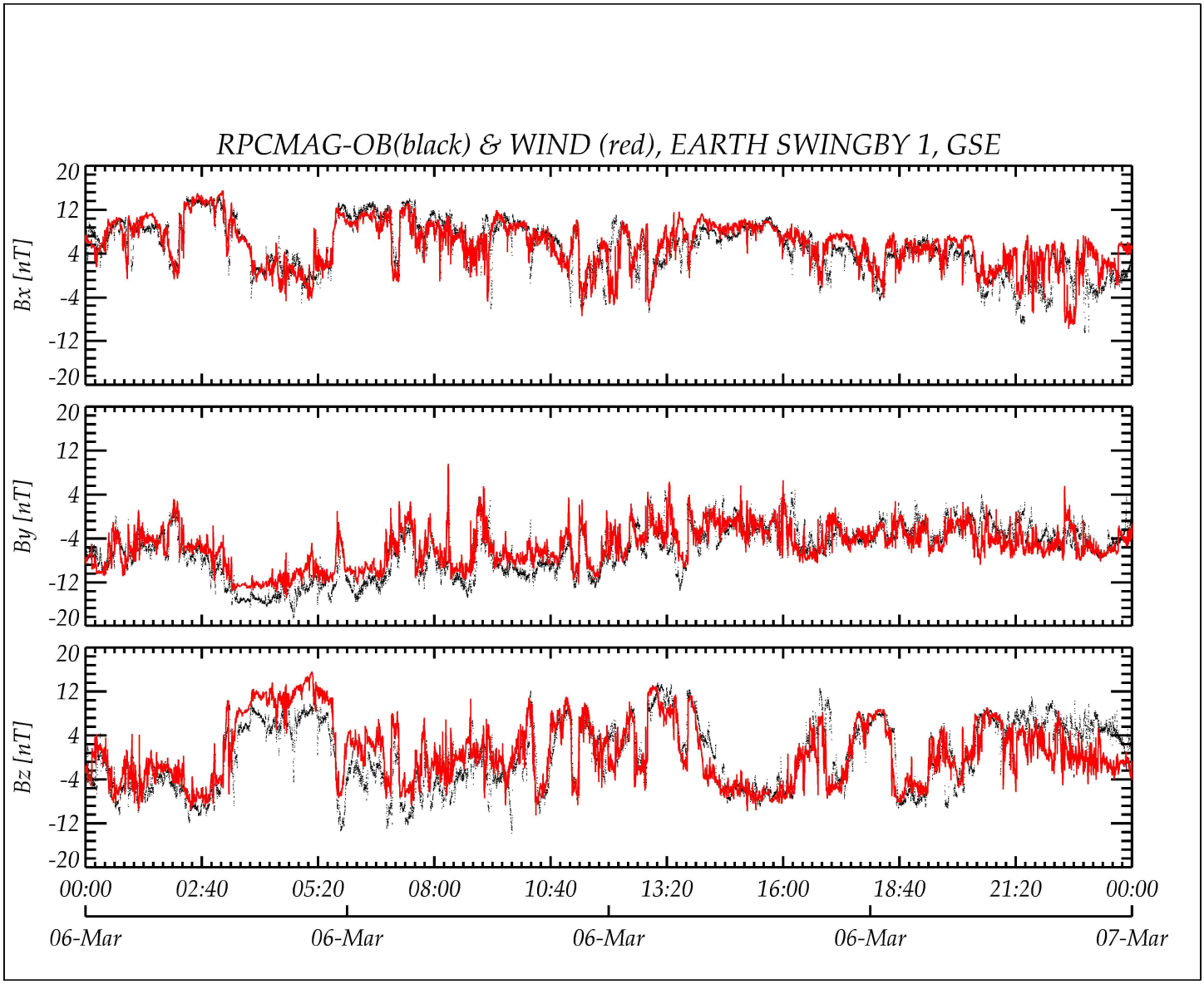

Figure 68: ROMAP OB versus WIND data

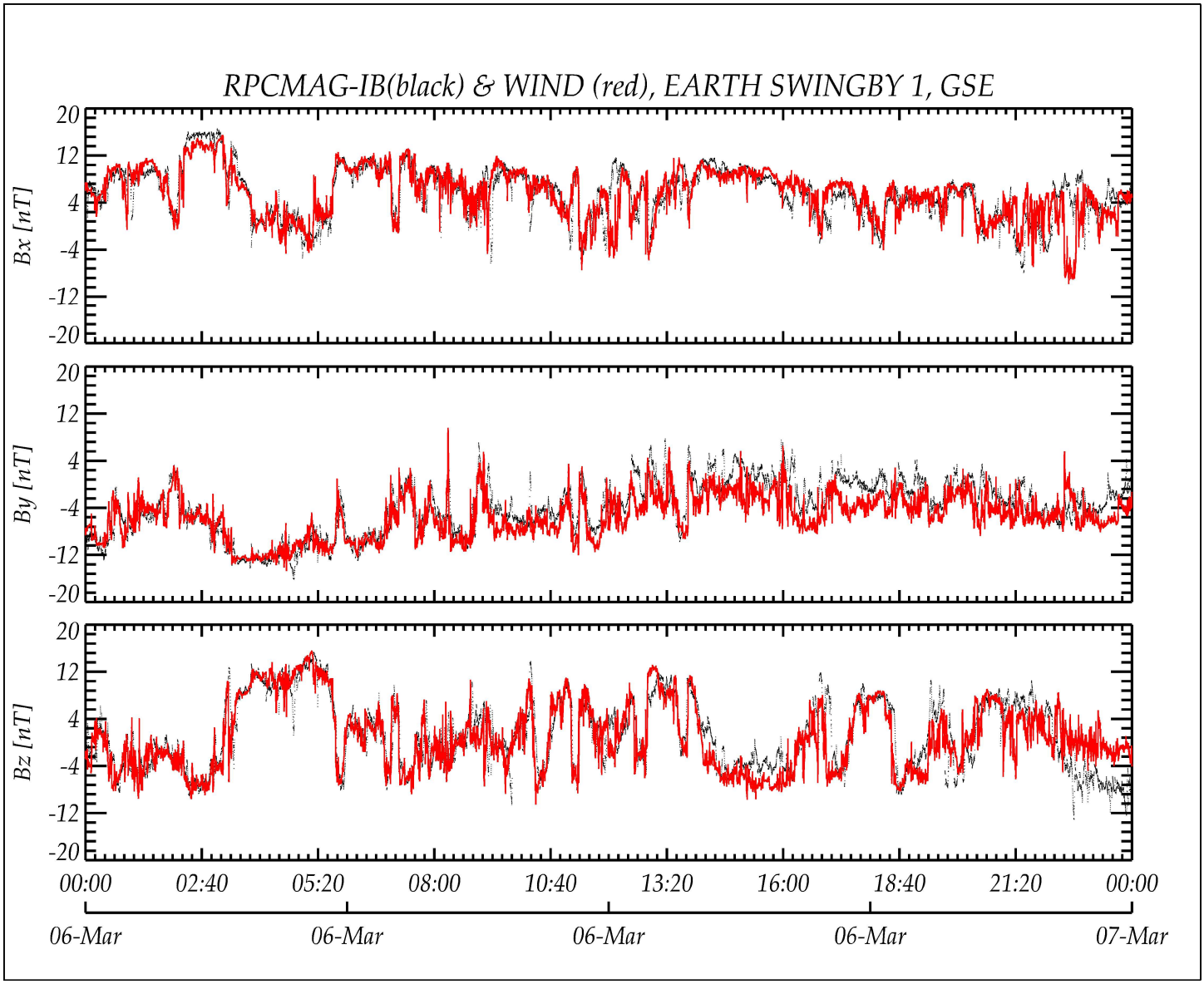

Figure 69: ROMAP IB versus WIND data

7 Dynamic Spectra of the Swing by

This section shows the dynamic spectra of the OB sensor in LEVEL_C = ECLIPJ2000 coordinates. As the sensor was operated as primary sensor in NORMAL mode, SID2, the maximum resolvable frequency is 0.5 Hz. The spectra show significant structures from afternoon of March 1 until the morning of March 5. These horizontal lines are harmonics of a base frequency of 1/30 Hz which is caused by pulsed heaters on the LANDER (refer to section 9)

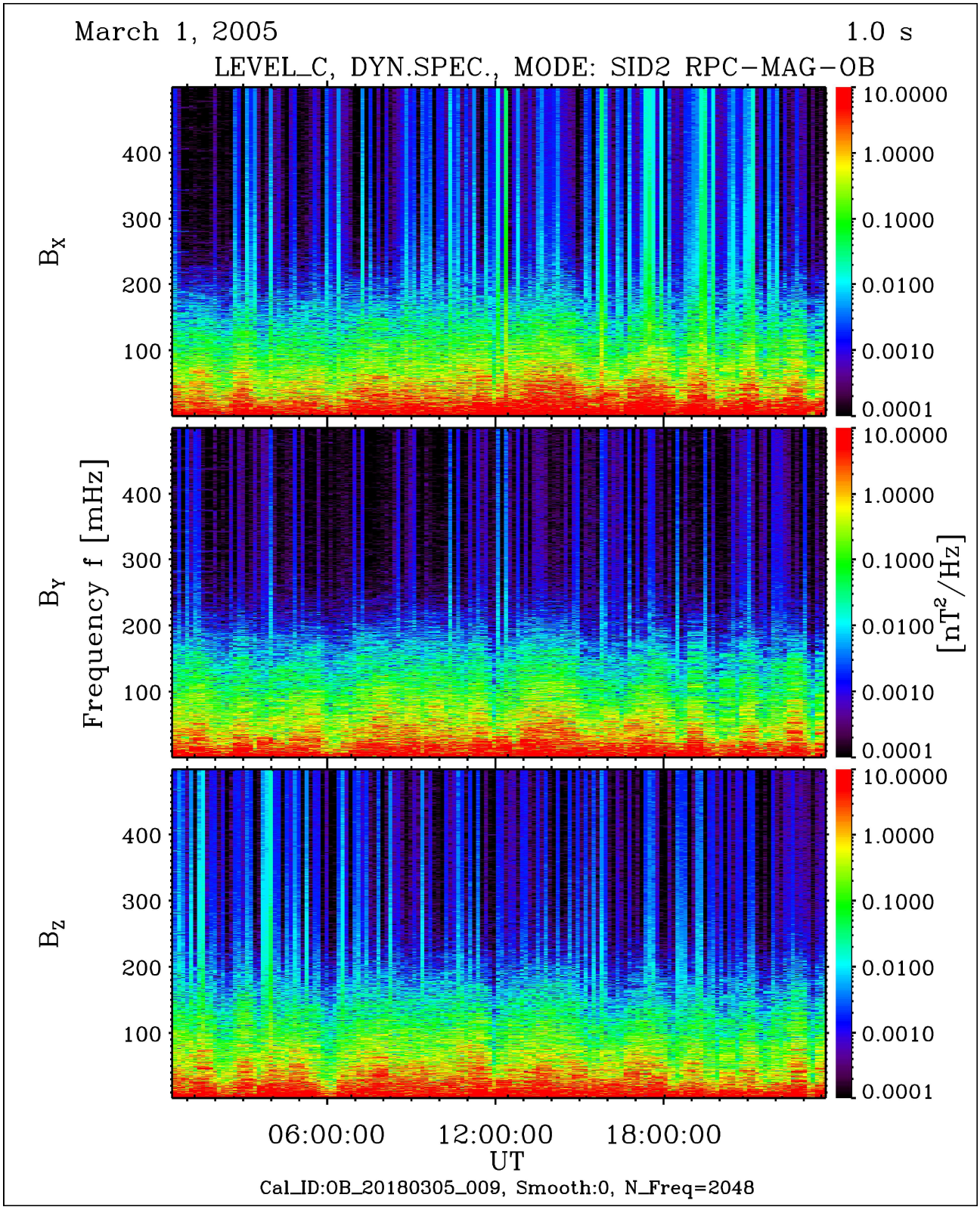

Figure 70: File: RPCMAG050301T0014_CLC_OB_M2_DS0_500_009

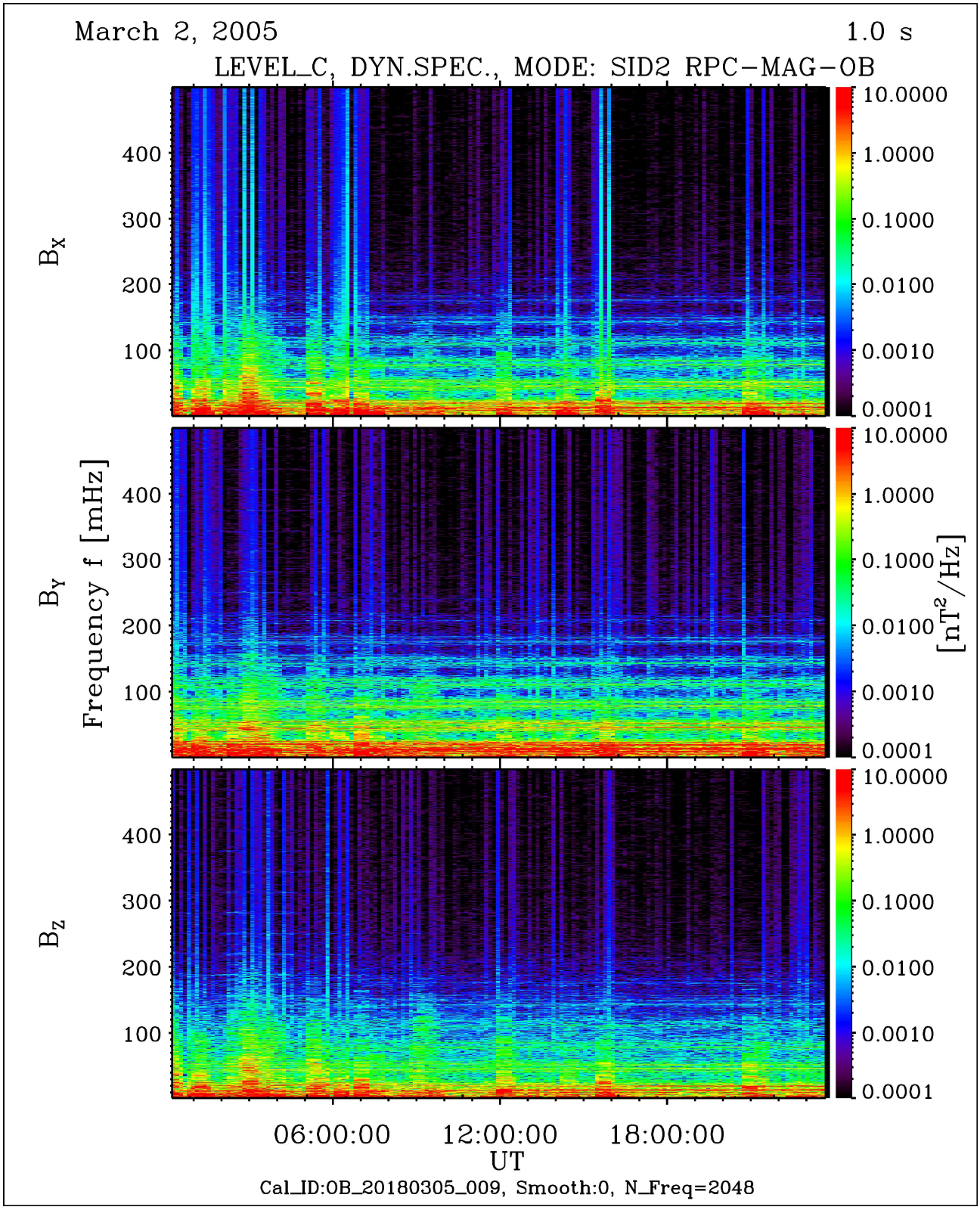

Figure 71: File: RPCMAG050302T0000_CLC_OB_M2_DS0_500_009

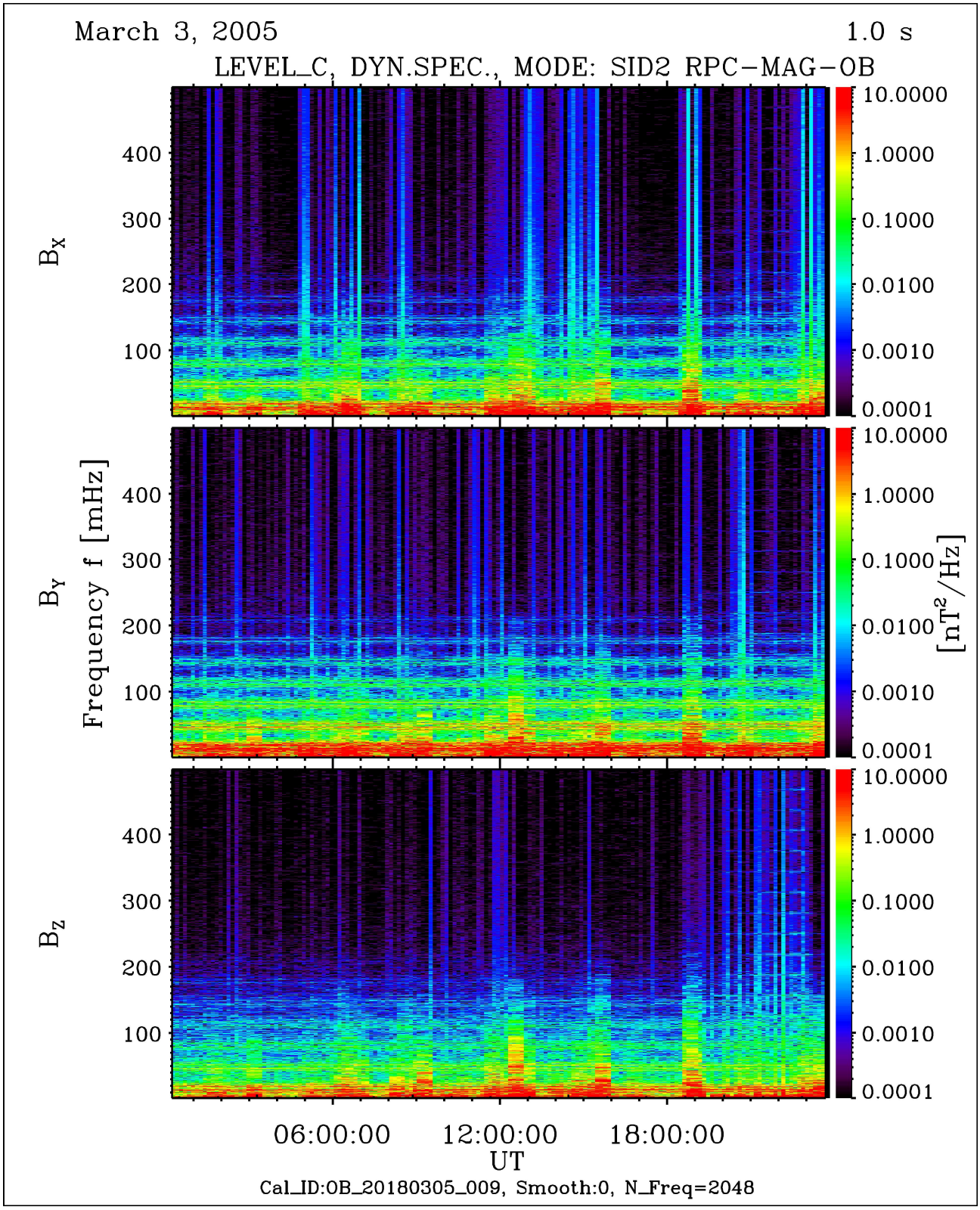

Figure 72: File: RPCMAG050303T0000_CLC_OB_M2_DS0_500_009

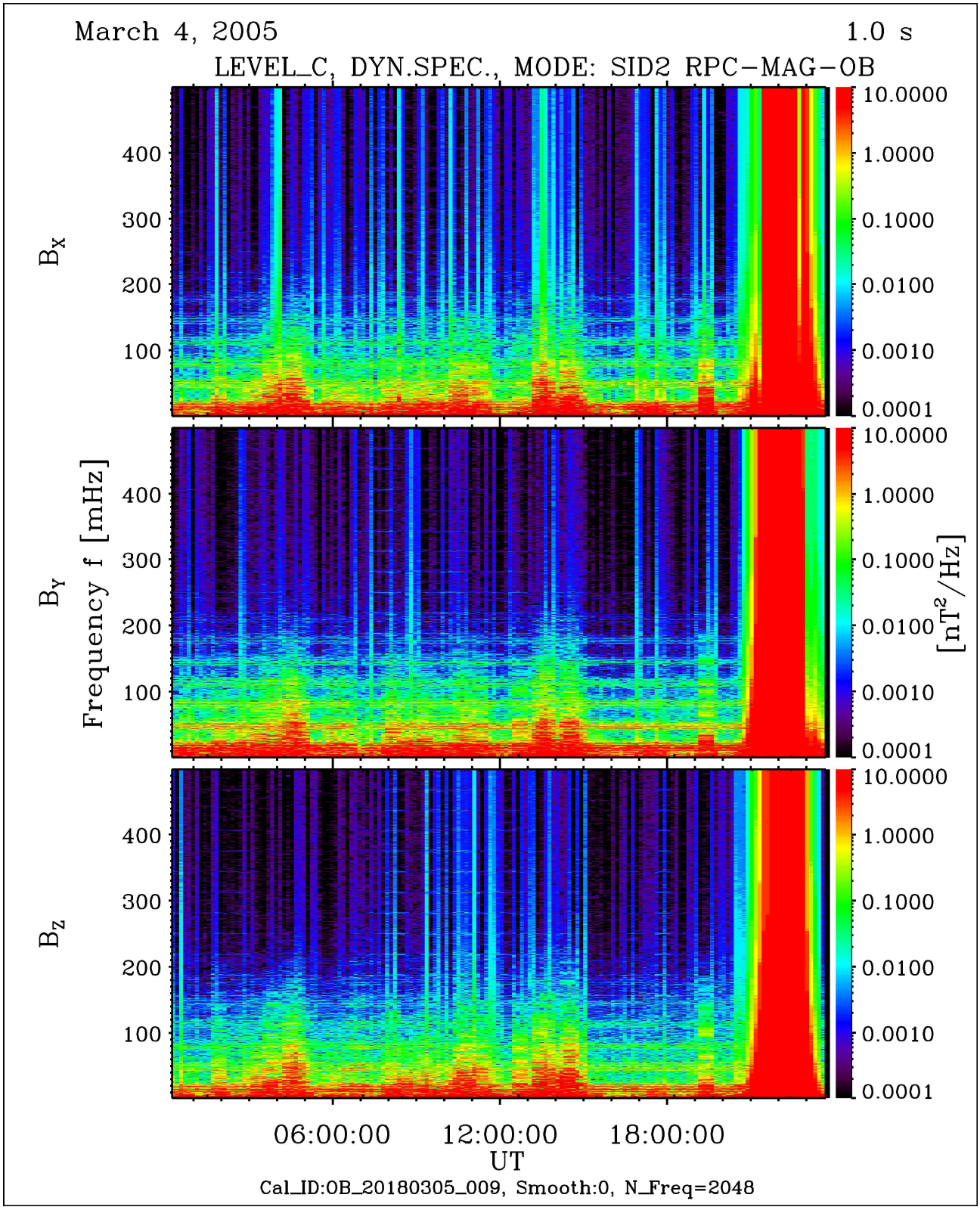

Figure 73: File: RPCMAG050304T0000_CLC_OB_M2_DS0_500_009

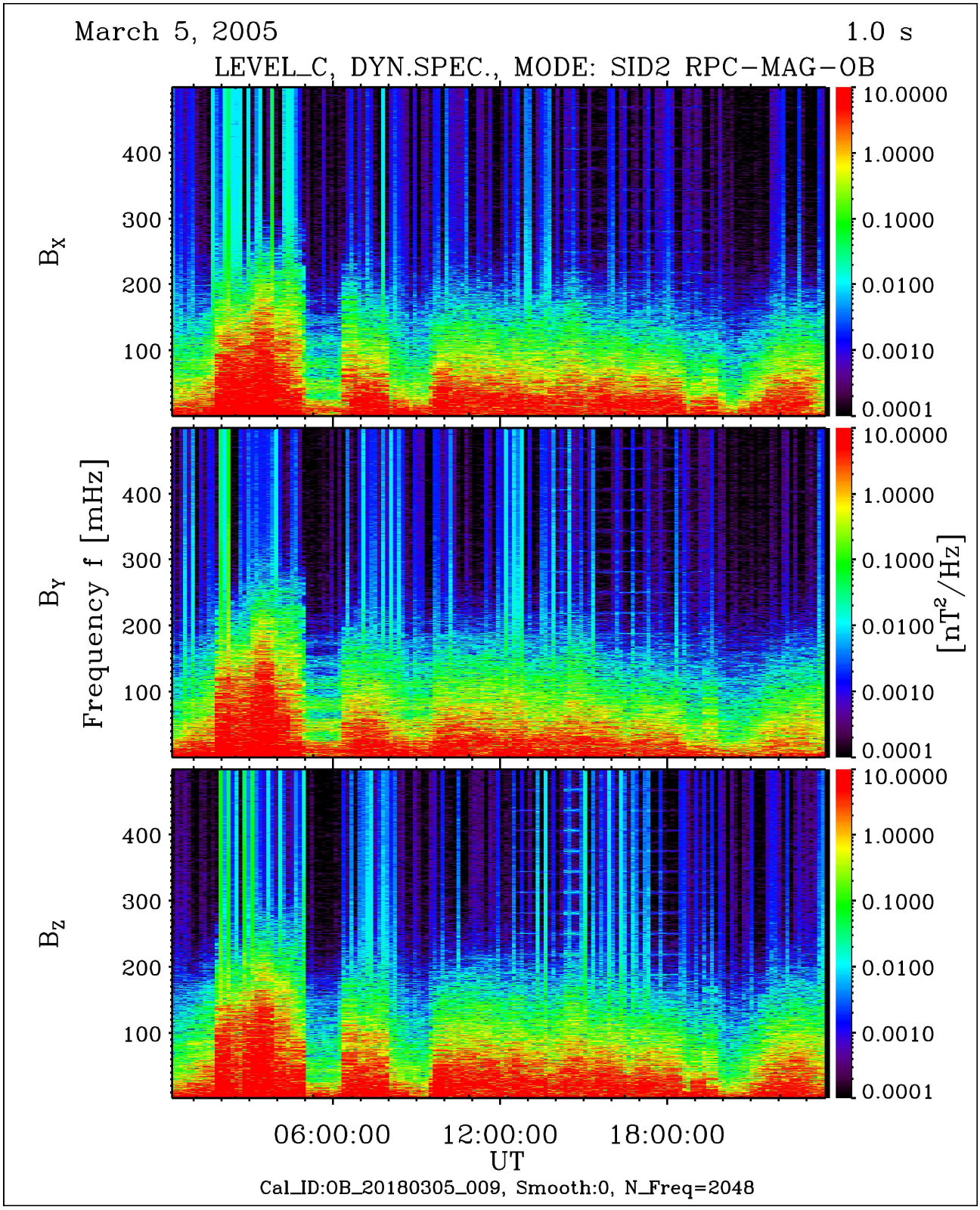

Figure 74: File: RPCMAG050305T0000_CLC_OB_M2_DS0_500_009

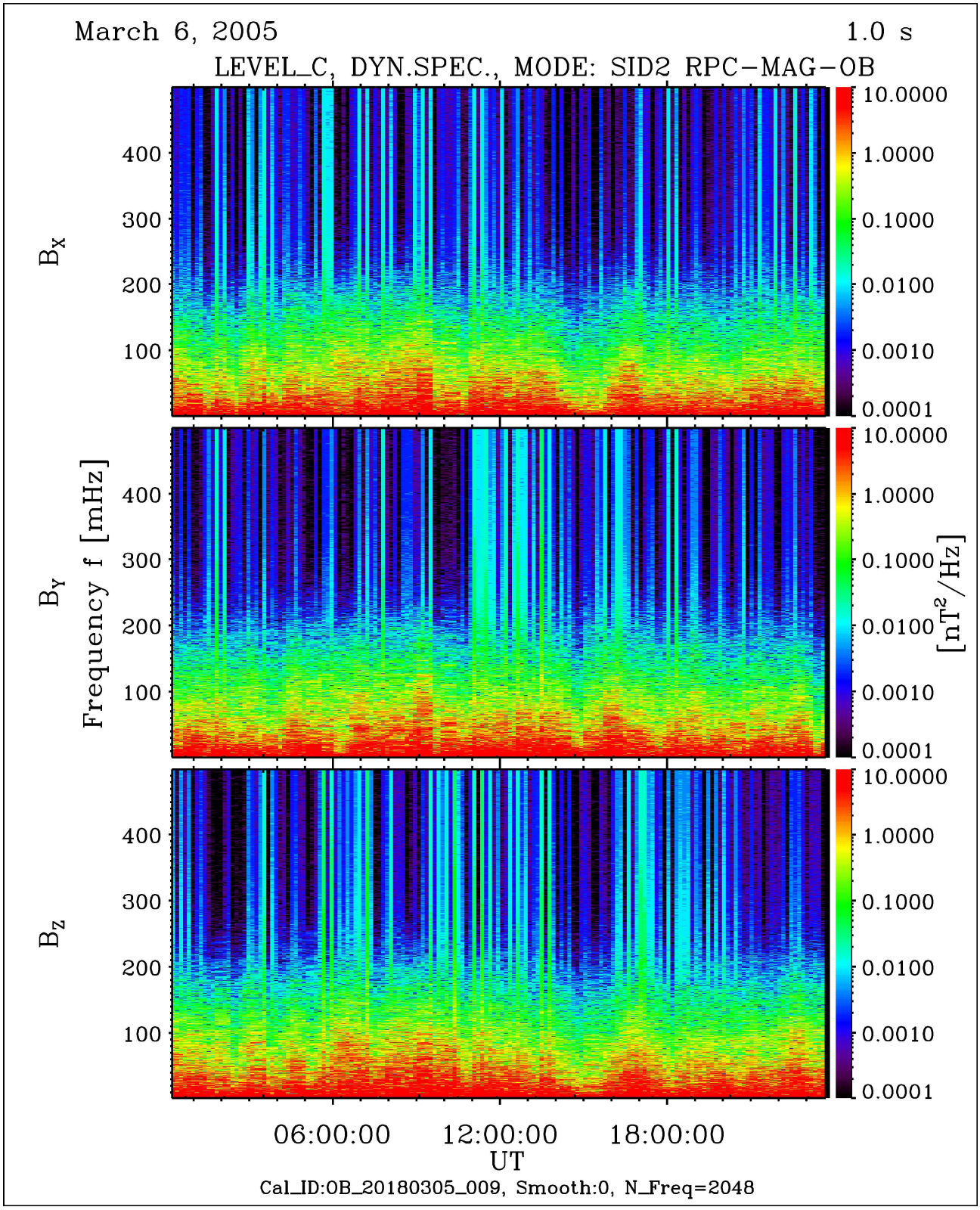

Figure 75: File: RPCMAG050306T0000_CLC_OB_M2_DS0_500_009

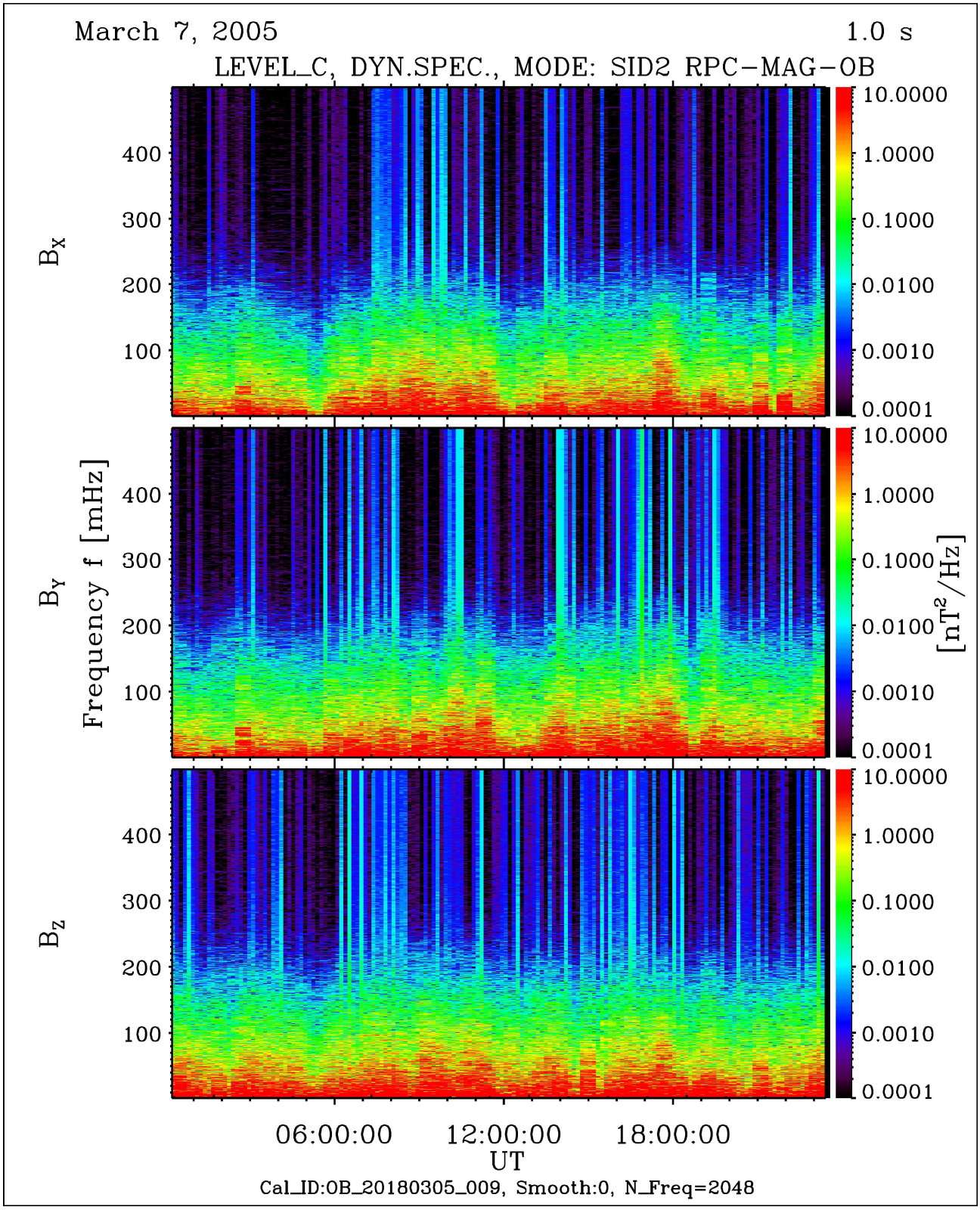

Figure 76: File: RPCMAG050307T0000_CLC_OB_M2_DS0_500_009

8 Dynamic Spectra of ROSETTAs REACTION WHEELS

This section shows the spectra of ROSETTAs Reaction Wheels (RW). There are 4 different wheels rotating with different frequencies. The plots do not show the original rotation frequencies but the signatures that would be expected using an data acquisition system operating at 1 Hz sampling frequency without any aliasing filter.
These signatures are expected to be seen on the OB sensor operated in NORMAL modes, SID2 due to our experiences from the commissioning phase.

However, a view to the spectra of the measured magnetic field (refer to section 7) shows , that there is actually no influence of the RWs. The magnetic field spectra are clean.

The MAG team is happy about this, although there is no explanation for the disappearance of the RW impact.

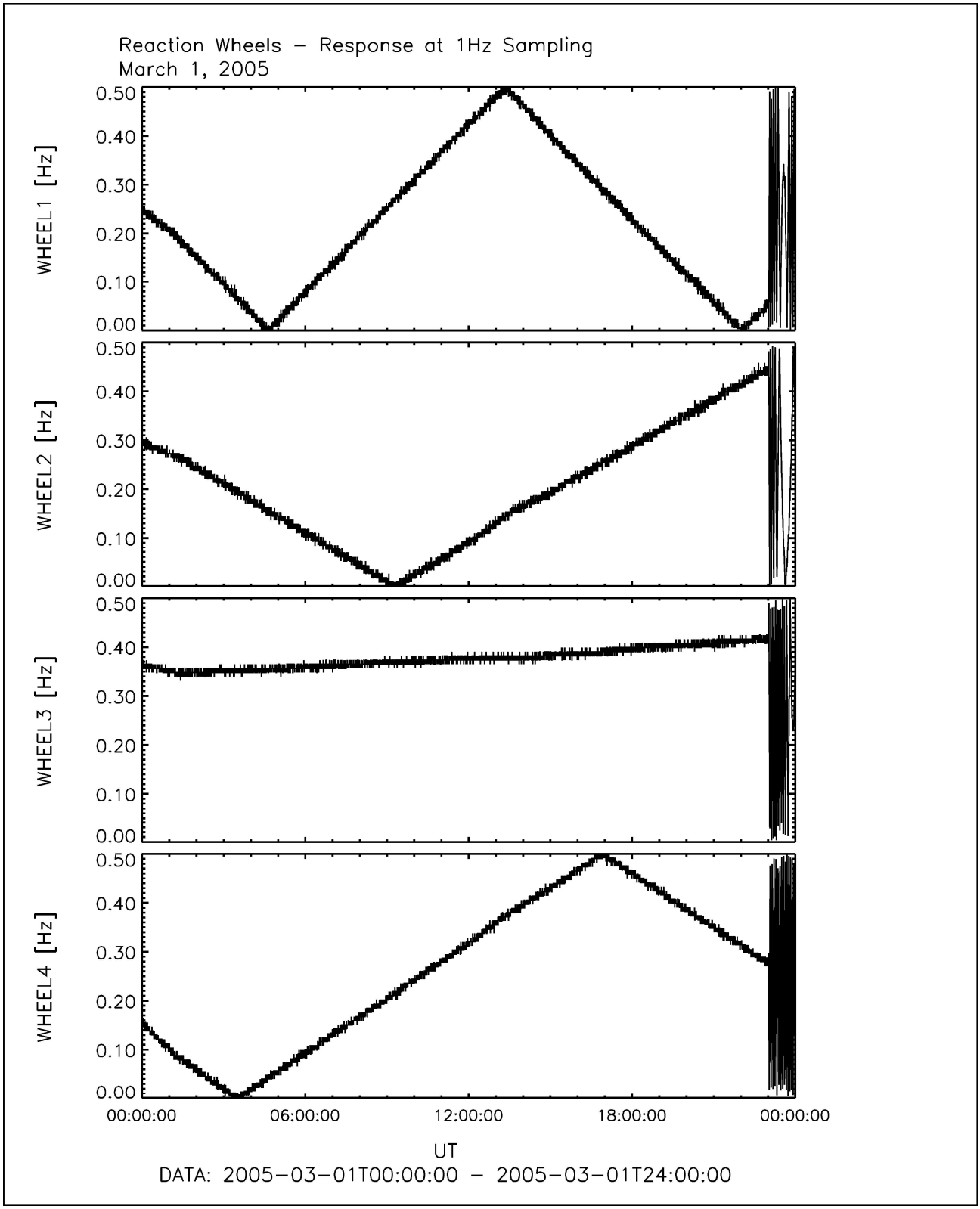

Figure 77: File: wheels_1Hz_Sampling2005-03-01T00-00

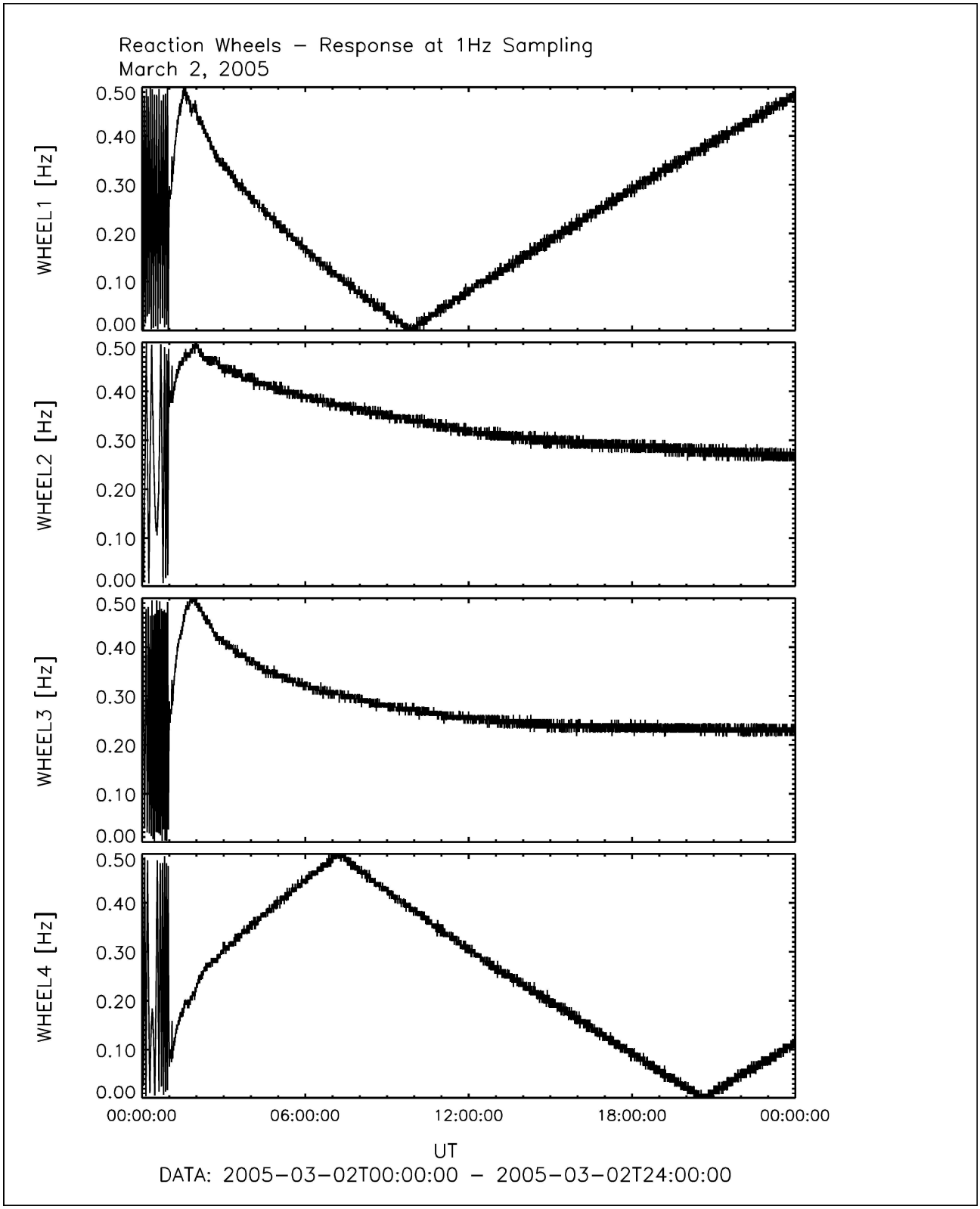

Figure 78: File: wheels_1Hz_Sampling2005-03-02T00-00

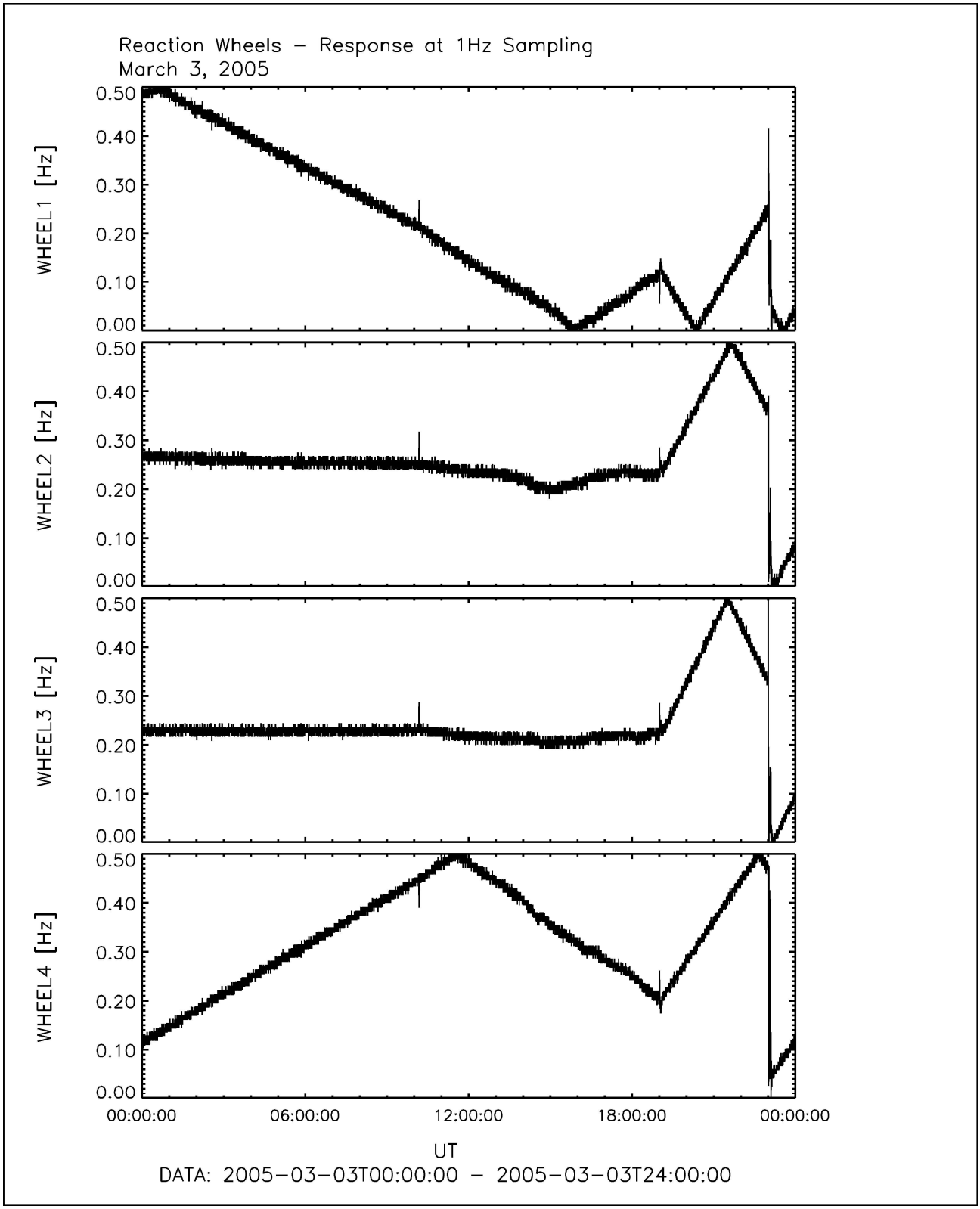

Figure 79: File: wheels_1Hz_Sampling2005-03-03T00-00

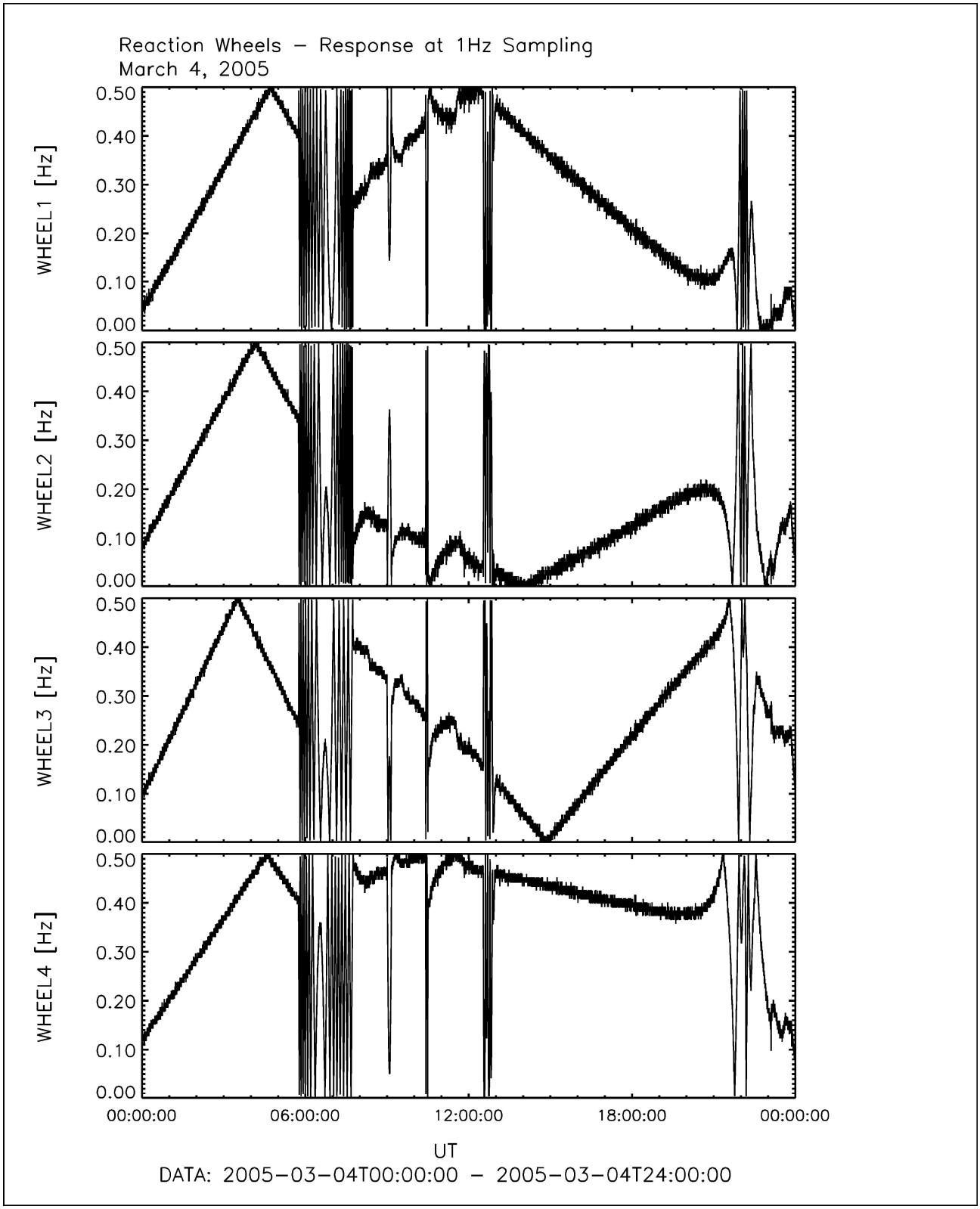

Figure 80: File: wheels_1Hz_Sampling2005-03-04T00-00

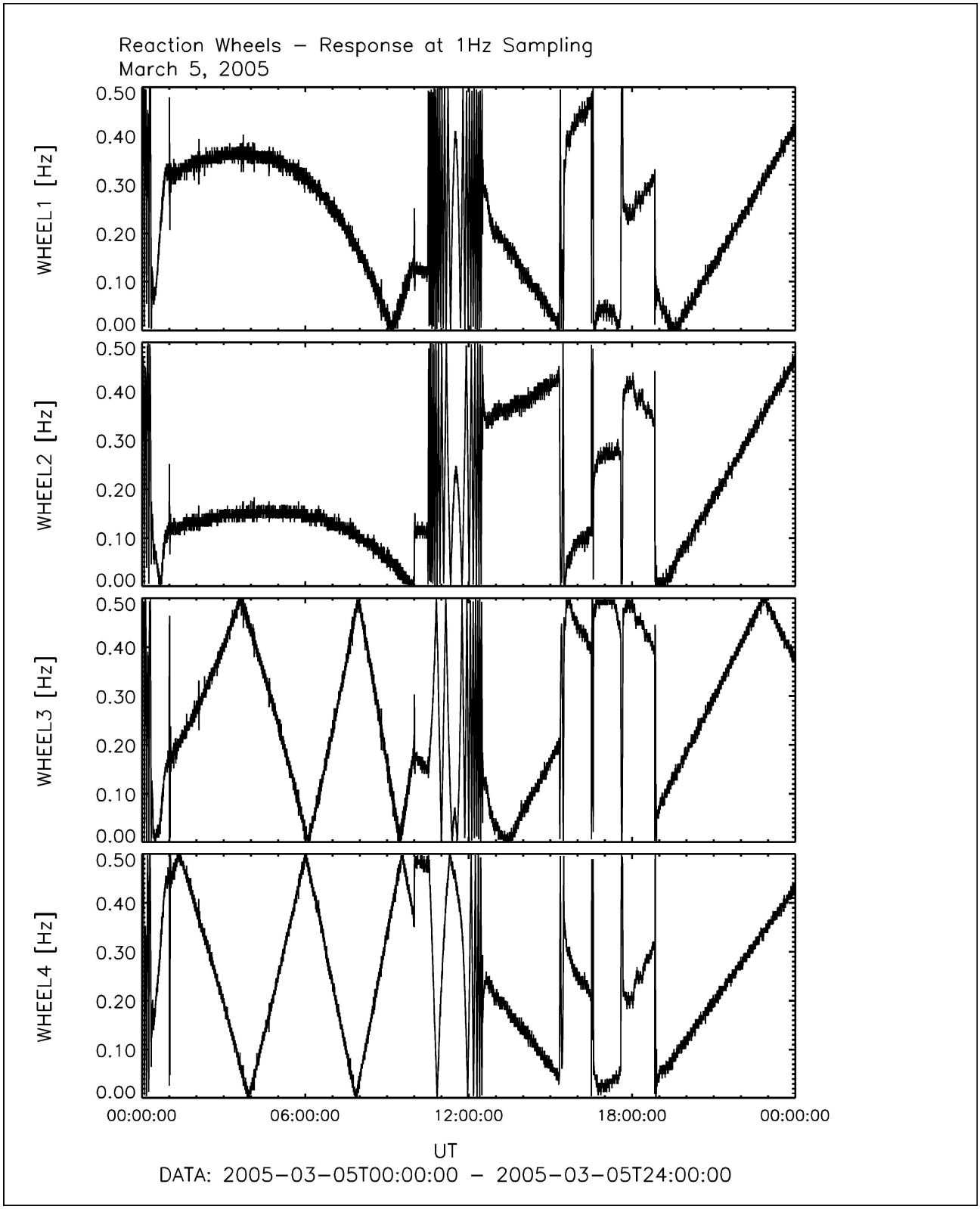

Figure 81: File: wheels_1Hz_Sampling2005-03-05T00-00

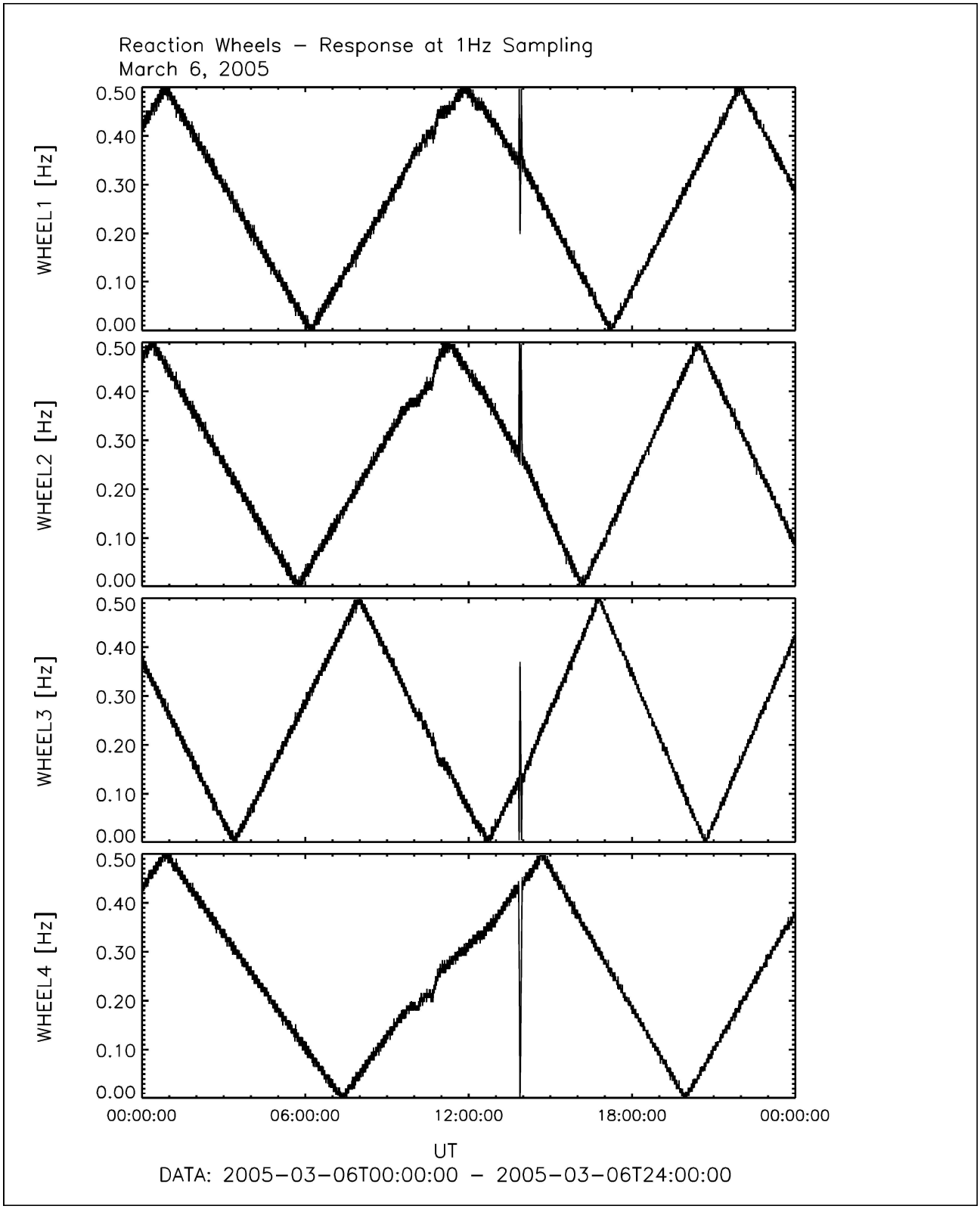

Figure 82: File: wheels_1Hz_Sampling2005-03-06T00-00

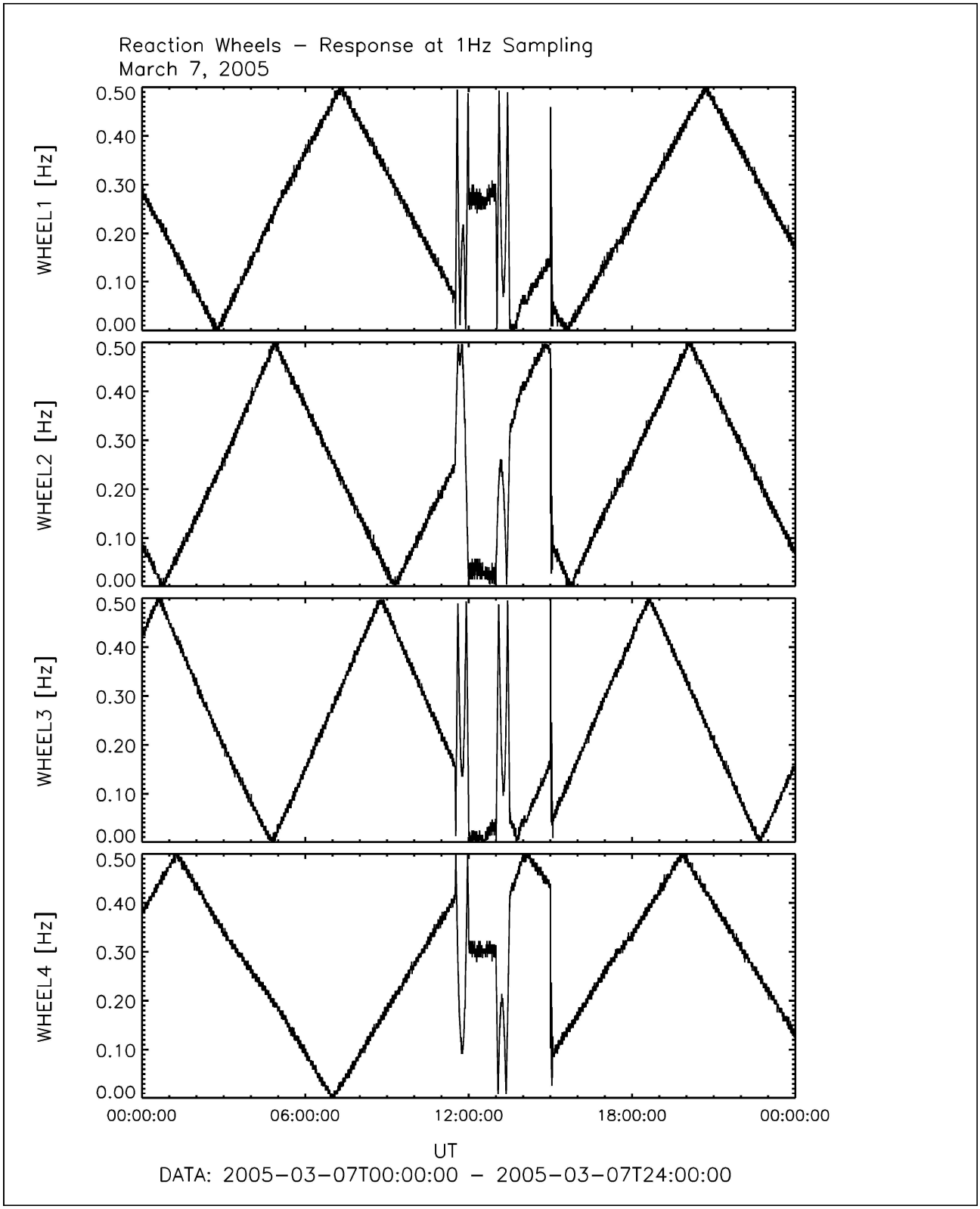

Figure 83: File: wheels_1Hz_Sampling2005-03-07T00-00

9 The impact and elimination of the LANDER heaters

During EAR1 RPCMAG had the worthy chance to perform parallel measurements with the Lander magnetometer ROMAP. ROMAP was switched on from 2005-03-01T01:00 until 2005-03-07T03:30. As, however, already mentioned, the Lander heaters were tested as well in the time from afternoon of March 1 until the morning of March 5. These heaters cause disturbances in the order of 1000—2000 nT at the ROMAP sensors and disturbances in the order of 0.5 — 1.5 nT at the RPCMAG OB sensor.

This section will show the impact of the heaters to the MAG OB sensor and the method to eliminate these disturbances.

Figure 84 shows a randomly chosen interval (March 3, 00:00 — 24:00) of RPCMAG OB data. On the first view these data look like proper magnetic field data. If we, however, zoom into the data, as done for randomly chosen interval of 30 minutes, we can clearly identify a disturbing signal in shape of a square wave with a period of T=30 s. The amplitude is not constant, but appearing with 4 different levels. This is related to three different kind of heaters (respective different currents) located on the Lander.

This disturbed signal in B_x, B_y, B_z components (ECLIPJ2000–coordinates) is redisplayed in Figure 85. As it is easier to perform a convenient signal processing on one component with a clearly disturbed signal rather than on three slightly disturbed ones, the idea arose to turn the measured magnetic field signal into a minimum variance system. The result of this preprocessing transformation can be impressively seen in Figure 86. The complete disturbance is now superimposed on the B_x signal whereas the B_y and B_z components in the MINVAR system completely purged.

The real processing is visualized in Figure 87. The most upper panels shows the preprocessed data rotated into the B_x component of the minimum variance system (which is actually the component with the maximum variance.)
The second panel shows the detection of the jumps. This is done using a moving variance indicator. A short time variance of just a few samples is evaluated and shifted step by step over the whole times series (dark blue curve). As a result strong positive peaks occur at the times of the jumps, and a nearly flat signal dominates the other times. In a second step a threshold (light blue line) has to be defined to separate between jumps and "normal" data. Everything below this threshold belongs to right data, everything above this threshold is interpreted as jump caused by the heaters.
The third panels shows the separated step in the B_x time series. The times of the jumps and intermediate values are cut out.

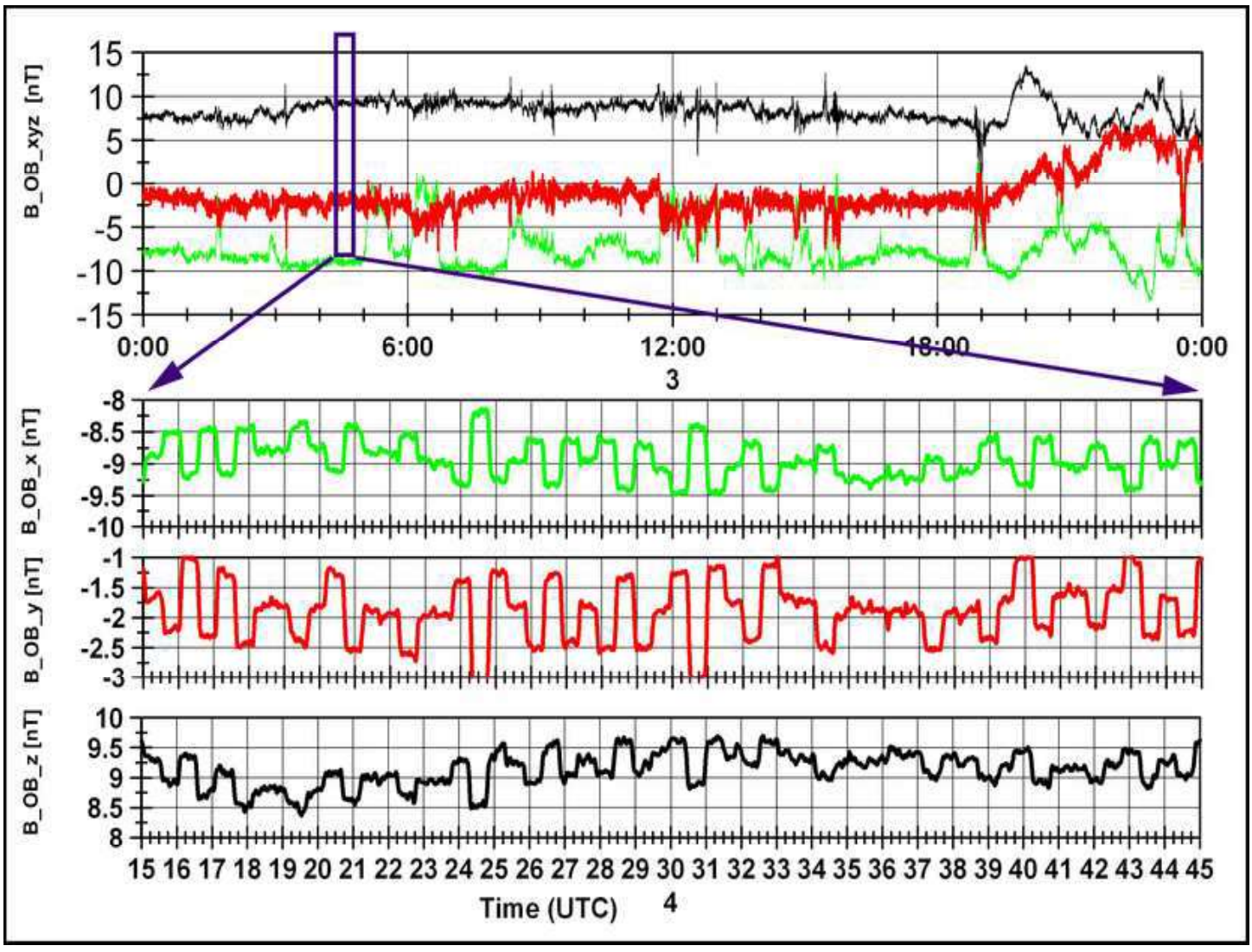

Figure 84: Original and zoomed Signal of March 3 (ECLIPJ2000).

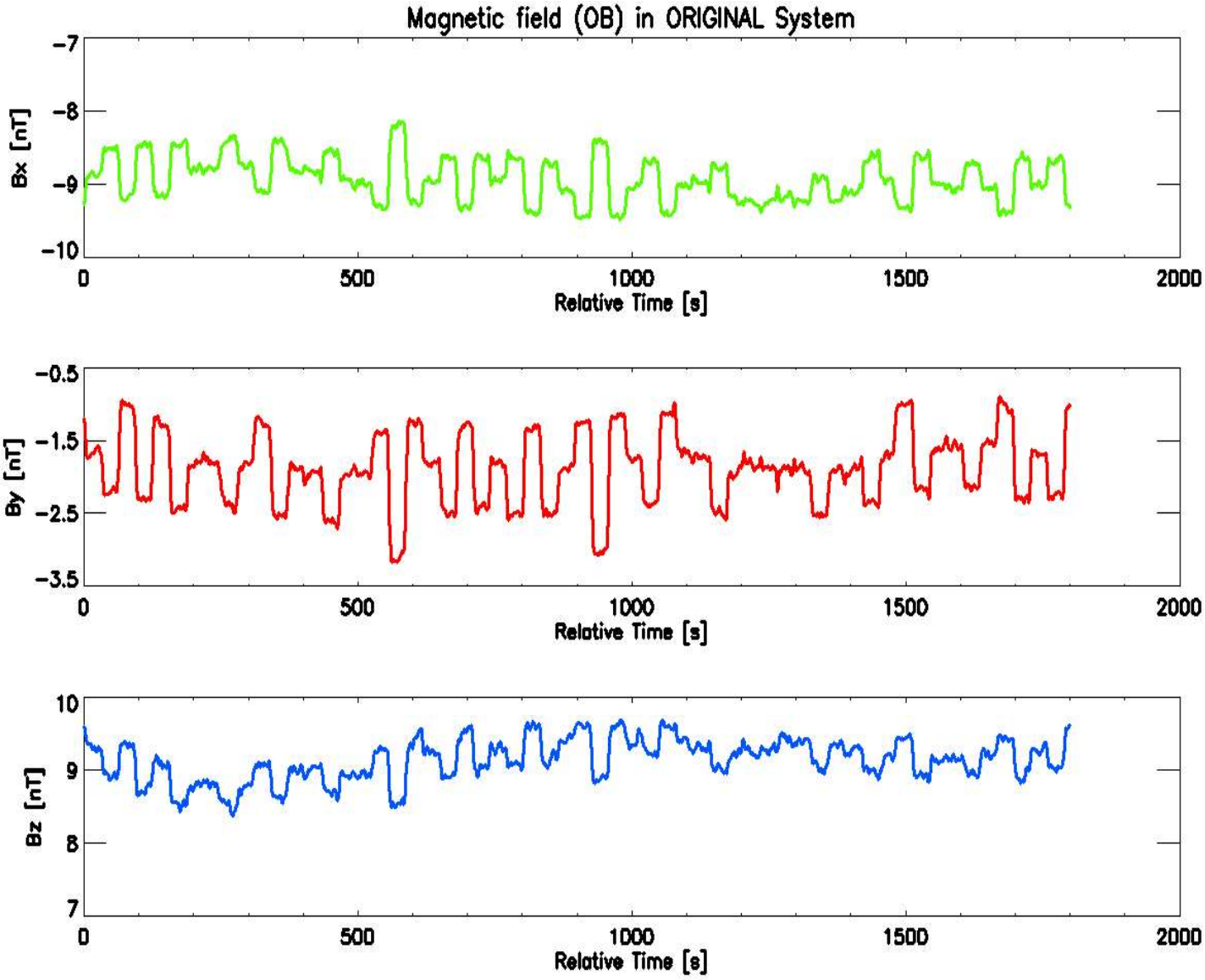

Figure 85: Original Signal disturbed by the LANDER heaters

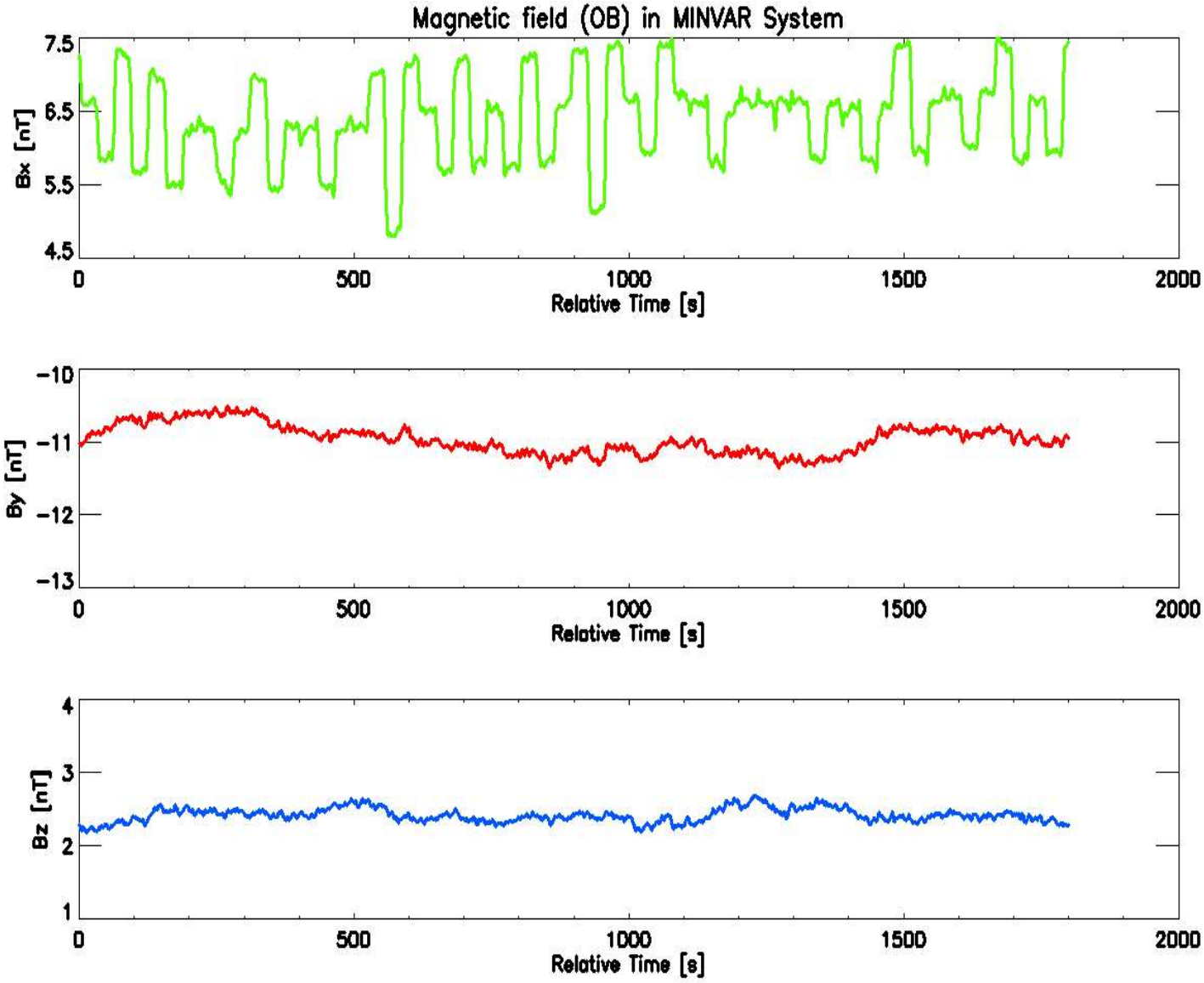

Figure 86: Disturbed signal rotated the Minimum Variance System

In the fourth panel the desired real time series is reconstructed. To do this the height of the jumps has to be computed individually for each jump. This height (level difference) is evaluated using short time averages of the last values of the level just before the jump and the average of the values just after the jump. With these data available it is possible to proceed step by step through the time series and to "flatten" all the infected levels. As the result the interrupted black–red time series is obtained.

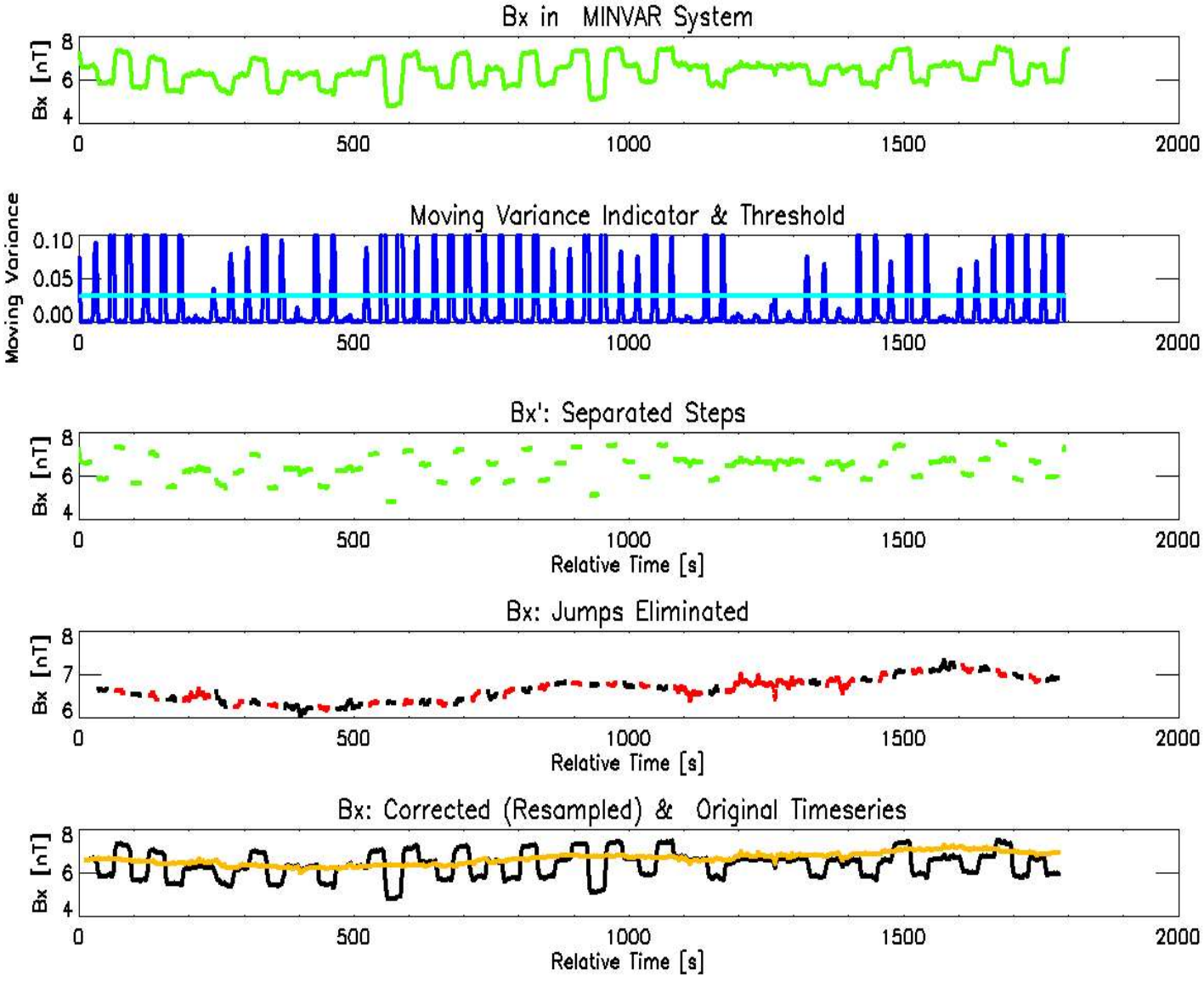

Figure 87: Processing of the heater disturbed Signal

The last step of the jump elimination can be seen in the bottom panels. The time gaps have been closed by resampling and interpolating the signal at the times of a jump. For a better comparison the original disturbed time series (black) and the improved signal (orange) are displayed.
At the very last processing step the corrected signal has to be rotated back from the min-var system to the original s/c frame. The result is shown in Figure 88.

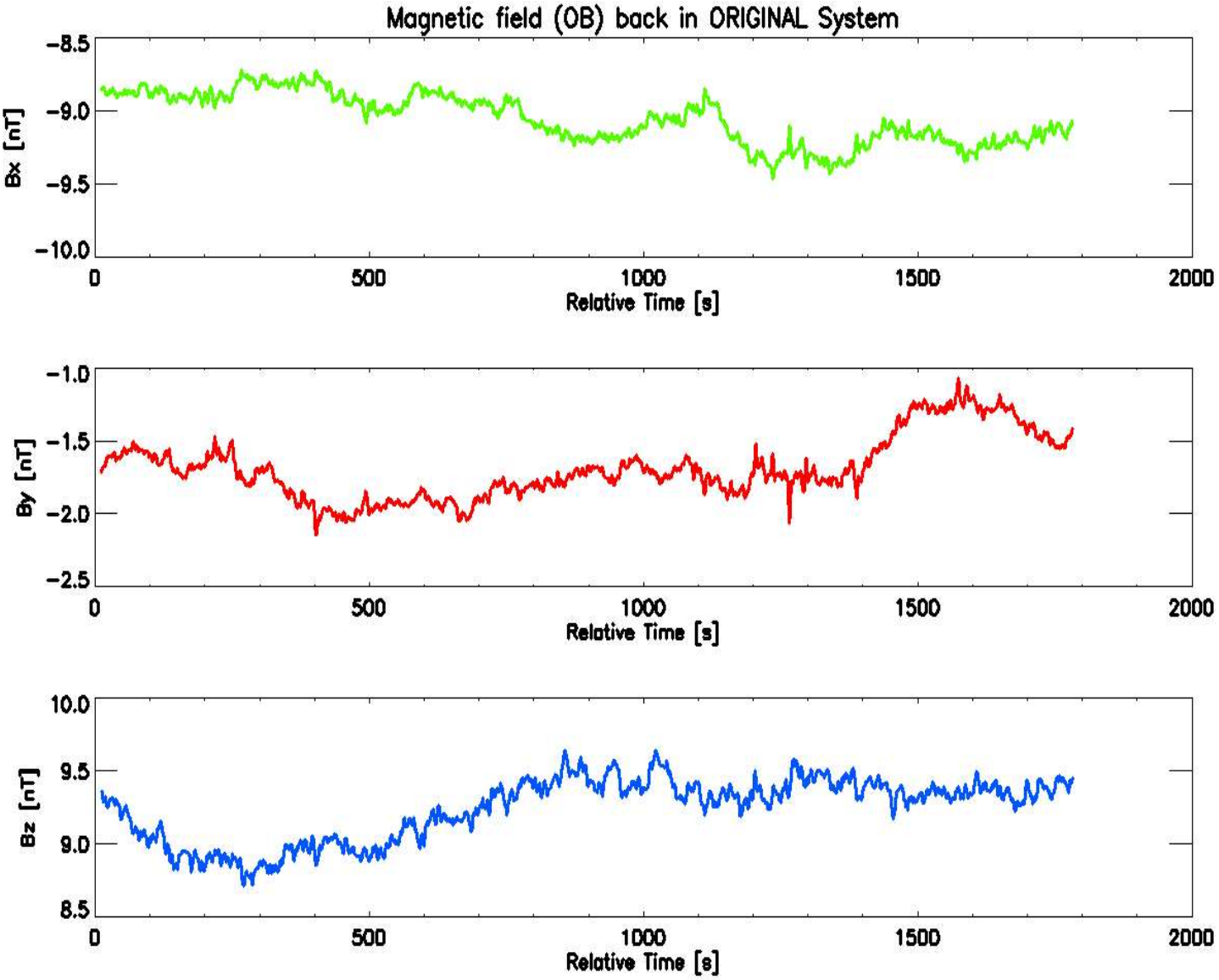

Figure 88: Processed Signal rotated back to s/c coordinate System

10 Temperature profile during EAR1

The following figure shows the measured temperatures of the OB and IB sensor during EAR1. The lower panels of the graph show the angles between x–, y–, and z–axis of the s/c frame and the sun direction.

The analysis of these plots shows that - as expected - most of the temperature changes are related to attitude changes. However, the steep increase of the temperatures at about 20:00 on March 3 can not be explained by a rotation.

A detailed model of ROSETTA using accurate SPICE kernels could possibly reveal all shadowing effects. Studies of this kind exceed, however, the scope of this report.

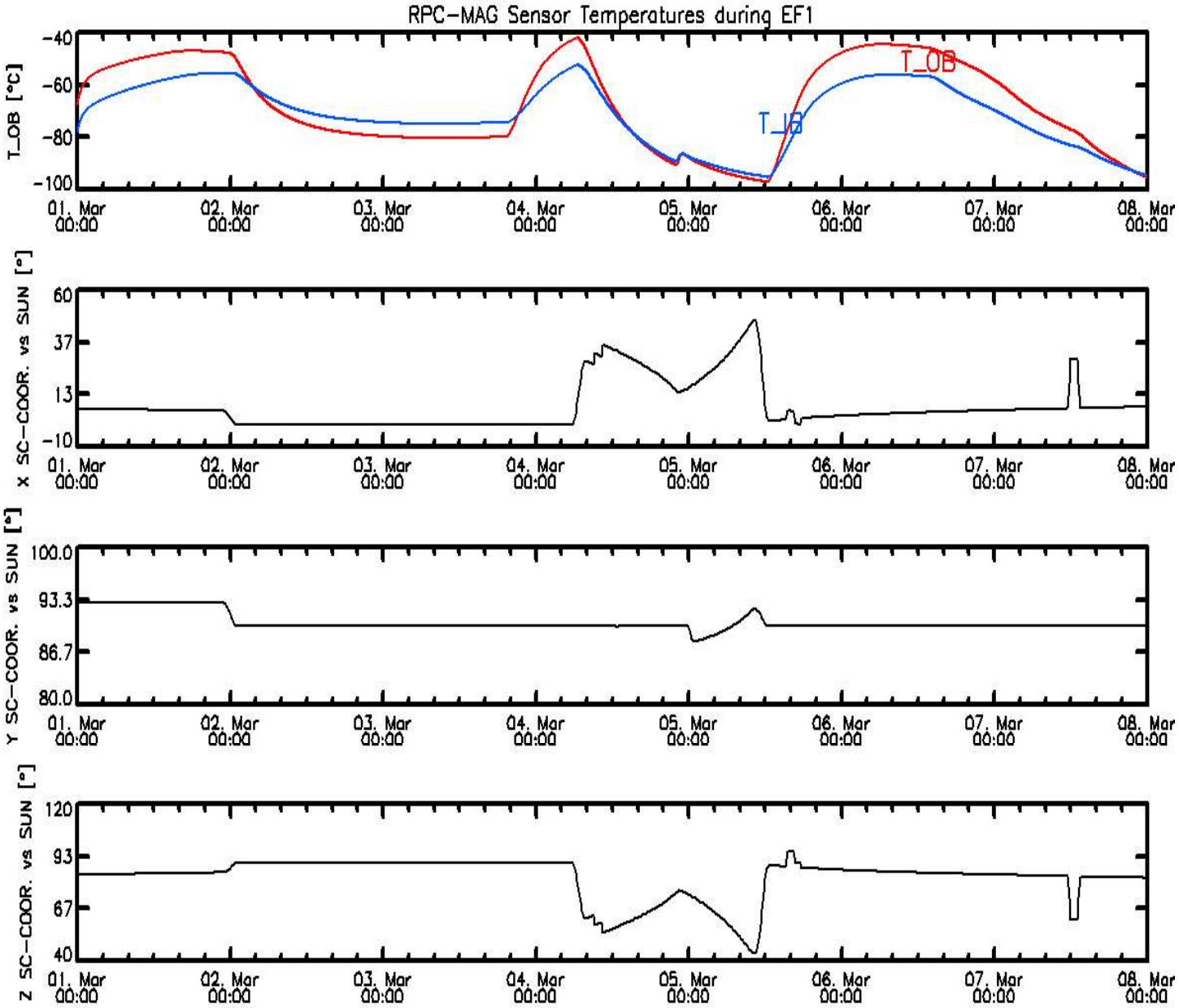

Figure 89: Measured Sensor Temperatures and attitudes during EAR1

11 Comparison of RPCMAG data with the ROMAP data

As an example for a comparison between RPCMAG and ROMAP the data of the OB (red) and the ROMAP sensor (black) of March 6, are plotted in Figures 90 (components) and 91 (differences). Here the heaters were off.

The higher frequent structures can be seen on both sensors in the same way. For the low frequencies the behavior is different, because the ROMAP sensor is not temperature calibrated at all . He shows a drift related to the temperature. After a proper temperature calibration, which is in the responsibility of the ROMAP PI, the data will probably match quite nice.

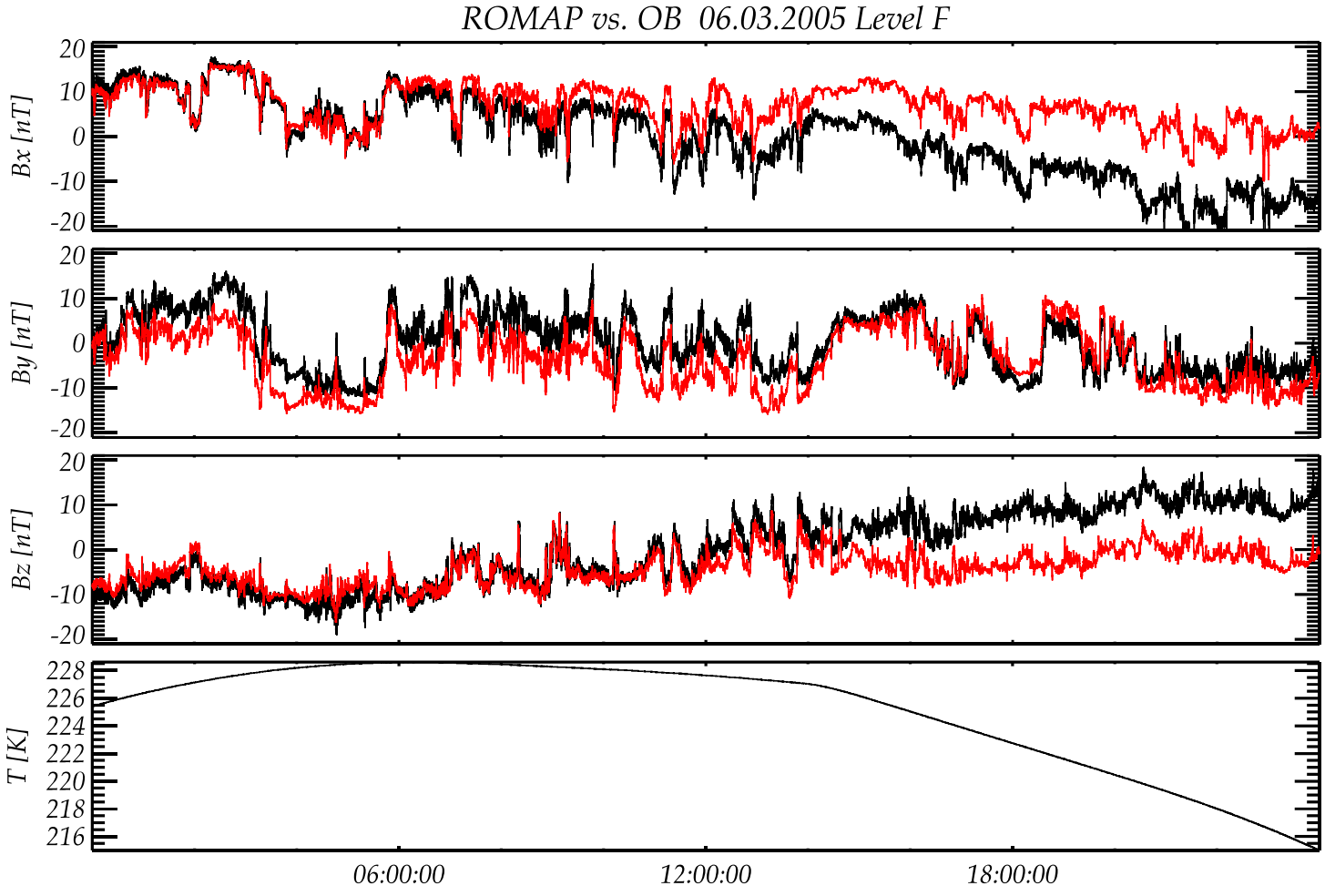

Figure 90: ROMAP versus OB: Data of March 6, 2005

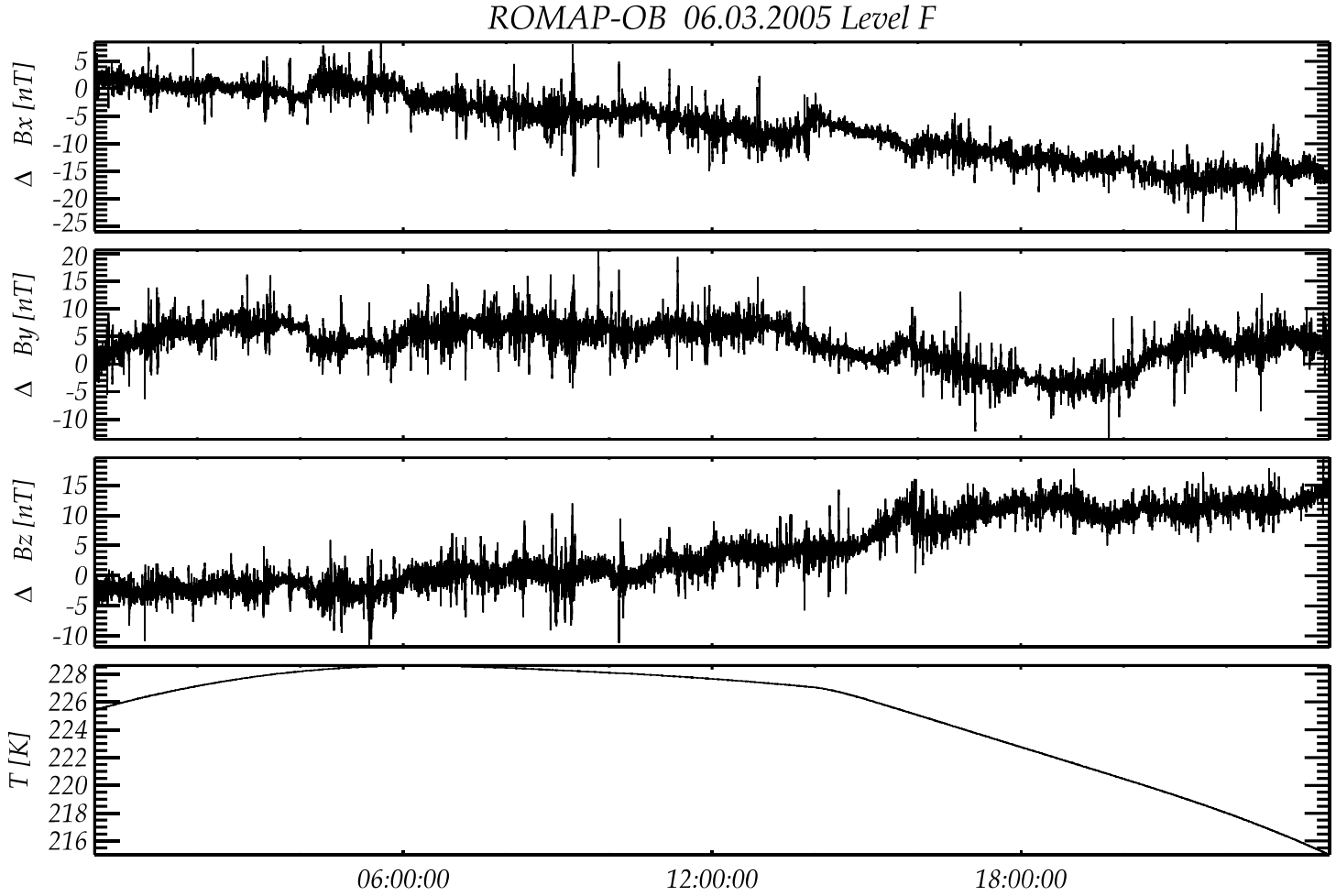

Figure 91: ROMAP versus OB: Data of March 6, 2005,Differences

12 Conclusions

- RPCMAG has performed amazing measurements during the Earth Swing by EAR1.
- A comparison of the MAG data with the forecast of a theoretical model (POMME) of the Earth's magnetic field shows only small differences in the order of less than 15 nT even in the components. This result was obtained by shifting the data in time (a few seconds [2]) and a slight rotation of the MAG URF in the order of less than 0.4 degrees.
  Thus, EAR 1 was a perfect opportunity to calibrate the actual sensor assembly matrices onboard the spacecraft.
- Comparison of RPCMAG-OB and RPCMAG-IB data with observations made by the solar wind monitor satellite WIND shows remarkable agreement.
- Disturbing heater signatures originated in the LANDER could be successfully eliminated.
- The spectra do not show any impact of ROSETTAs reaction wheels anymore.
- The comparison between IB and OB data showed that the measurements are very sensitive to specific temperature changes at the single sensors. The behavior can be used to build a data quality indicator.
- RPCMAG and ROMAP data will be in good agreement, when the temperature drifts and the heater effects are eliminated.

[2] an investigation of the onboard filter S/W has been done after EAR1 and all data have been reprocessed. Refer to the EAICD.